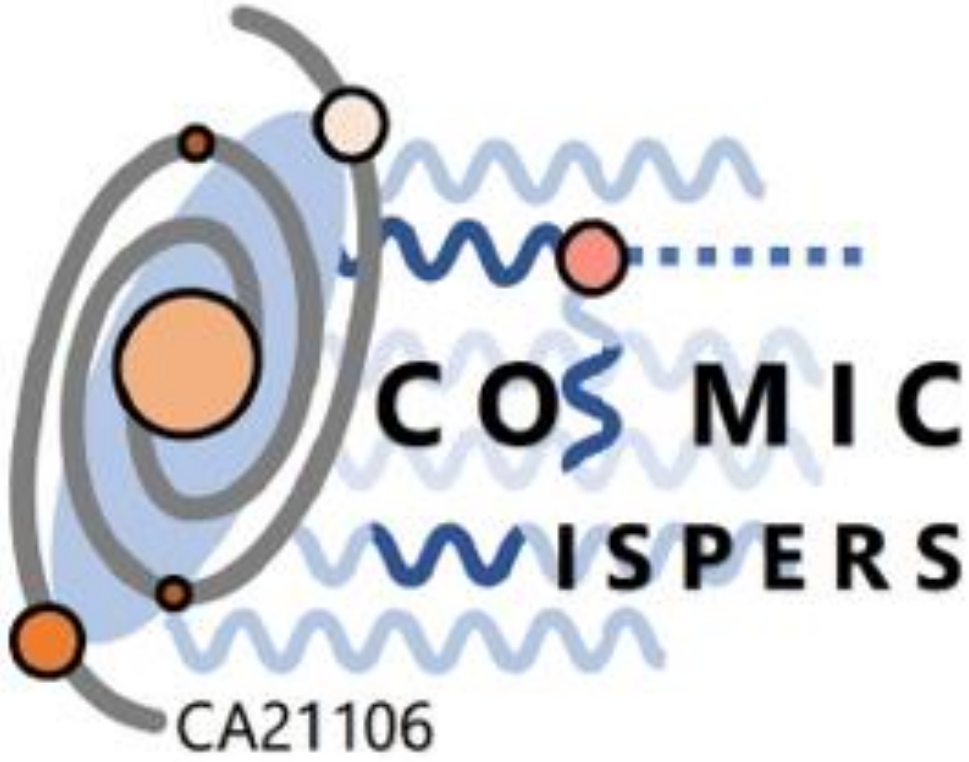

Axion field tomography: cosmic birefringence from the epochs of recombination and reionization

Patricia Diego-Palazuelos, Roger de Belsunce, Steven Gratton, Blake Sherwin

1st Training School COST Action COSMIC WISPers
Universita' del Salento, Lecce
September 11 – 14 2023

Searching for ULA through their coupling to EM

ALP can couple to EM through a Chern-Simons interaction

$$\frac{1}{4} g_{\phi\gamma} \phi F_{\mu\nu} \tilde{F}_{\mu\nu}$$

rotation of the plane of linear polarization clockwise on the sky

$$\beta = -\frac{1}{2} g_{\phi\gamma} \int \frac{\partial \phi}{\partial t} dt$$

Komatsu [arXiv:2202.13919]

Searching for ULA through their coupling to EM

ALP can couple to EM through a Chern-Simons interaction

$$\frac{1}{4} g_{\phi\gamma} \phi F_{\mu\nu} \tilde{F}_{\mu\nu}$$

rotation of the plane of linear polarization clockwise on the sky

$$\beta = -\frac{1}{2} g_{\phi\gamma} \int \frac{\partial \phi}{\partial t} dt$$

Komatsu [arXiv:2202.13919]

ALP as dark energy

10^{-32} eV $\lesssim m_\phi \lesssim 10^{-28}$ eV

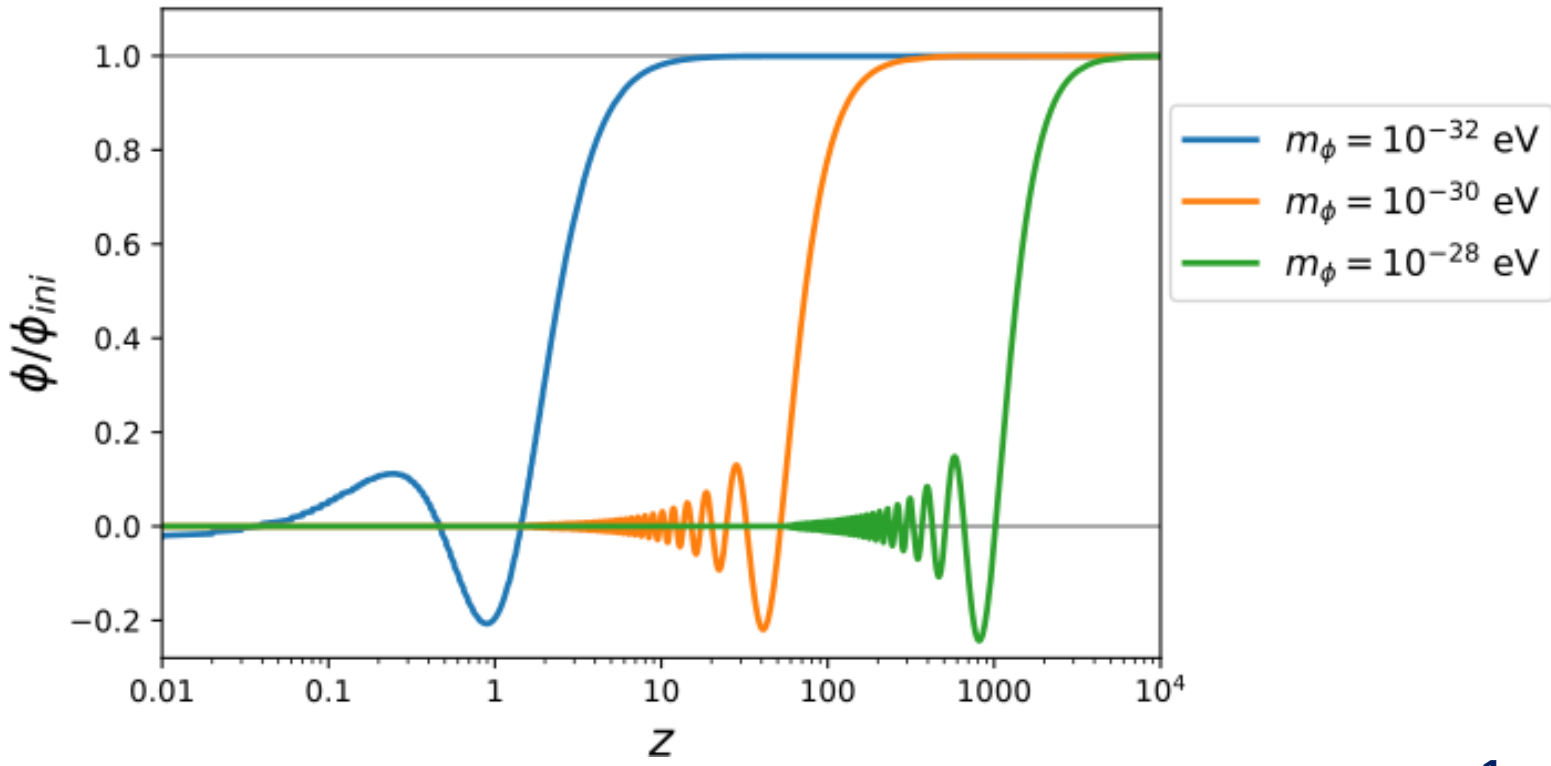

Searching for ULA through their coupling to EM

ALP can couple to EM through a Chern-Simons interaction

$$\frac{1}{4} g_{\phi\gamma} \phi F_{\mu\nu} \tilde{F}_{\mu\nu}$$

rotation of the plane of linear polarization clockwise on the sky

$$\beta = -\frac{1}{2} g_{\phi\gamma} \int \frac{\partial \phi}{\partial t} dt$$

Komatsu [arXiv:2202.13919]

ALP as dark energy

10^{-32} eV $\lesssim m_\phi \lesssim 10^{-28}$ eV

CMB offers two observational windows

- Small angular scales (high-ℓ) are sensitive to β_{dec}
- Large angular scales (low-ℓ) are sensitive to β_{reio}

Tomographic view of the ULA field at z≈10 and z≈1000

Sherwin&Namikawa[arXiv:2108.09287]
Nakatsuka+[arXiv:2203.08560]

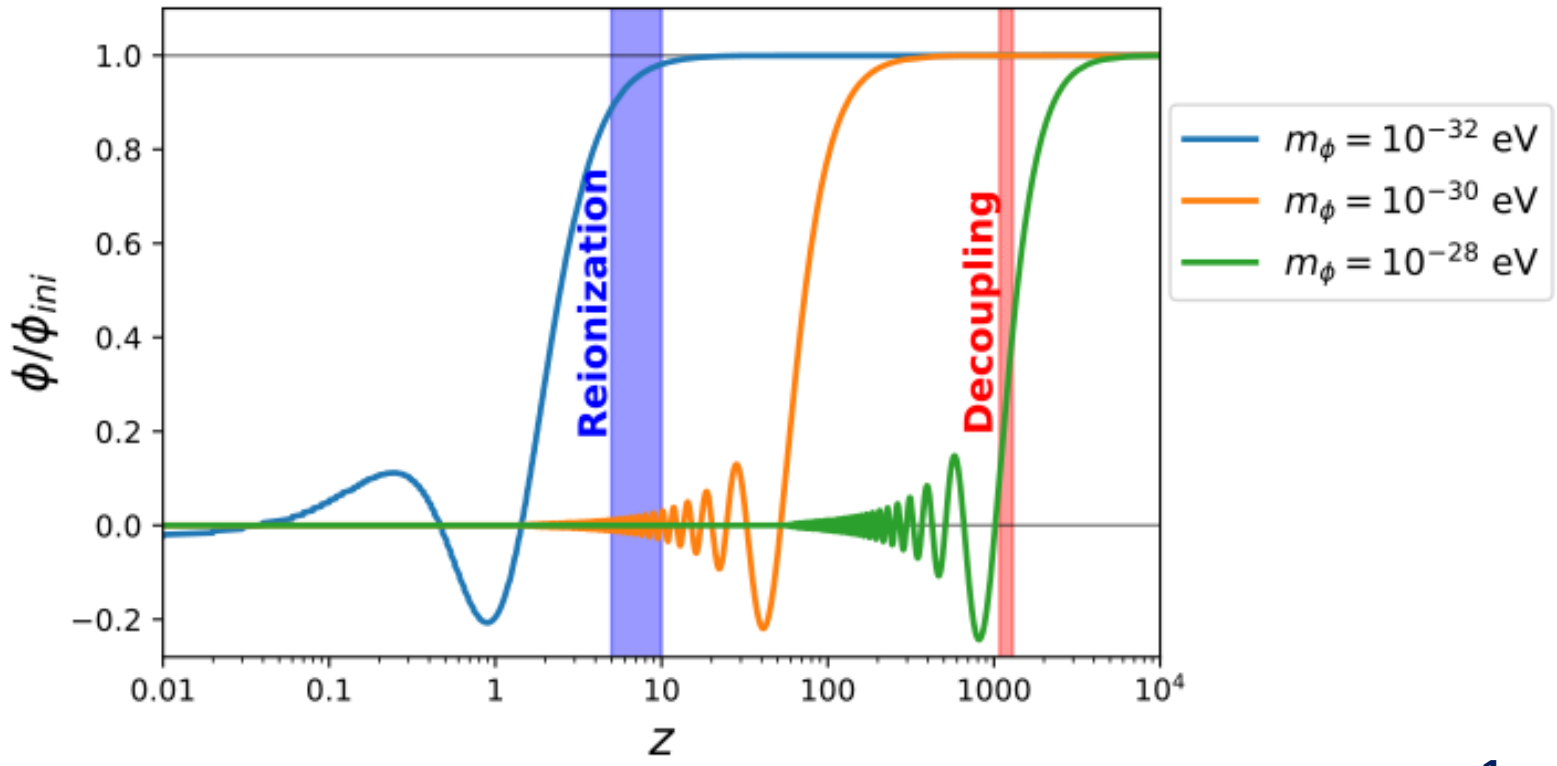

Cosmic birefringence rotates the observed CMB

$$\begin{pmatrix} E^{\rm o}_{\ell m} \\ B^{\rm o}_{\ell m} \end{pmatrix} = \begin{pmatrix} \cos(2\beta) & -\sin(2\beta) \\ \sin(2\beta) & \cos(2\beta) \end{pmatrix} \begin{pmatrix} E^{\rm cmb}_{\ell m} \\ B^{\rm cmb}_{\ell m} \end{pmatrix}$$

so the observed angular power spectrum becomes

$$C_\ell^{EB,{\rm o}} = \frac{1}{2}\sin(4\beta)\left(C_\ell^{EE,{\rm cmb}} - C_\ell^{BB,{\rm cmb}}\right) + \cos(4\beta) C_\ell^{EB,{\rm cmb}}$$

ΛCDM

Cosmic birefringence

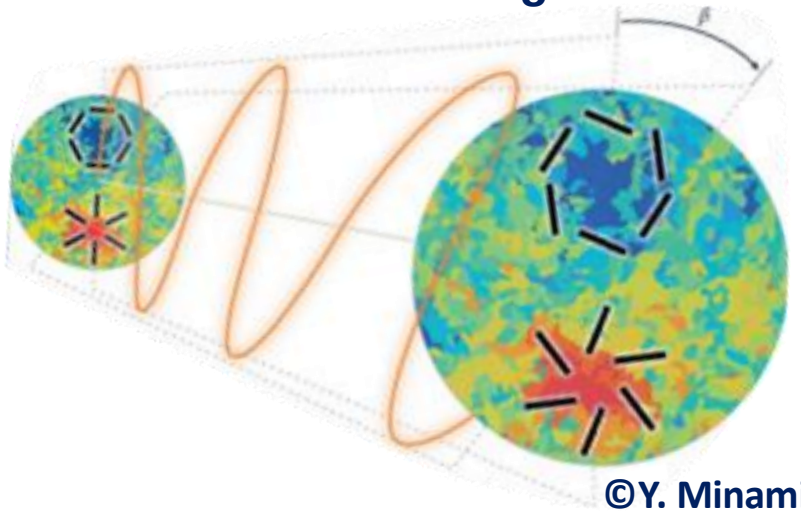

©Y. Minami

Cosmic birefringence rotates the observed CMB

$$\begin{pmatrix} E^{\rm o}_{\ell m} \\ B^{\rm o}_{\ell m} \end{pmatrix} = \begin{pmatrix} \cos(2\beta) & -\sin(2\beta) \\ \sin(2\beta) & \cos(2\beta) \end{pmatrix} \begin{pmatrix} E^{\rm cmb}_{\ell m} \\ B^{\rm cmb}_{\ell m} \end{pmatrix}$$

so the observed angular power spectrum becomes

$$C_\ell^{EB,{\rm o}} = \frac{1}{2}\sin(4\beta)\left(C_\ell^{EE,{\rm cmb}} - C_\ell^{BB,{\rm cmb}}\right) + \cos(4\beta)\cancel{C_\ell^{EB,{\rm cmb}}}$$

ΛCDM

$$C_\ell^{EB,{\rm o}} = \frac{1}{2}\tan(4\beta)\left(C_\ell^{EE,{\rm o}} - C_\ell^{BB,{\rm o}}\right)$$

Base of most methodologies applied in the past

Cosmic birefringence

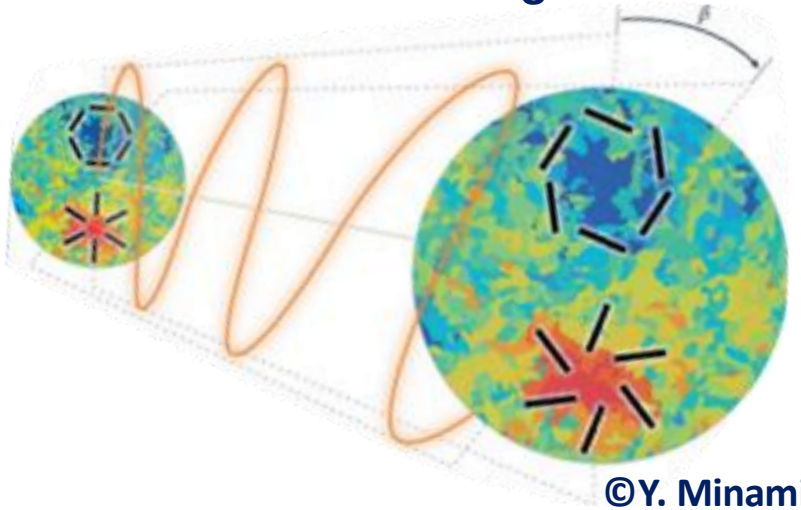

©Y. Minami

Cosmic birefringence rotates the observed CMB

$$\begin{pmatrix} E^{\rm o}_{\ell m} \\ B^{\rm o}_{\ell m} \end{pmatrix} = \begin{pmatrix} \cos(2\beta) & -\sin(2\beta) \\ \sin(2\beta) & \cos(2\beta) \end{pmatrix} \begin{pmatrix} E^{\rm cmb}_{\ell m} \\ B^{\rm cmb}_{\ell m} \end{pmatrix}$$

so the observed angular power spectrum becomes

$$C_\ell^{EB,{\rm o}} = \frac{1}{2}\sin(4\beta)\left(C_\ell^{EE,{\rm cmb}} - C_\ell^{BB,{\rm cmb}}\right) + \cos(4\beta)\cancel{C_\ell^{EB,{\rm cmb}}}$$

ΛCDM

$$C_\ell^{EB,{\rm o}} = \frac{1}{2}\tan(4\beta)\left(C_\ell^{EE,{\rm o}} - C_\ell^{BB,{\rm o}}\right)$$

Base of most methodologies applied in the past

Cosmic birefringence

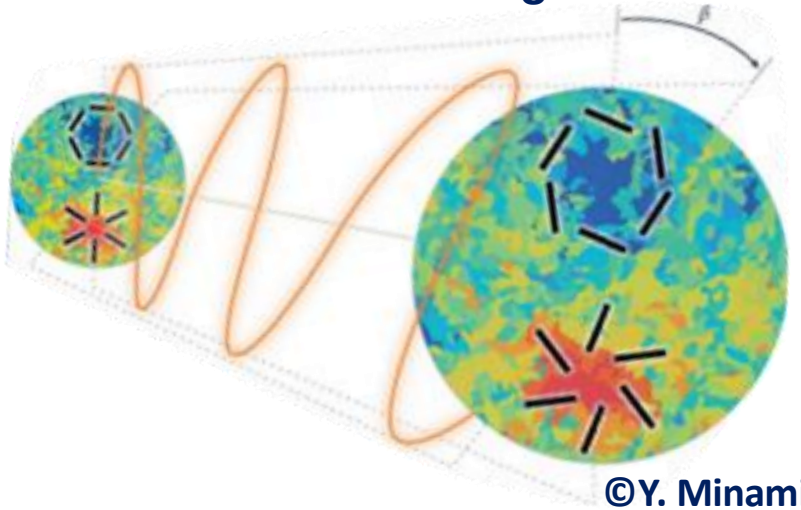

©Y. Minami

OR

Miscalibration of the detector's polarisation angle

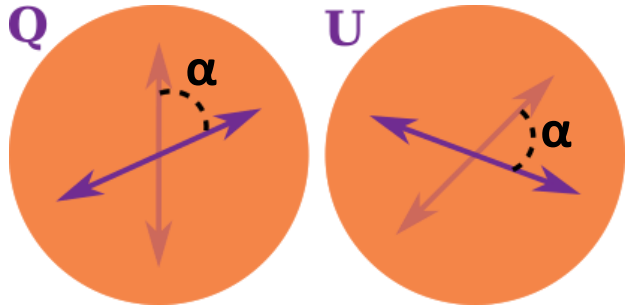

Unknown α miscalibration
Completely degenerate with birefringence

Krachmalnicoff+[arXiv:2111.09140]

The observed signal is actually

$$\begin{pmatrix} E^{\rm o}_{\ell m} \\ B^{\rm o}_{\ell m} \end{pmatrix} = \begin{pmatrix} \cos(2\alpha+2\beta) & -\sin(2\alpha+2\beta) \\ \sin(2\alpha+2\beta) & \cos(2\alpha+2\beta) \end{pmatrix} \begin{pmatrix} E^{\rm cmb}_{\ell m} \\ B^{\rm cmb}_{\ell m} \end{pmatrix}$$

so that EB yields α+β

$$C_\ell^{EB,{\rm o}} = \frac{1}{2}\tan(4\alpha+4\beta)\left(C_\ell^{EE,{\rm o}} - C_\ell^{BB,{\rm o}}\right)$$

Cosmic birefringence

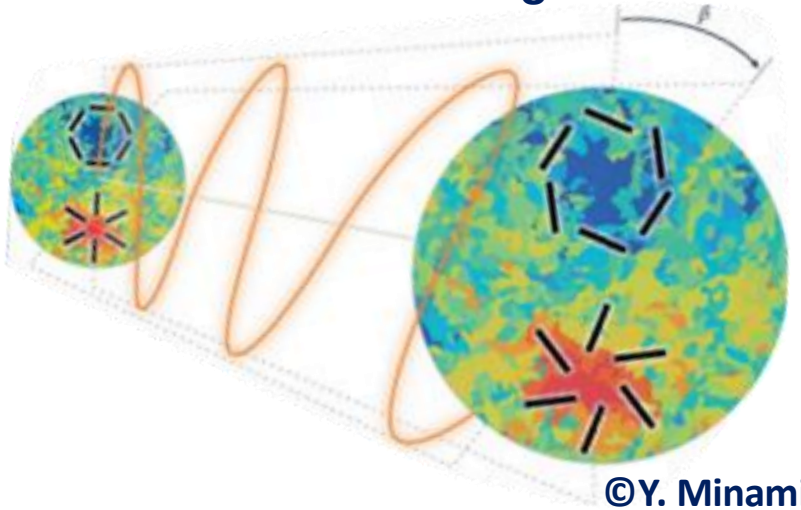

©Y. Minami

OR

Miscalibration of the detector's polarisation angle

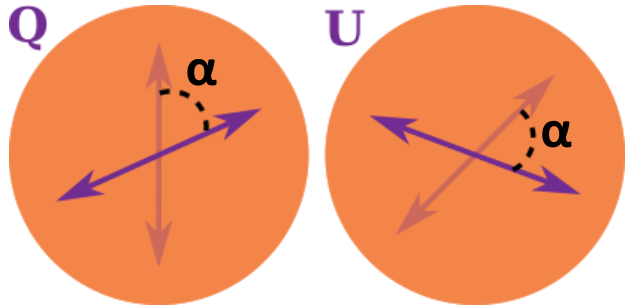

Unknown α miscalibration
Completely degenerate with birefringence

Krachmalnicoff+[arXiv:2111.09140]

The observed signal is actually

$$\begin{pmatrix} E^{\rm o}_{\ell m} \\ B^{\rm o}_{\ell m} \end{pmatrix} = \begin{pmatrix} \cos(2\alpha+2\beta) & -\sin(2\alpha+2\beta) \\ \sin(2\alpha+2\beta) & \cos(2\alpha+2\beta) \end{pmatrix} \begin{pmatrix} E^{\rm cmb}_{\ell m} \\ B^{\rm cmb}_{\ell m} \end{pmatrix}$$

so that EB yields α+β

$$C_\ell^{EB,{\rm o}} = \frac{1}{2}\tan(4\alpha+4\beta)\left(C_\ell^{EE,{\rm o}} - C_\ell^{BB,{\rm o}}\right)$$

Requires absolute calibration of instrumental polarisation angles

Previous measurements limited to ≈ 0.5°- 1°

Cosmic birefringence

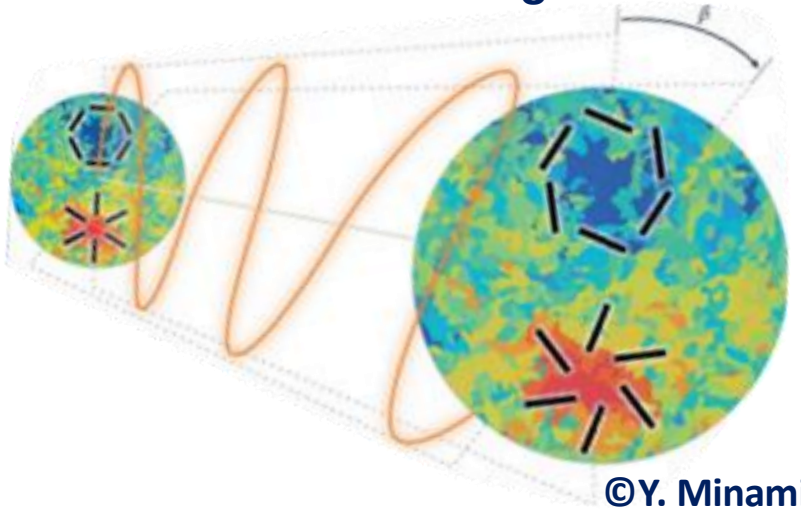

©Y. Minami

OR

Miscalibration of the detector's polarisation angle

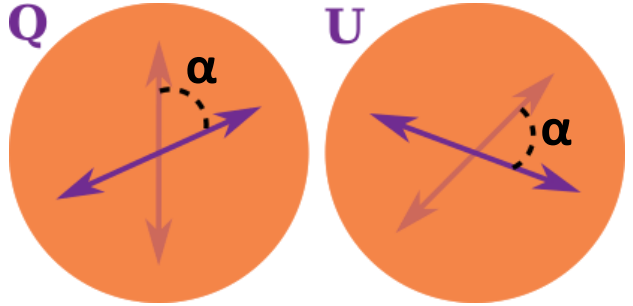

Unknown α miscalibration

Completely degenerate with birefringence

Krachmalnicoff+[arXiv:2111.09140]

$$\beta = -\frac{1}{2} g_{\phi\gamma} \int \frac{\partial \phi}{\partial t} dt$$

Galactic foreground emission not significantly affected by birefringence

Use foregrounds as our calibrator

Minami+[arXiv:1904.12440]
Minami&Komatsu[arXiv:2006.15982]

$$\beta = -\frac{1}{2} g_{\phi\gamma} \int \frac{\partial \phi}{\partial t} dt$$

Galactic foreground emission not significantly affected by birefringence

Use foregrounds as our calibrator

Minami+[arXiv:1904.12440]
Minami&Komatsu[arXiv:2006.15982]

Observed signal is a rotation of the CMB and Galactic foreground emissions

$$\begin{pmatrix} E^{\rm o}_{\ell m} \\ B^{\rm o}_{\ell m} \end{pmatrix} = \begin{pmatrix} \cos(2\alpha) & -\sin(2\alpha) \\ \sin(2\alpha) & \cos(2\alpha) \end{pmatrix} \begin{pmatrix} E^{\rm fg}_{\ell m} \\ B^{\rm fg}_{\ell m} \end{pmatrix} + \begin{pmatrix} \cos(2\alpha+2\beta) & -\sin(2\alpha+2\beta) \\ \sin(2\alpha+2\beta) & \cos(2\alpha+2\beta) \end{pmatrix} \begin{pmatrix} E^{\rm cmb}_{\ell m} \\ B^{\rm cmb}_{\ell m} \end{pmatrix}$$

so the observed EB angular power spectrum is

$$C_\ell^{EB,{\rm o}} = \frac{\tan(4\alpha)}{2}\left(C_\ell^{EE,{\rm o}} - C_\ell^{BB,{\rm o}}\right) + \frac{1}{\cos(4\alpha)} C_\ell^{EB,{\rm fg}} + \frac{\sin(4\beta)}{2\cos(4\alpha)}\left(C_\ell^{EE,{\rm cmb}} - C_\ell^{BB,{\rm cmb}}\right)$$

$$\beta = -\frac{1}{2} g_{\phi\gamma} \int \frac{\partial \phi}{\partial t} dt$$

Galactic foreground emission not significantly affected by birefringence

Use foregrounds as our calibrator

Minami+[arXiv:1904.12440]
Minami&Komatsu[arXiv:2006.15982]

Observed signal is a rotation of the CMB and Galactic foreground emissions

$$\begin{pmatrix} E^{\rm o}_{\ell m} \\ B^{\rm o}_{\ell m} \end{pmatrix} = \begin{pmatrix} \cos(2\alpha) & -\sin(2\alpha) \\ \sin(2\alpha) & \cos(2\alpha) \end{pmatrix} \begin{pmatrix} E^{\rm fg}_{\ell m} \\ B^{\rm fg}_{\ell m} \end{pmatrix} + \begin{pmatrix} \cos(2\alpha+2\beta) & -\sin(2\alpha+2\beta) \\ \sin(2\alpha+2\beta) & \cos(2\alpha+2\beta) \end{pmatrix} \begin{pmatrix} E^{\rm cmb}_{\ell m} \\ B^{\rm cmb}_{\ell m} \end{pmatrix}$$

so the observed EB angular power spectrum is

$$C_\ell^{EB,{\rm o}} = \frac{\tan(4\alpha)}{2}\left(C_\ell^{EE,{\rm o}} - C_\ell^{BB,{\rm o}}\right) + \frac{1}{\cos(4\alpha)} C_\ell^{EB,{\rm fg}} + \frac{\sin(4\beta)}{2\cos(4\alpha)}\left(C_\ell^{EE,{\rm cmb}} - C_\ell^{BB,{\rm cmb}}\right)$$

Synchrotron

Synch EB **statistically compatible with null**

Martire+[arXiv:2110.12803]
QUIJOTE [arXiv:2301.05113]

Dust

Misalignment between dust filaments and Galactic magnetic fields creates TB and EB correlations Clark+[arXiv:2105.00120] Cukierman+[arXiv:2208.07382]

***Planck* reported :**

- **Dust TB > 0**
- **A hint of dust EB > 0** *Planck* Collab [arXiv:1801.04945]

Promising hint of a non-null β_{dec} at high-ℓ

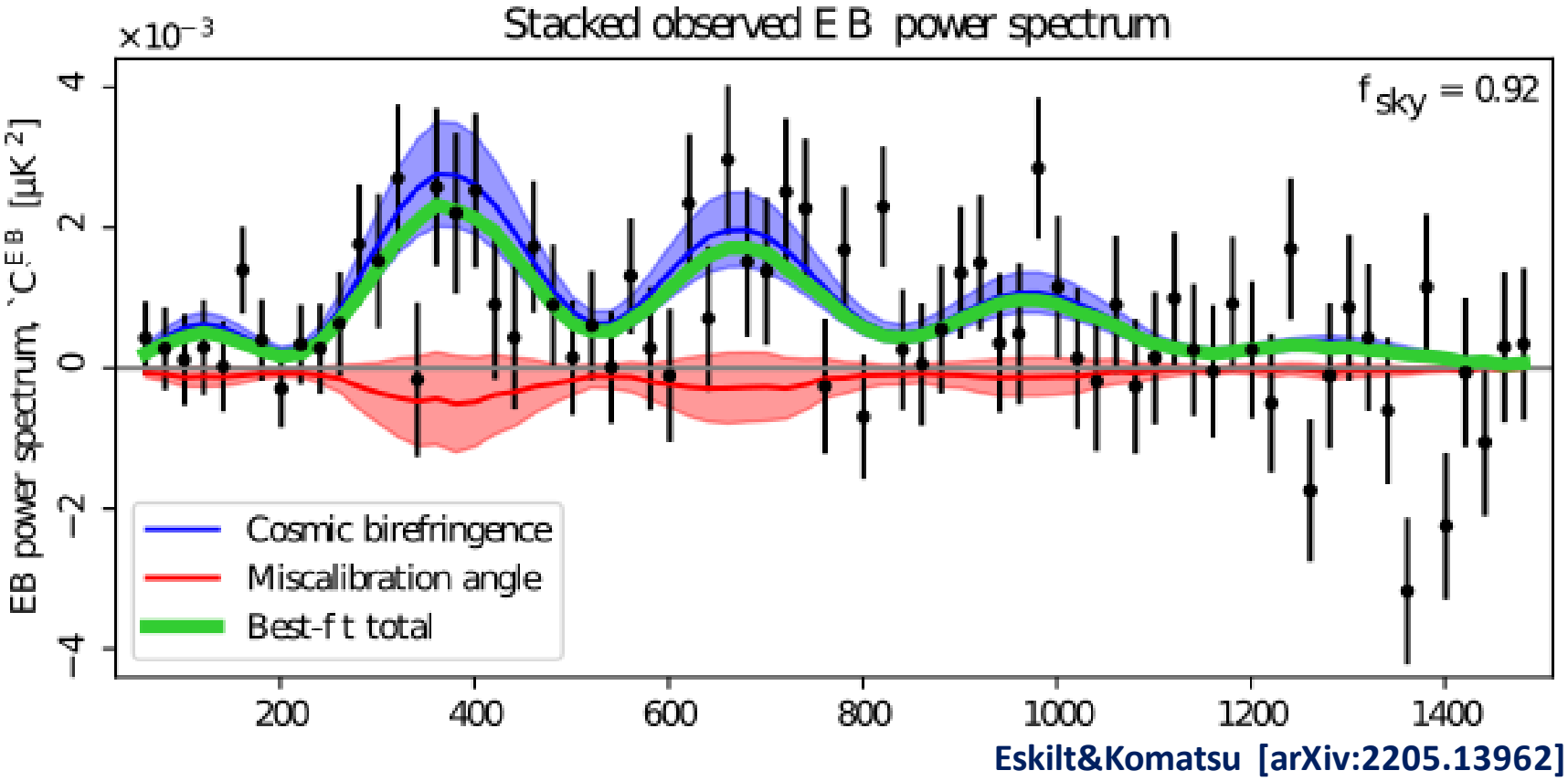

Eskilt&Komatsu [arXiv:2205.13962]

Tighthest constraint to date (3.6σ)

$$\beta = 0.342^\circ\,^{+0.094^\circ}_{-0.091^\circ}$$

from the analysis of *Planck* and WMAP data

Eskilt&Komatsu [arXiv:2205.13962]

Promising hint of a non-null β_{dec} at high-ℓ

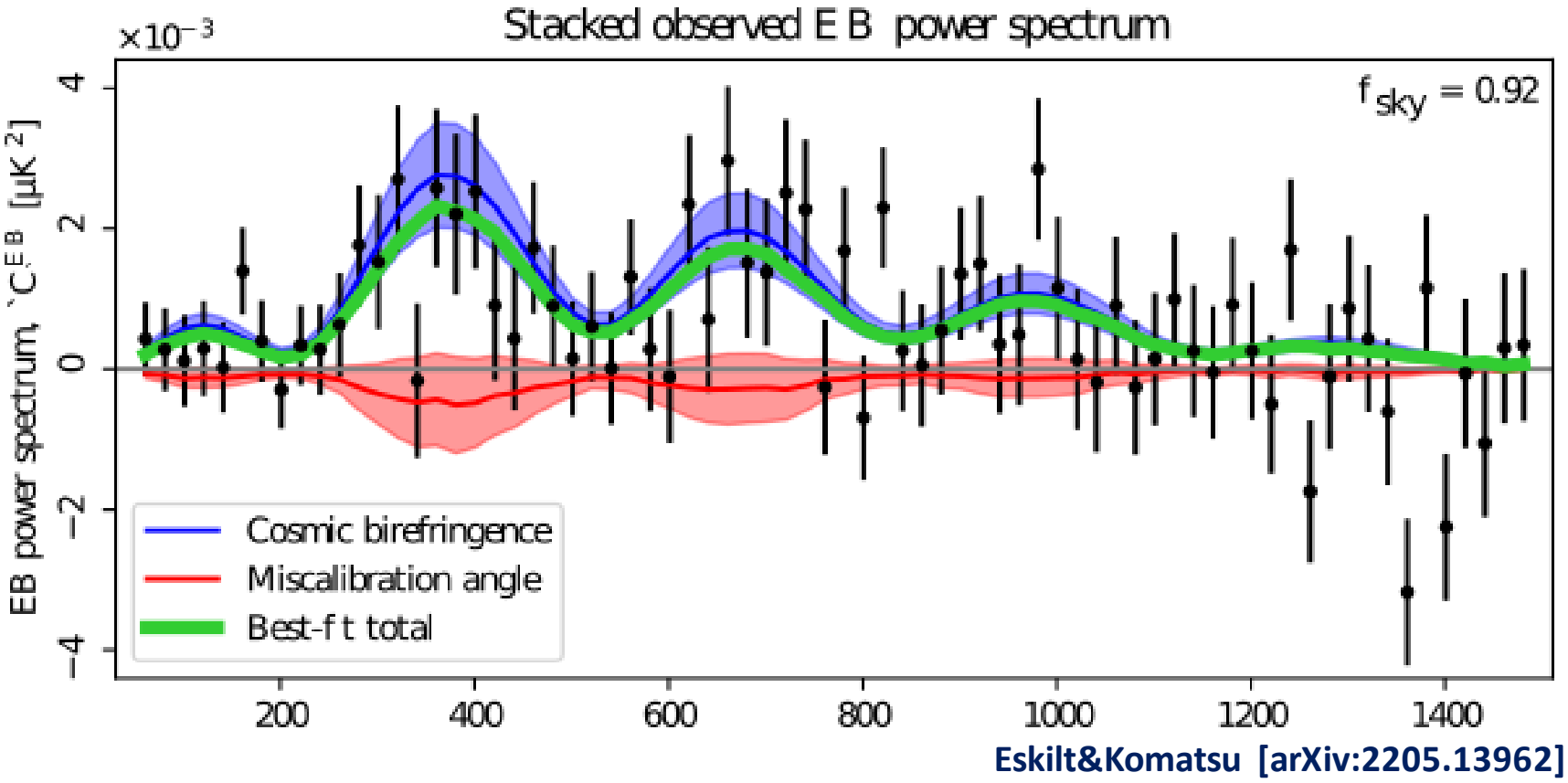

Eskilt&Komatsu [arXiv:2205.13962]

Tighthest constraint to date (3.6σ)

$$\beta = 0.342^\circ\,^{+0.094^\circ}_{-0.091^\circ}$$

from the analysis of *Planck* and WMAP data

Eskilt&Komatsu [arXiv:2205.13962]

Robust against instrumental systematics

PDP+[arXiv:2210.07655]
Eskilt+[arXiv:2305.02268]

Sensitive to dust EB

- **Templates modeling dust as a modified blackbody**
- **Estimate the misalignment between filaments and magnetic fields**

PDP+[arXiv:2201.07682]

Measuring β_{reio} from $\ell \leq 10$

Work with CMB instead of frequency maps

Remove foregrounds by fitting and subtracting templates of synchrotron and dust emission

CMB spectra from 100 GHz x 143 GHz of *Planck* SRoll2.0

Delouis+[arXiv:1901.11386]

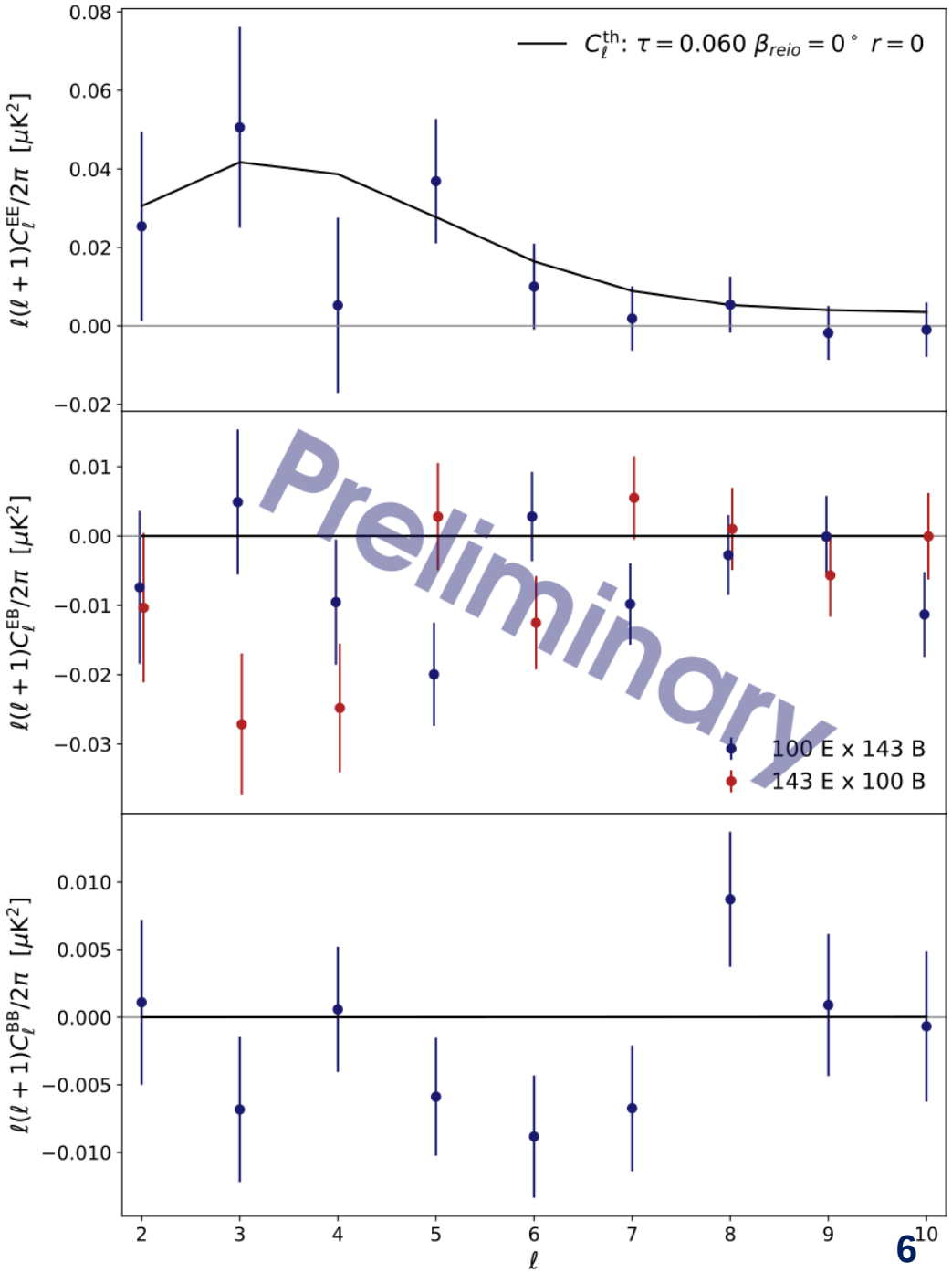

Measuring β_{reio} from $\ell \leq 10$

Work with CMB instead of frequency maps

Remove foregrounds by fitting and subtracting templates of synchrotron and dust emission

CMB spectra from 100 GHz x 143 GHz of *Planck* SRoll2.0

Delouis+[arXiv:1901.11386]

$$P(\Theta|d,\mathcal{M}) \propto \mathcal{L}(d|\Theta,\mathcal{M})\Pi(\Theta|\mathcal{M})$$

Sample over $\Theta = \{\tau,\ \beta_{reio},\ \beta_{dec},\ \alpha_{100},\ \alpha_{143},\ r=0\}$

Gaussian prior on β_{dec}, α_{100}, α_{143} from high-ℓ analysis

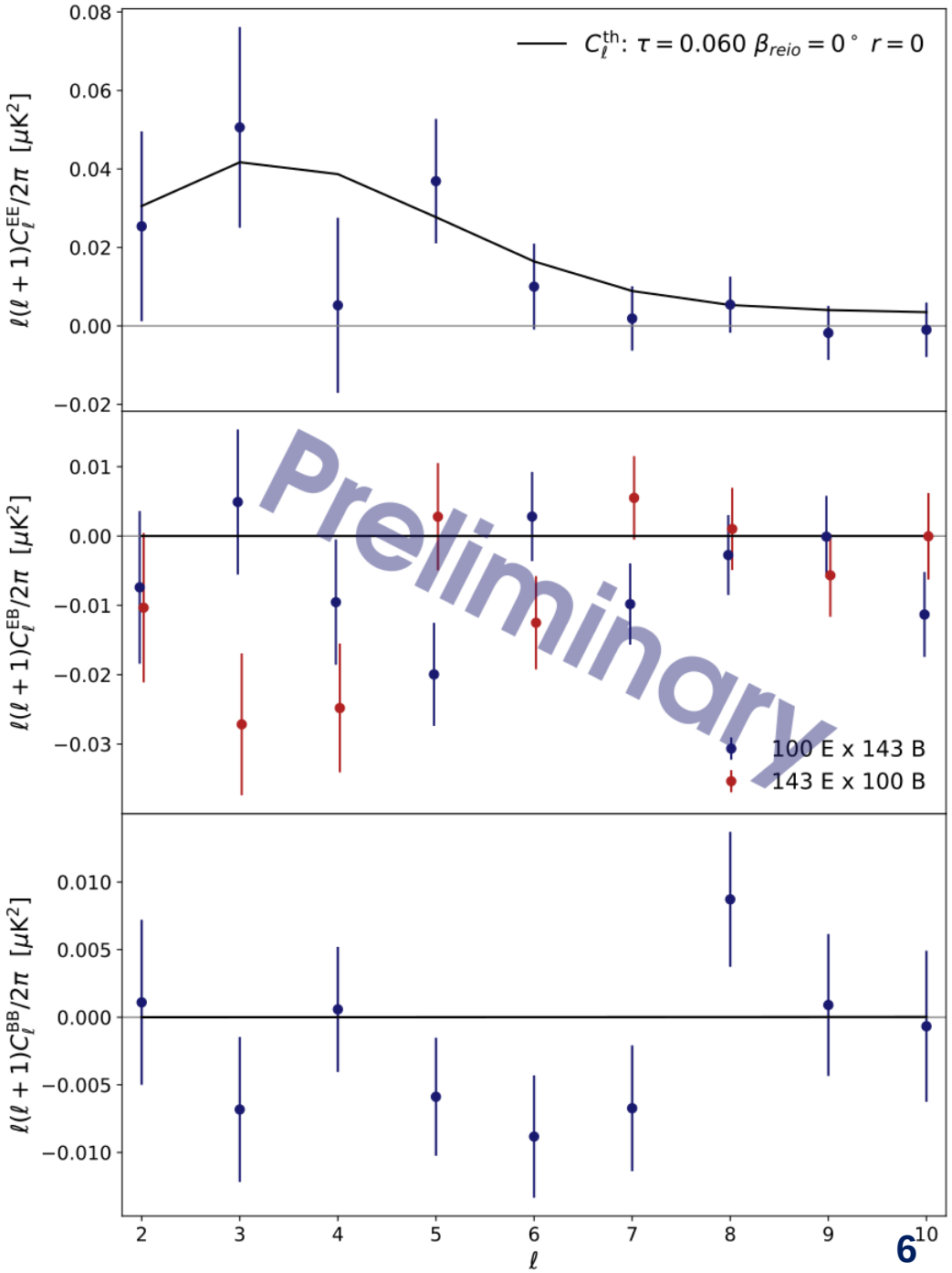

Measuring β_{reio} from $\ell \leq 10$

Work with CMB instead of frequency maps

Remove foregrounds by fitting and subtracting templates of synchrotron and dust emission

CMB spectra from 100 GHz x 143 GHz of *Planck* SRoll2.0

Delouis+[arXiv:1901.11386]

$$P(\Theta|d,\mathcal{M}) \propto \mathcal{L}(d|\Theta,\mathcal{M})\Pi(\Theta|\mathcal{M})$$

Sample over $\Theta = \{\tau,\ \beta_{reio},\ \beta_{dec},\ \alpha_{100},\ \alpha_{143},\ r=0\}$

Gaussian prior on β_{dec}, α_{100}, α_{143} from high-ℓ analysis

momento

Semi-analytical likelihood-approximation based on the principle of maximum entropy

Gratton [arXiv:1708.08479]

de Belsunce+[arXiv:2103.14378]

de Belsunce+[arXiv:2207.04903]

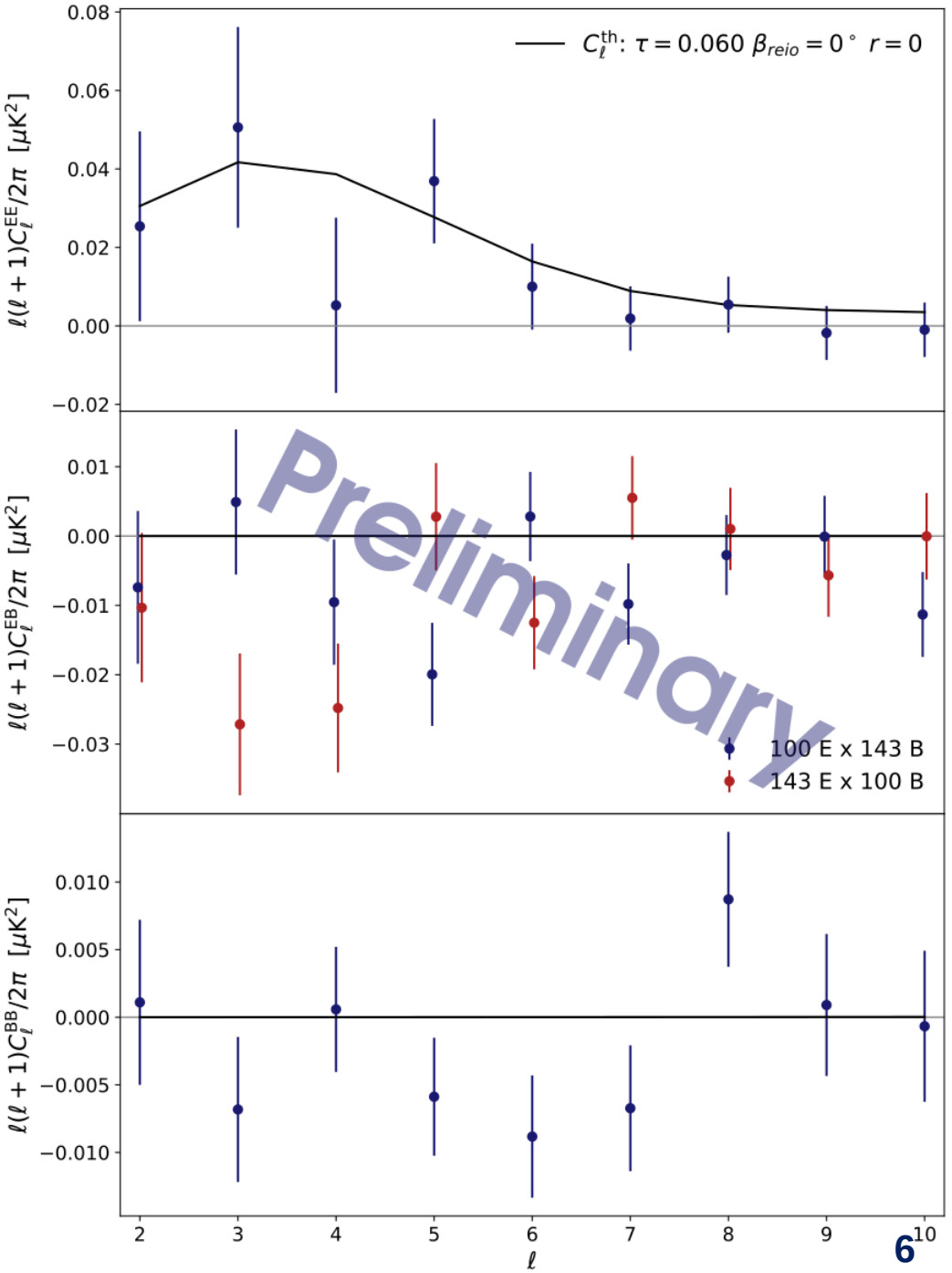

EE – BB information

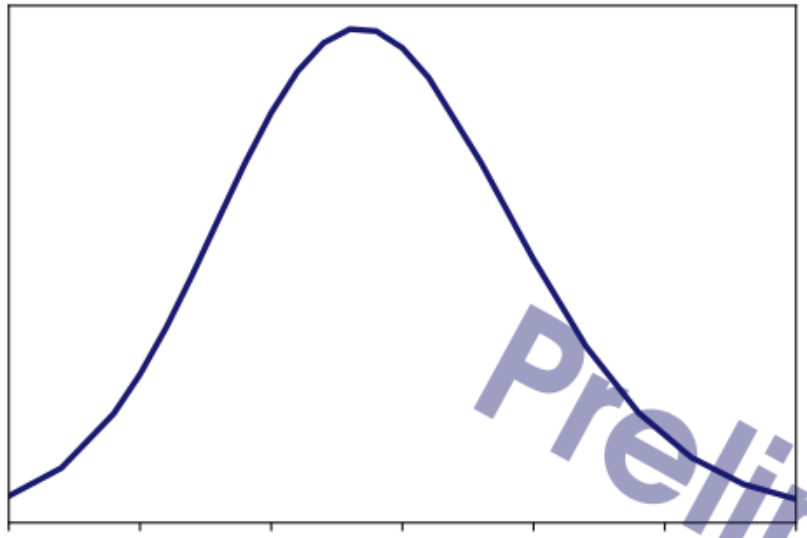

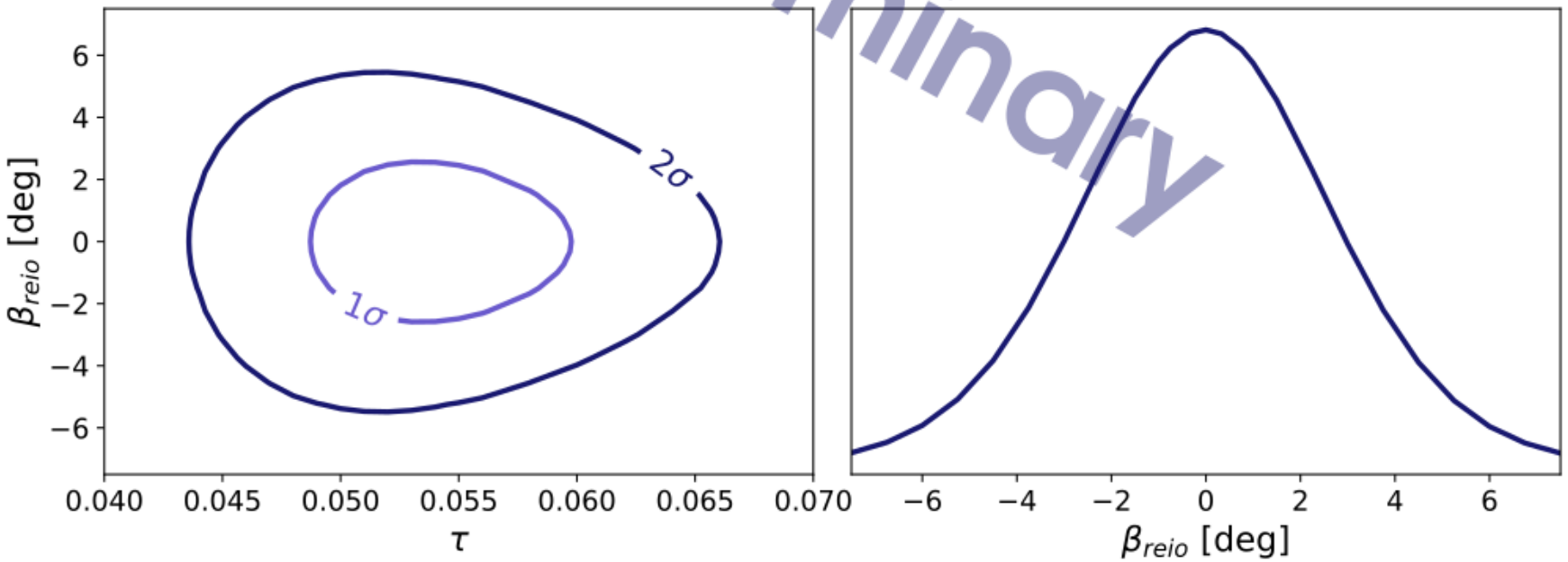

Recover the expected τ - β_{reio} degeneracy

$$C_\ell^{EE,\mathrm{o}} \approx \cos^2(2\alpha + 2\beta_{reio}) C_\ell^{EE,\mathrm{reio}}$$

$$C_\ell^{BB,\mathrm{o}} \approx \sin^2(2\alpha + 2\beta_{reio}) C_\ell^{EE,\mathrm{reio}}$$

$$C_\ell^{EB,\mathrm{o}} \approx \frac{1}{2}\sin(4\alpha + 4\beta_{reio}) C_\ell^{EE,\mathrm{reio}}$$

Best fit	
τ	0.054 ± 0.005
β_{reio} [deg]	-0.02 ± 2.68
β_{dec} [deg]	0.38 ± 0.15
α_{100} [deg]	-0.38 ± 0.16
α_{143} [deg]	0.06 ± 0.15

Outlook

CMB polarization offers a tomographic view into of ALP at z≈10 and z≈1000 through the birefringence angles measured at the largest and smallest angular scales

Promising hint of a ≈ 0.3° birefringence angle from the epoch of recombination

Preliminary results on the first-ever attempt at simultaneously measuring miscalibration angles and the birefringence angle from the epoch of reionization

- 2.7° sensitivity with EE - BB information
- Working towards extending the analysis to EB

Currently limited by data → take this work as a demonstrator of the methodology's potential

If confirmed, the observed signal …

- Could be attributed to an ultra-light axion field with masses around 10^{-31} eV $\lesssim m_\phi \lesssim 10^{-28}$ eV
- Would rule out some simple Grand Unified Theory models Agrawal+[arXiv:2206.07053]
- Would be evidence of parity-violating physics outside the weak interaction

Backup slides

Effect of birefringence on low-ℓ CMB spectra

$$C_\ell^{EE,\mathrm{o}} \approx \cos^2(2\alpha + 2\beta_{reio}) C_\ell^{EE,\mathrm{reio}} + \cos^2(2\alpha + 2\beta_{dec}) C_\ell^{EE,\mathrm{dec}}$$

$$C_\ell^{EB,\mathrm{o}} \approx \frac{1}{2}\sin(4\alpha + 4\beta_{reio}) C_\ell^{EE,\mathrm{reio}} + \frac{1}{2}\sin(4\alpha + 4\beta_{dec}) C_\ell^{EE,\mathrm{dec}}$$

$$C_\ell^{BB,\mathrm{o}} \approx \sin^2(2\alpha + 2\beta_{reio}) C_\ell^{EE,\mathrm{reio}} + \sin^2(2\alpha + 2\beta_{dec}) C_\ell^{EE,\mathrm{dec}} + C_\ell^{BB,\mathrm{cmb}}$$

Planck Collab [arXiv:1807.06208]

Delouis+[arXiv:1901.11386]

Commander as our sky model

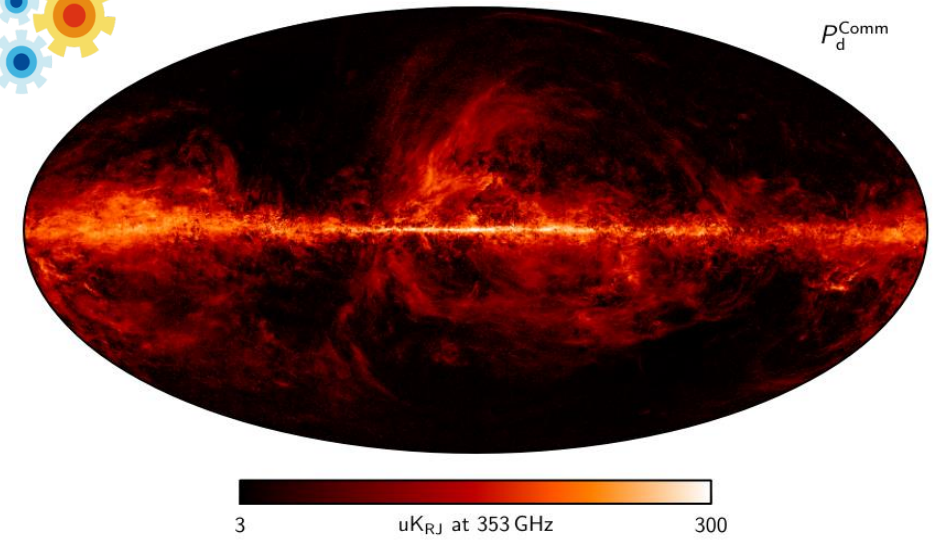

$$\frac{1}{f(\nu)}\left(\frac{\nu}{\nu_d}\right)^{\beta_d-2}\frac{B(\nu,T_d)}{B(\nu_d,T_d)}\begin{pmatrix}q^{\mathrm{dust}}\\ u^{\mathrm{dust}}\end{pmatrix}_p$$

Planck SRoll 2.0 data
100, 143, 217, 353 GHz half-mission splits

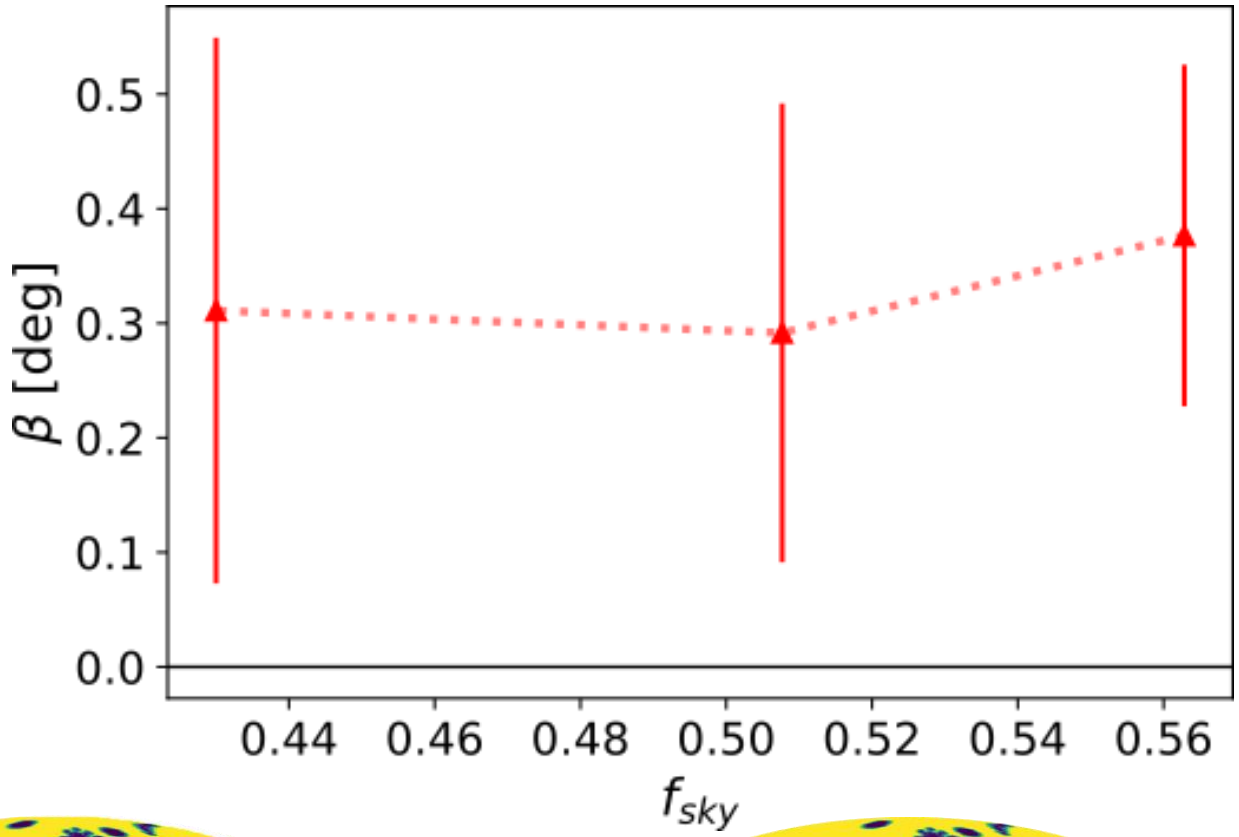

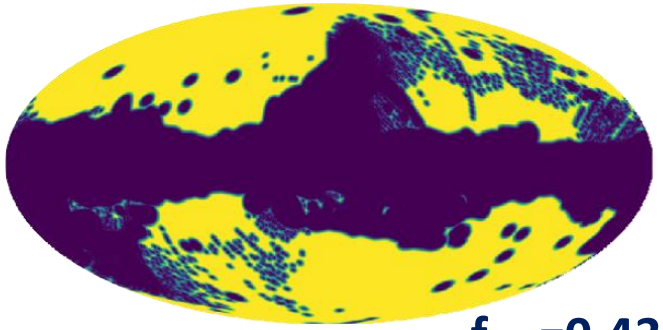

f_{sky}=0.43

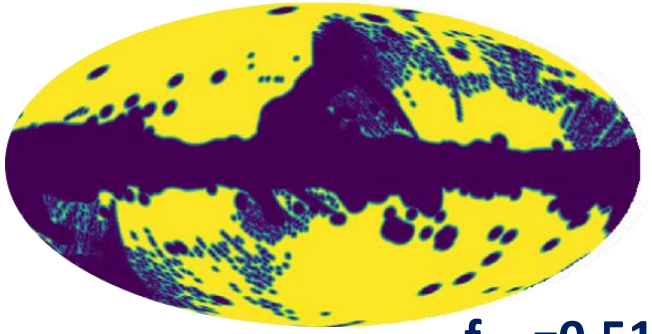

f_{sky}=0.51

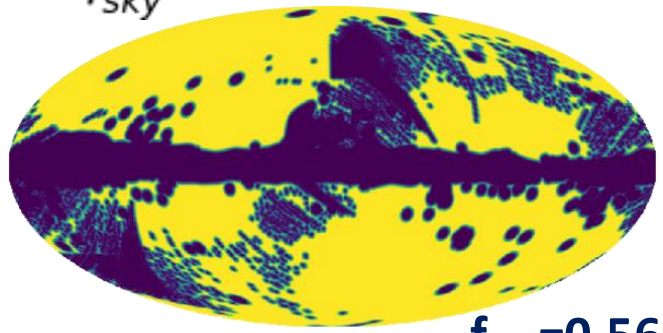

f_{sky}=0.56

High-ℓ best fit [deg]	
β_{dec}	0.38 ± 0.15
α_{100}	-0.38 ± 0.16
α_{143}	0.06 ± 0.15
α_{217}	0.01 ± 0.14
α_{353}	-0.15 ± 0.13

Planck SRoll 2.0 data
100, 143, 217, 353 GHz half-mission splits
Commander as our sky model

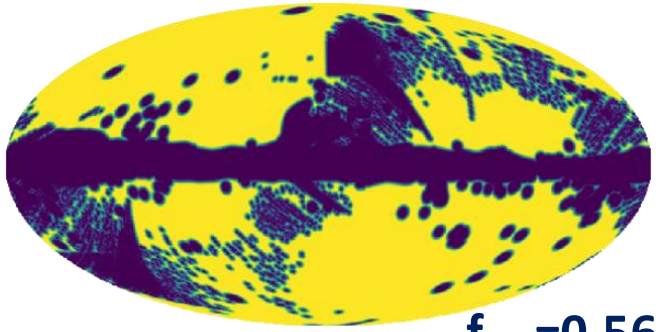

$f_{sky}=0.56$

Gaussian prior for low-ℓ analysys

$$\begin{pmatrix} \sigma_\beta^2 & \rho_{\beta\text{-}100}\sigma_\beta\sigma_{100} & \rho_{\beta\text{-}143}\sigma_\beta\sigma_{143} \\ \rho_{\beta\text{-}100}\sigma_\beta\sigma_{100} & \sigma_{100}^2 & \rho_{100\text{-}143}\sigma_{100}\sigma_{143} \\ \rho_{\beta\text{-}143}\sigma_\beta\sigma_{143} & \rho_{100\text{-}143}\sigma_{100}\sigma_{143} & \sigma_{143}^2 \end{pmatrix} = \begin{pmatrix} (0.15°)^2 & & \\ -0.9307 & (0.16°)^2 & \\ -0.9595 & 0.8939 & (0.15°)^2 \end{pmatrix}$$

EE – BB information

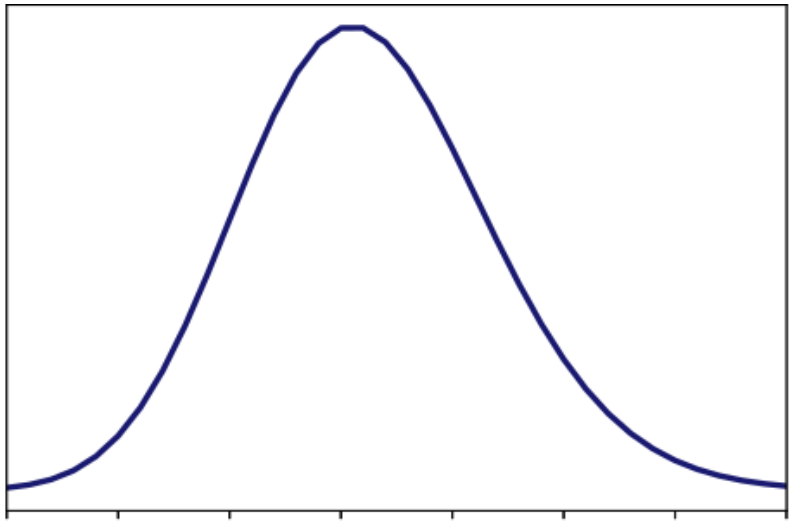

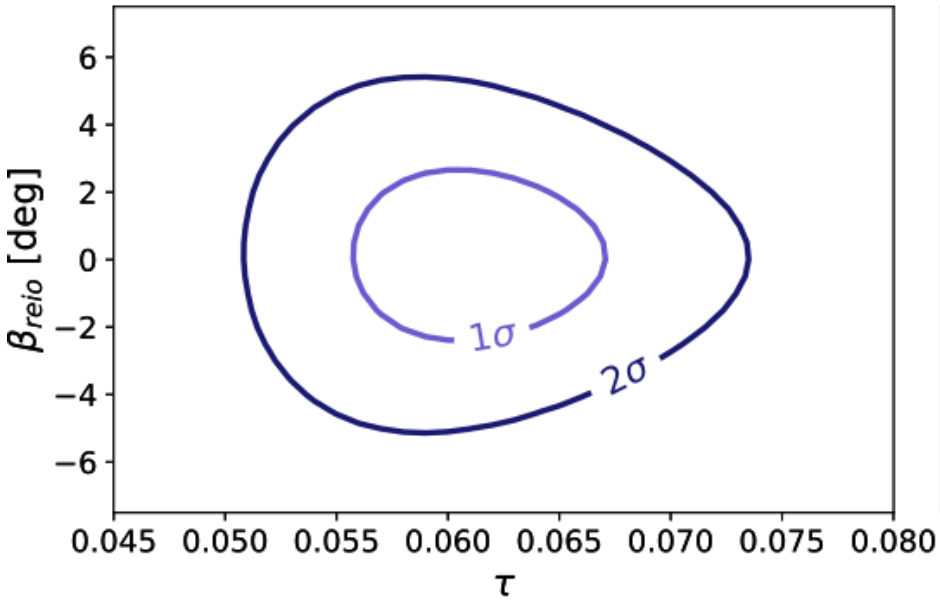

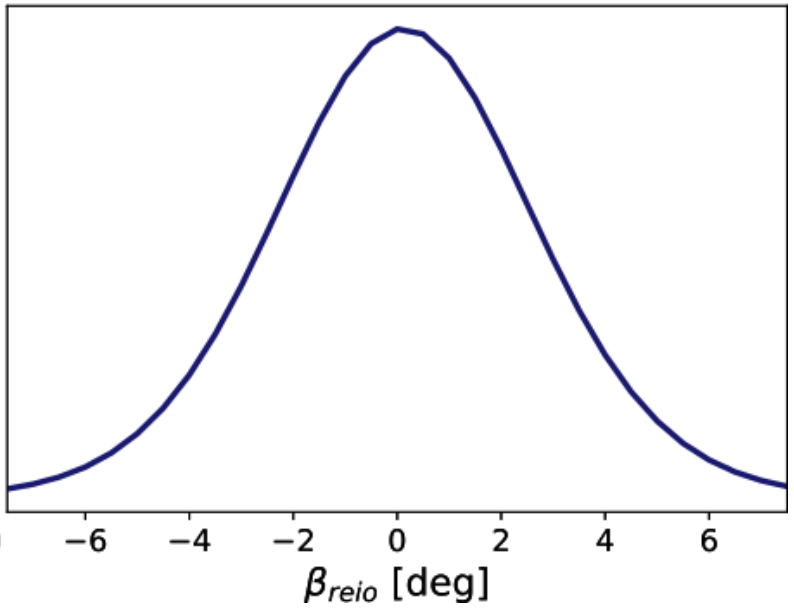

Test on CMB + realistic noise simulations

Not affected by foreground residuals
Covariance matrix perfectly describes the data

Parameter	Input	Recovered
τ	0.060	0.061 ± 0.006
β_{reio} [deg]	0.15	0.12 ± 2.56

Searching for ULA through their gravitational imprint

CMB Rogers+[arXiv:2301.08361]
kSZ Farren+[arXiv:2109.13268]
Galaxy clustering Laguë+[arXiv:2104.07802]
Galaxy weak lensing Dentler+[arXiv:2111.01199]
Lyman-alpha forest Rogers&Peiris[arXiv:2007.12705]
Dwarf galaxies Dalal&Kravtsov[arXiv:2203.05750]
21cm observations Flitter&Kovetz[arXiv:2207.05083]

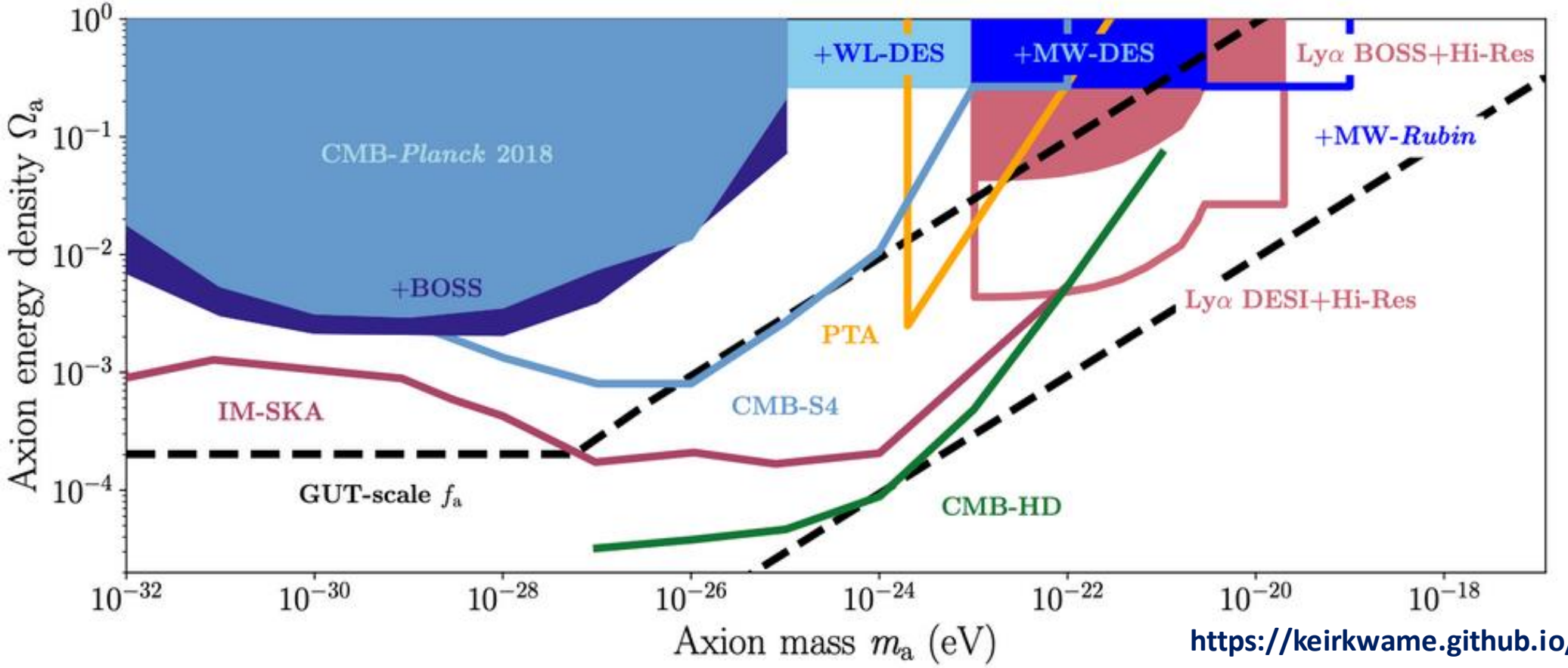

https://keirkwame.github.io/DM_limits

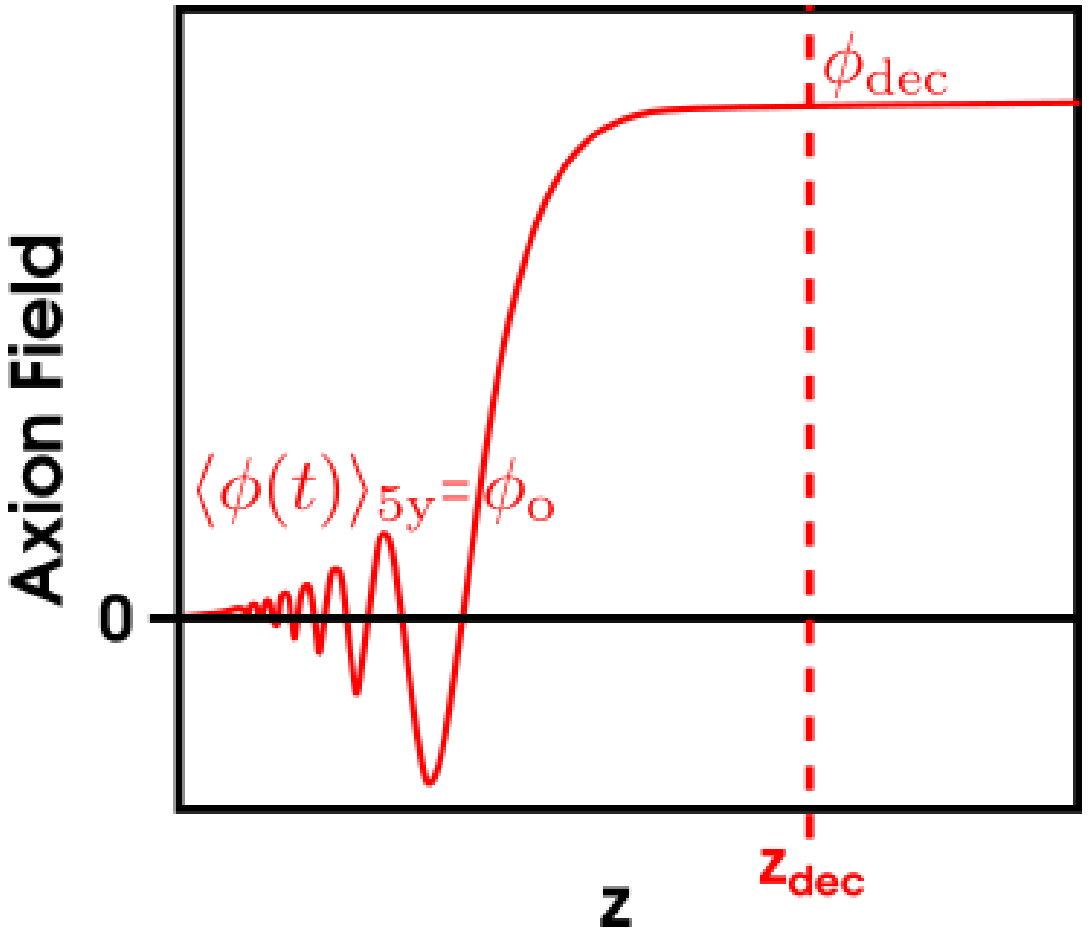

Suppose that ALP field is homogeneous and varies with time

$m_\phi \leq H_{\rm dec}$ **For ALP to start oscillating after decoupling**

$m_\phi \geq H_{\rm o}$ **For ALP to start oscillating before today**

$$10^{-33}\text{eV} \leq m_\phi \leq 10^{-28}\text{eV}$$

Constant birefringence angle, mainly sensitive to the ALP field value during decoupling

$$\beta = -\frac{1}{2}g_{\phi\gamma}\int \frac{\partial\phi}{\partial t}dt = -\frac{1}{2}g_{\phi\gamma}(\phi_{\rm o}-\phi_{\rm dec}) \approx \frac{1}{2}g_{\phi\gamma}\phi_{\rm dec}$$

Improved calibration strategies for upcoming data

Artificial calibrators:

- Rotating polarised source
  BICEP3 recently achieved ≈ 0.03° precision Cornelison+[arXiv:2207.14796]
  Exciting results coming soon!

- Drone/satellite carrying a polarised source
  Expected to reach ≈ 0.01° Nati+[arXiv:1704.02704], Casas-Reinares+[DOI:10.3390/s21103361]

Astrophysical calibrators:

- Crab Nebula
  Measured to 0.33° precision Ritacco+[arXiv:1804.09581], Aumont+[arXiv:1805.10475]

- Galactic thermal dust emission Minami+[arXiv:1904.12440], Minami&Komatsu[arXiv:2011.11254]

Using dust as a calibrator, birefringence measurements are…

… robust against the miscalibration of polarisation angles and other systematics

… sensitive to dust EB

PDP+[arXiv:2201.07682]
PDP+[arXiv:2210.07655]

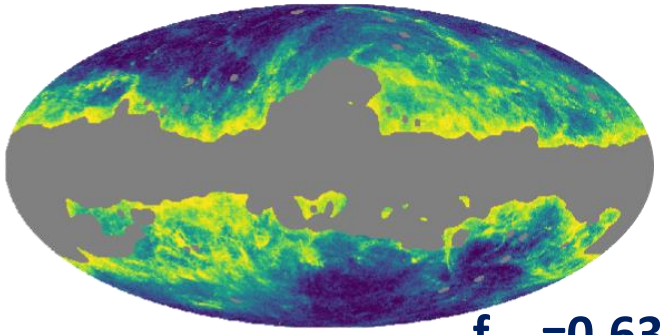

f_{sky}=0.63

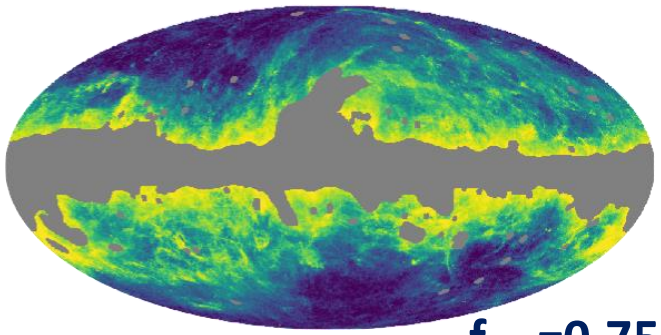

f_{sky}=0.75

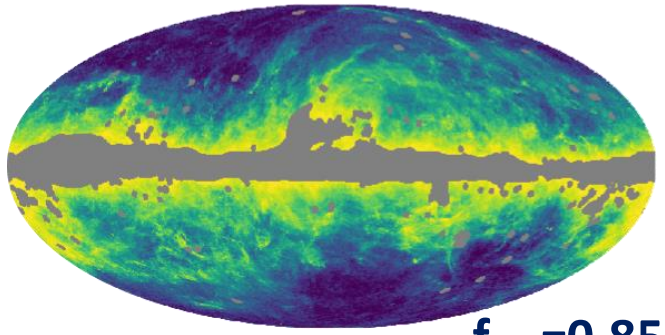

f_{sky}=0.85

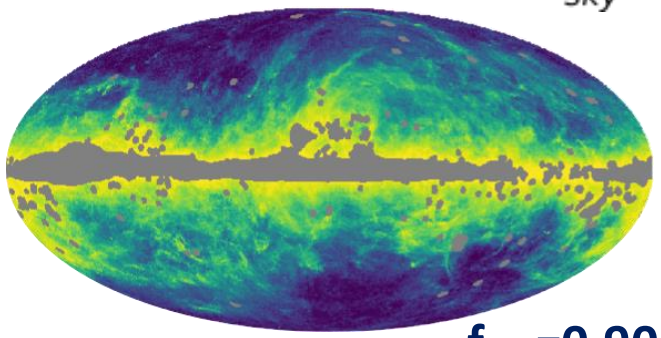

f_{sky}=0.90

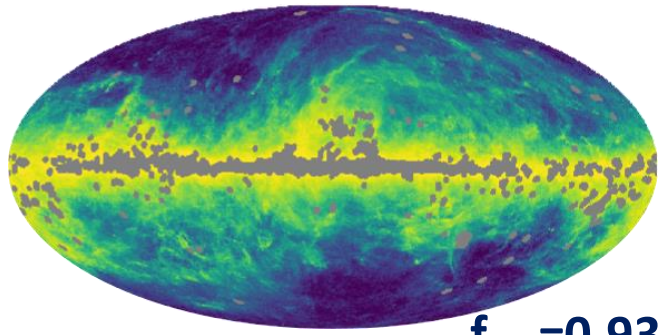

f_{sky}=0.93

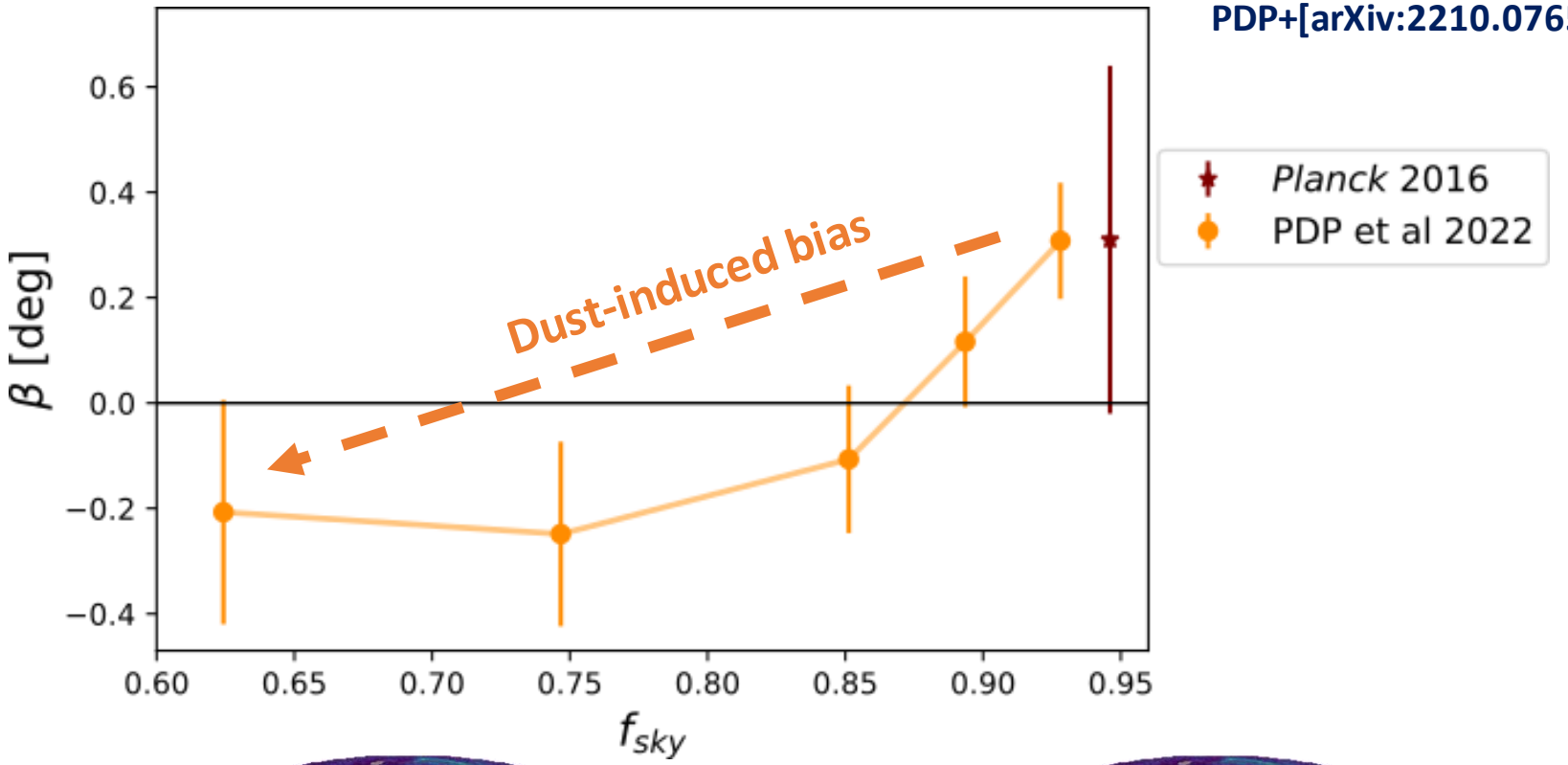

Constraining power of CMB observations alone was the β ≈ 0.3° measurement confirmed

Fujita+[arXiv:2008.02473]

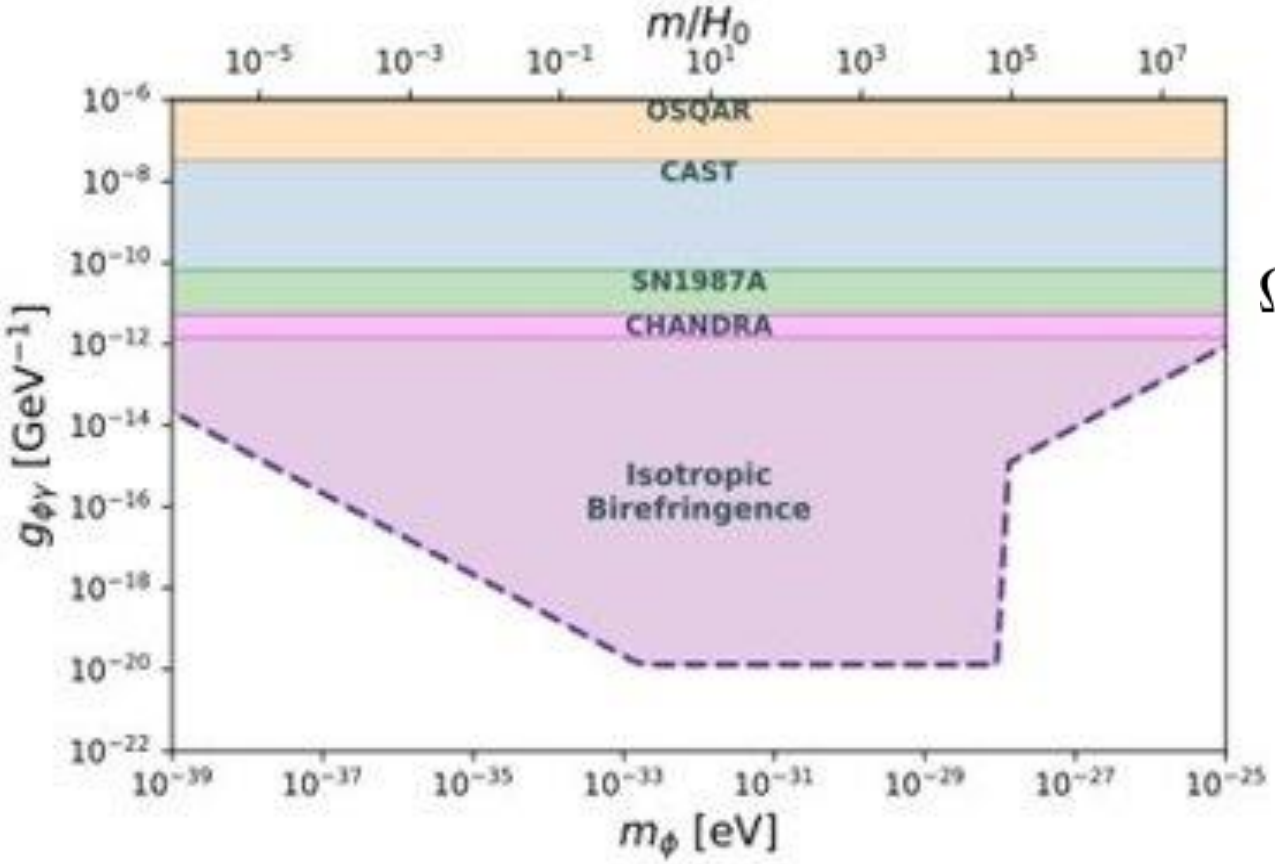

Assuming the largest ALP abundance allowed

$$\Omega_\phi \begin{cases} \Omega_\Lambda = 0.69 & m_\phi \leq 9.26 \times 10^{-34}\mathrm{eV} \\ 0.006h^{-2} & 10^{-32}\mathrm{eV} \leq m_\phi \leq 10^{-25.5}\mathrm{eV} \end{cases}$$

Planck Collab [arXiv:1807.06209]

with ALP density only bounded from above, putting an upper constraint on the ALP-photon coupling is not possible

Nakatsuka+[arXiv:2203.08560]

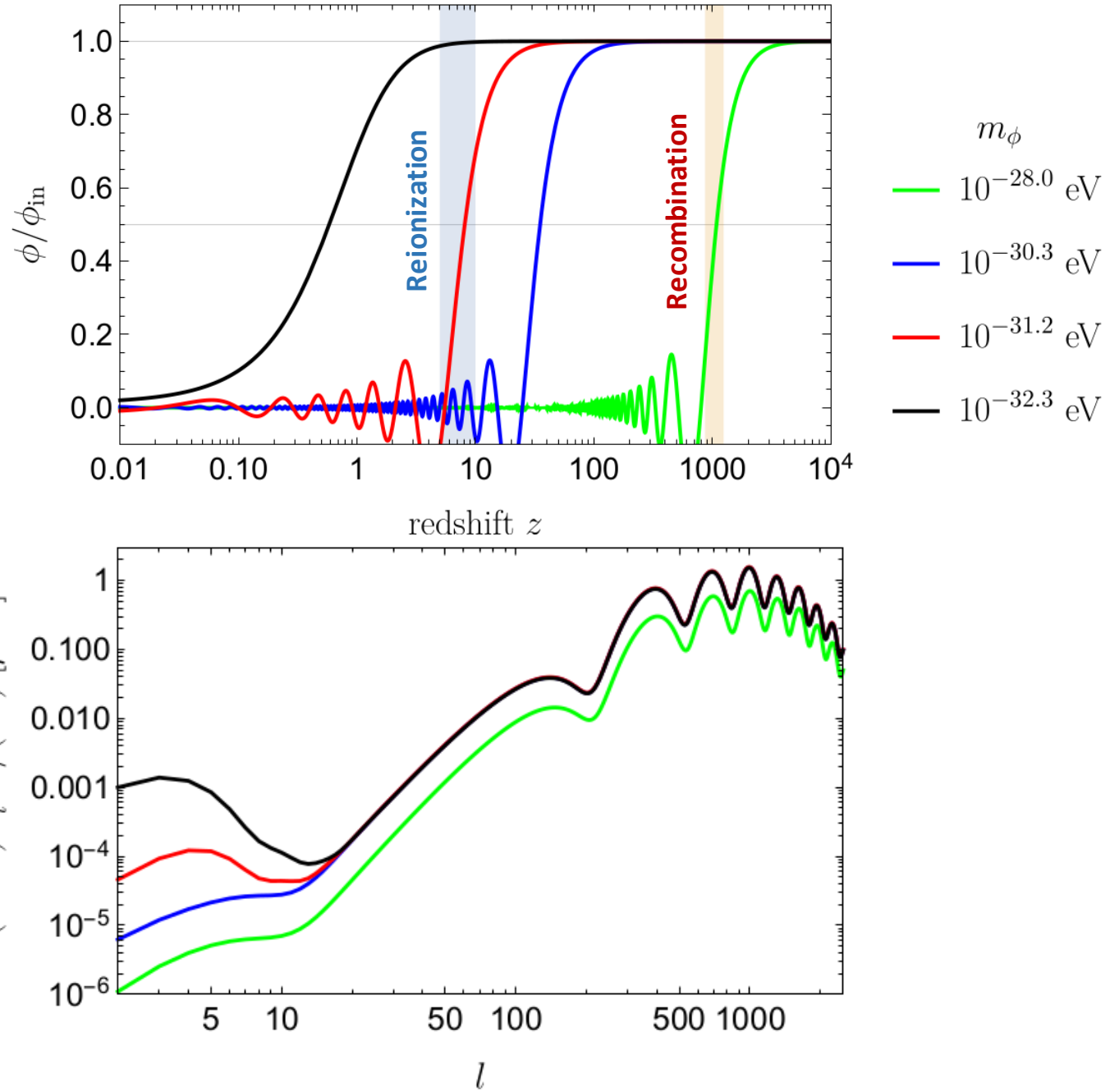

$$\beta(z) = \begin{cases} 0 & \text{for} \quad z = 0 \\ \beta_{\rm rei} & \text{for} \quad 0 < z \leq 10 \\ \beta_{\rm rec} & \text{for} \quad 10 < z \end{cases},$$

CMB photons emitted at recombination and reionization will suffer different rotations

$$C_\ell^{EB,{\rm o}} \approx \frac{1}{2}\sin(4\beta_{\rm rec})C_\ell^{E_{\rm rec}E_{\rm rec}} + \frac{1}{2}\sin(4\beta_{\rm rei})C_\ell^{E_{\rm rei}E_{\rm rei}} + \sin(2\beta_{\rm rec}+2\beta_{\rm rei})C_\ell^{E_{\rm rec}E_{\rm rei}}$$

The study of low-multipoles gives a tomographic view of the ALP field

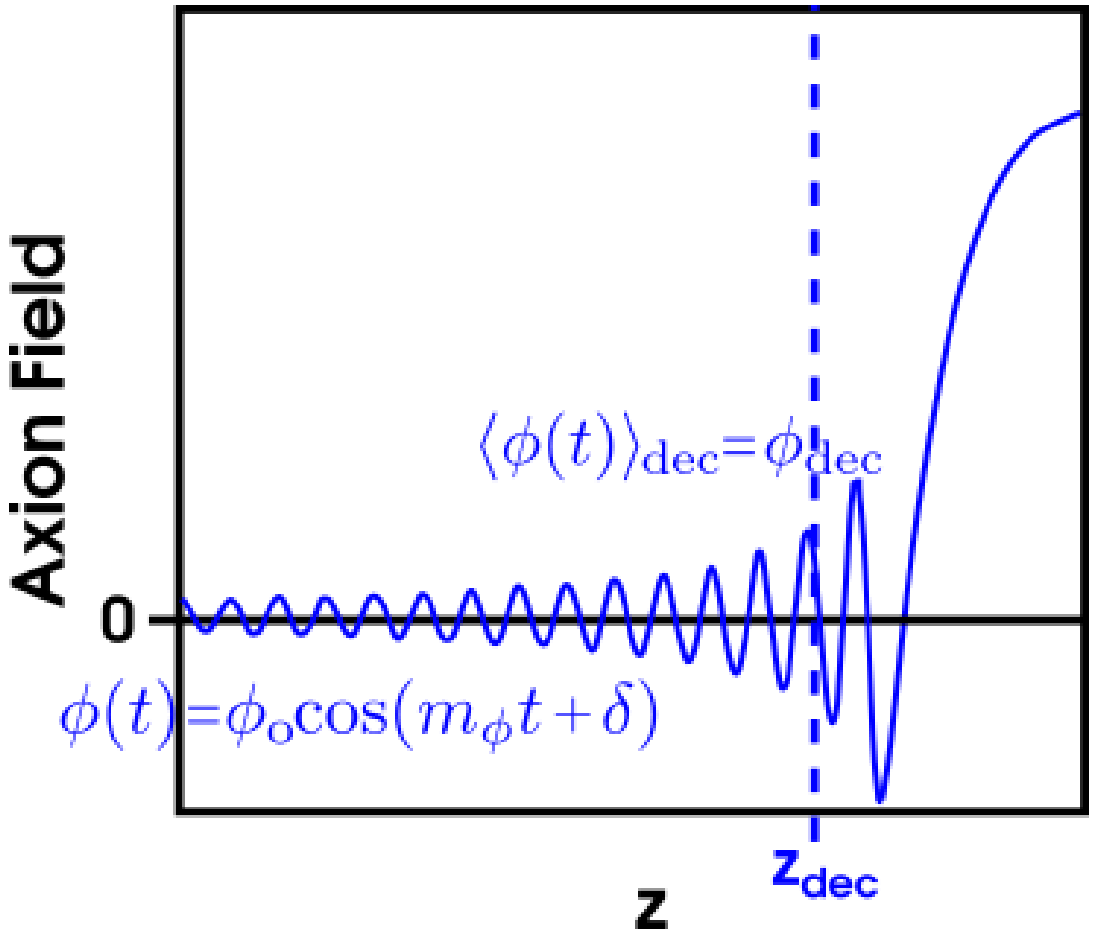

Suppose that ALP field is homogeneous and varies with time

$$m_\phi \geq H_{\rm dec}$$

For ALP to start oscillating before decoupling

$$10^{-28}{\rm eV} \leq m_\phi$$

(Q,U) rotating as if the polarisation angle oscillated with a period

$$T_\phi \sim 1{\rm y}\left(\frac{10^{-22}{\rm eV}}{m_\phi}\right)$$

***Planck*, LiteBIRD** $\sim 1{\rm y}$

BICEP/Keck, SPT $\sim 1{\rm h}$

$$10^{-24}{\rm eV} \leq m_\phi \leq 10^{-19}{\rm eV}$$

Oscillation depending on ALP field at absorption

$$(Q \pm iU)(t,\vec{n}) = J_0[g_{\phi\gamma}\phi_{\rm dec}]\exp\left[\mp 2i\left(\frac{g_{\phi\gamma}}{2}\phi_{\rm o}\cos(m_\phi t+\delta)\right)\right](Q \pm iU)_0(\vec{n})$$

Washout depending on ALP field at emission

Fedderke+[arXiv:1903.02666]

Fedderke+[arXiv:1903.02666]

Washout is a consequence of **decoupling not being an instantaneous** process

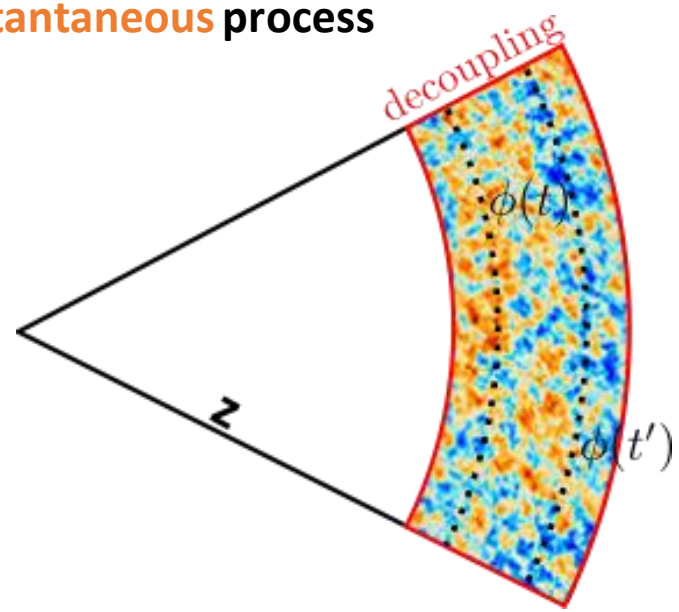

Photons emitted at different times…
… see a slightly different ALP field
… are rotated by a slightly different angle

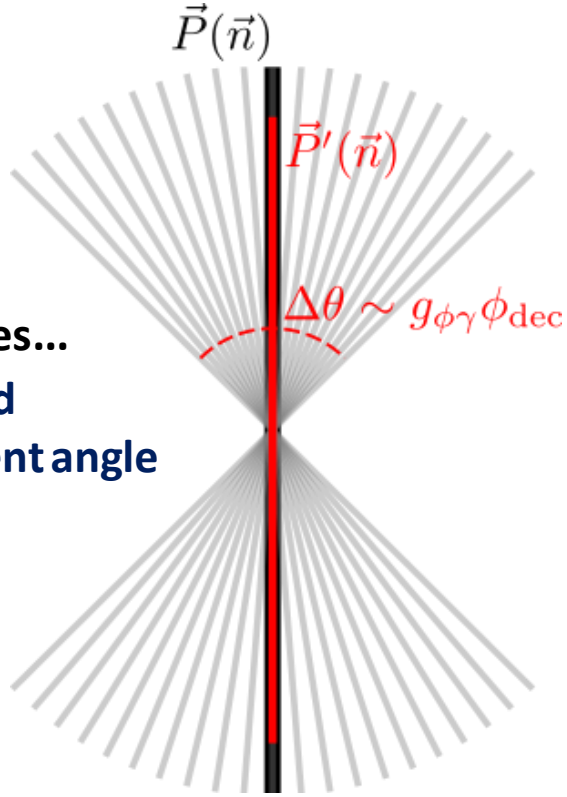

CMB detectors do an incoherent sum over the fanned-out states

Reduction of polarization intensity

$$J_0[g_{\phi\gamma}\phi_{\rm dec}] \approx 1 - \frac{1}{4}(g_{\phi\gamma}\phi_{\rm dec})^2$$

Constraints from time-dependent birefringence

Planck washout

Fedderke+[arXiv:1903.02666]

$$g_{\phi\gamma} \lesssim 9.6 \times 10^{-13}\,\mathrm{GeV}^{-1} \times \left(\frac{m_\phi}{10^{-21}\,\mathrm{eV}}\right) \times \left(\kappa \times \frac{\Omega_c^0 h^2}{0.11933}\right)^{-1/2}$$

SPT-3G data

Ferguson+[arXiv:2203.16567]

For periods 1 day ≤ T_φ ≤ 100 days …
… probing 10^{-22}eV ≤ m_φ ≤ 10^{-19}eV
… upper limit (β+α)(t) ≤ 0.071°

Assuming DM made of one ALP species with local density of 0.3 GeV/cm^3

$$g_{\phi\gamma} < 1.18 \times 10^{-12}\ \mathrm{GeV}^{-1} \times \left(\frac{m_\phi}{1.0 \times 10^{-21}\ \mathrm{eV}}\right)$$

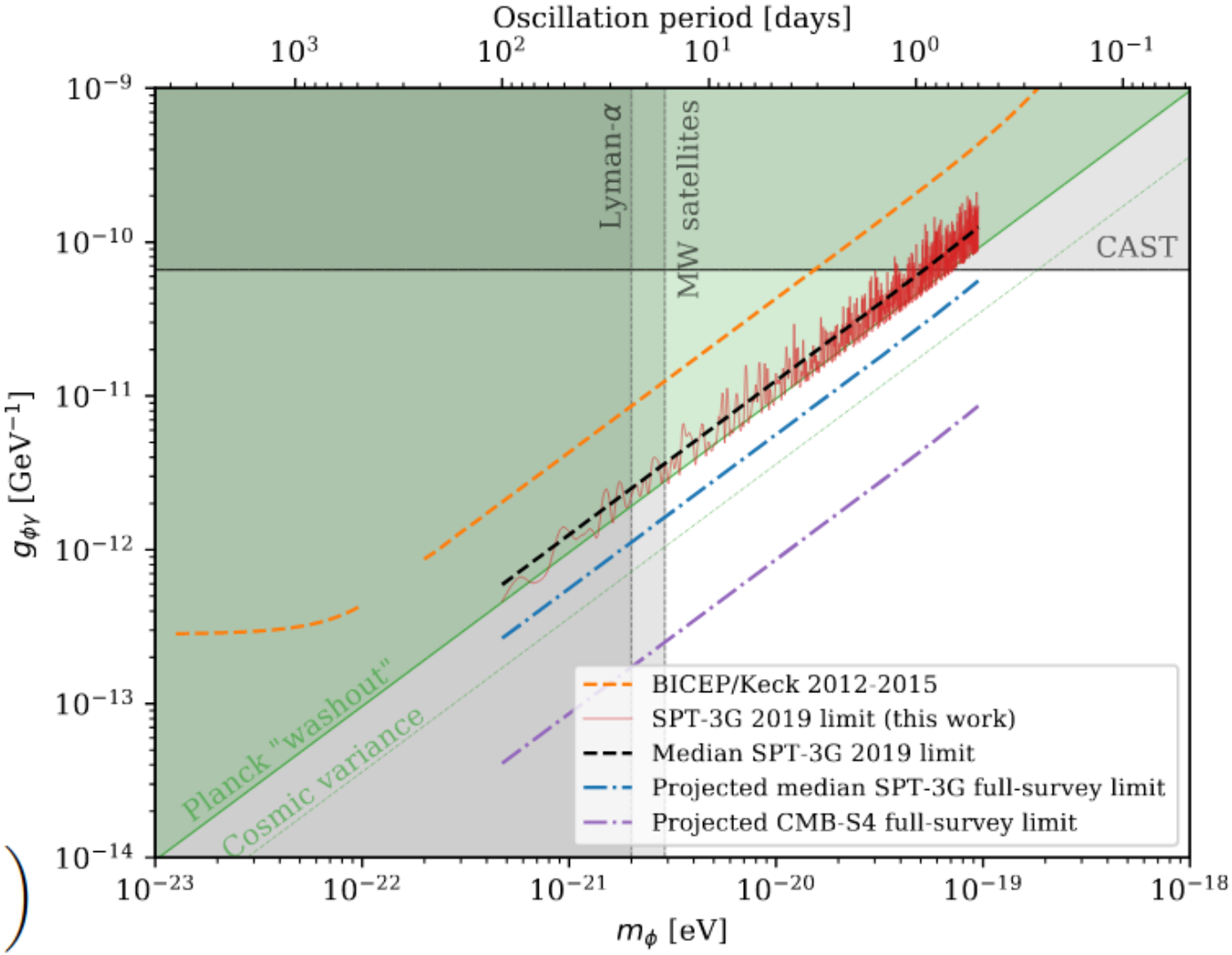

Based on...

Minami et al 2019, PTEP, 083E02	The original presentation of the methodology
Minami 2020, PTEP, 063E01	Extension to partial-sky observations
Minami & Komatsu 2020, PTEP, 103E02	Extension to frequency cross-spectra
Minami & Komatsu 2020, PRL, 125, 221301	Application to *Planck* HFI PR3 Without foreground modeling
PDP et al 2022, PRL, 128, 091302	Application to *Planck* HFI PR4 With foreground modeling
Eskilt 2022, A&A, 662, A10	Application to *Planck* LFI & HFI PR4 Study of the frequency dependence of birefringence
Eskilt & Komatsu 2022, PRD, 106, 063503	Joint analysis of *Planck* LFI & HFI PR4 and WMAP 9-year
PDP et al 2022 [arXiv:2210.07655] Accepted at JCAP	Alternative semi-analytical implementation Simulation study and assessment of the impact of systematics

Polarization primer

Cabella & Kamionkowski 2003 [arXiv:astro-ph/0403392]

Linearly polarized light propagating along the z direction

$$E_x = a_x \cos(\omega t - \delta_x) \; E_y = a_y \cos(\omega t - \delta_y)$$

can be described through the Stoke's parameters

$$I = a_x^2 + a_y^2$$
$$Q = a_x^2 - a_y^2$$
$$U = 2a_x a_y \cos(\delta_x - \delta_y)$$

Relative to the chosen coordinate system

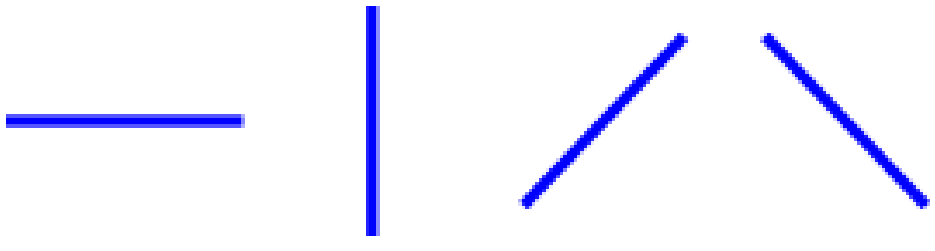

Q > 0 U = 0 | Q < 0 U = 0 | Q = 0 U > 0 | Q = 0 U < 0

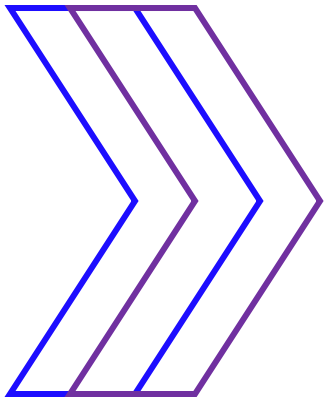

Helmholtz's theorem

Express vector fields as the sum of curl-free and divergence-free fields

Q and U define a spin-2 field

$$P_{ab} = \frac{1}{2}\begin{pmatrix} Q(\vec{r}) & U(\vec{r}) \\ U(\vec{r}) & -Q(\vec{r}) \end{pmatrix}$$

Express the polarization field in terms of its gradient and curl components

$$\nabla^2 E = \partial_a \partial_b P_{ab} \quad \nabla^2 B = \epsilon_{ac} \partial_b \partial_c P_{ab}$$

Locally independent

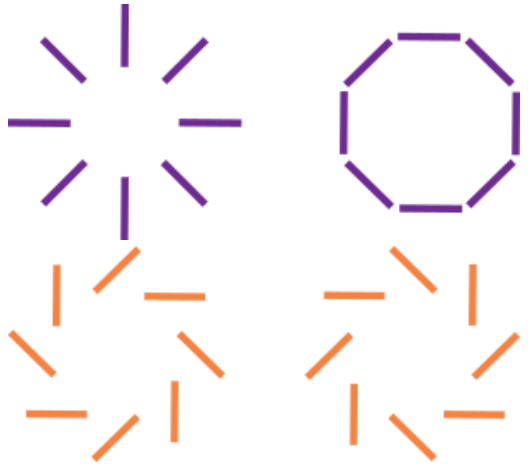

E-modes

B-modes

Decompose CMB maps into spherical harmonics

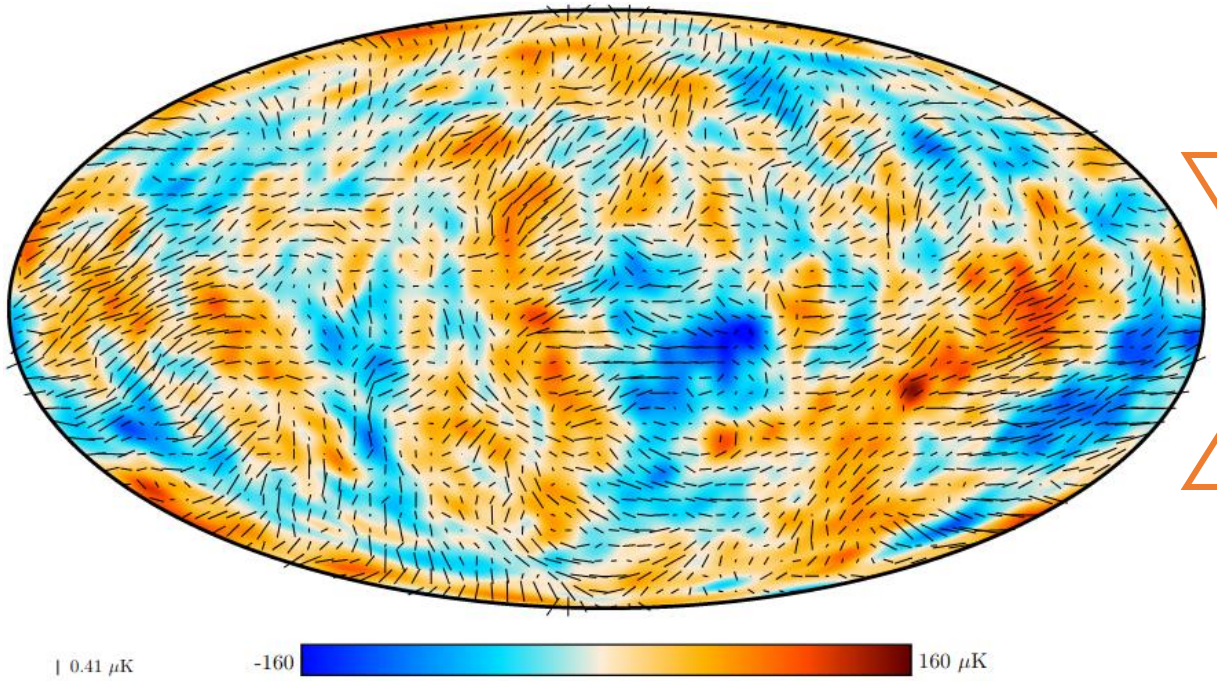

Planck Collaboration I. 2020, A&A, 641, A1

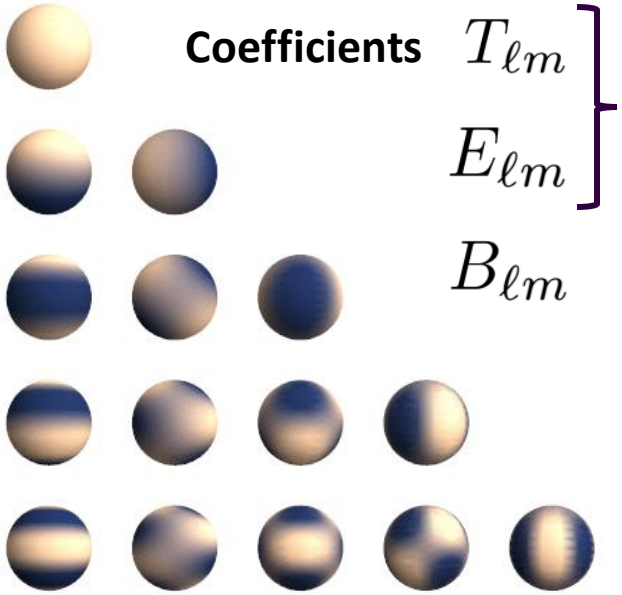

Coefficients $T_{\ell m}$, $E_{\ell m}$ — Parity-even

$B_{\ell m}$ — Parity-odd

Zaldarriaga & Seljak 1997, PRD, 55, 1830
Kamionkowski et al 1997, PRD, 55, 7368

Analyzing CMB polarization in terms of spherical harmonics

$$\langle E_{\ell m} E^*_{\ell' m'} \rangle = \delta_{mm'} \delta_{\ell \ell'} C_\ell^{EE}$$
$$\langle B_{\ell m} B^*_{\ell' m'} \rangle = \delta_{mm'} \delta_{\ell \ell'} C_\ell^{BB}$$

Parity-even

$$\langle E_{\ell m} B^*_{\ell' m'} \rangle = \delta_{mm'} \delta_{\ell \ell'} C_\ell^{EB}$$

Parity-odd

ΛCDM

The Universe has no preferred direction so the statistics of CMB anisotropies must be invariant under parity transformation

EB≠0 evidence of parity-violating physics

Lue et al 1999, PRL, 83, 1506

Past measurements

early WMAP & BOOMERANG	$\alpha+\beta = -6.0° \pm 4.0°$ (stat) $\pm$?? (sys)	Feng et al 2006, PRL, 96, 221302
QUaD	$\alpha+\beta = 0.55° \pm 0.82°$ (stat) $\pm 0.5°$ (sys)	Wu et al 2009, PRL, 102, 161302
WMAP 9-year	$\alpha+\beta = -0.36° \pm 1.24°$ (stat) $\pm 1.5°$ (sys)	Hinshaw et al 2013, ApJS, 208, 19
Planck 2015	$\alpha+\beta = 0.31° \pm 0.05°$ (stat) $\pm 0.28°$ (sys)	*Planck* Collaboration XLIX. 2016, A&A, 596, A110
POLARBEAR 2020	$\alpha+\beta = -0.61° \pm 0.22°$ (stat) $\pm$?? (sys)	Polarbear Collaboration 2020, ApJ, 897, 55
ACT 2020	$\alpha+\beta = -0.07° \pm 0.09°$ (stat) $\pm$?? (sys)	Choi et al 2020, JCAP, 12, 045
SPT 2020	$\alpha+\beta = 0.63° \pm 0.04°$ (stat) $\pm$?? (sys)	Bianchini et al 2020, PRD, 102, 083504

Systematic uncertainties dominate the analysis

Current calibration strategies set a ≈0.5°-1° limit

DM/DE could be a parity-violating pseudoscalar field $\phi(-\vec{n}) = -\phi(\vec{n})$

Carroll at al 1990, PRD, 41, 1231
Carroll & Field 1991, PRD, 43, 3789
Harari & Sikivie 1992, PLB, 289, 67

Chern-Simons coupling to EM $\frac{1}{4} g_{\phi\gamma} \phi F_{\mu\nu} \tilde{F}_{\mu\nu}$

Axion-like particles

Marsh 2016, Phys Rep, 643, 1

Early Dark Energy

Murai et al 2022 [arXiv:2209.07804]

rotation of the plane of linear polarization clockwise on the sky

$$\beta = -\frac{1}{2} g_{\phi\gamma} \int \frac{\partial \phi}{\partial t} dt$$

Cosmic birefringence

Faraday rotation from primordial magnetic fields

Subramanian 2016, Rep Prog Phys, 79, 076901

Superluminal Lorentz-violating electrodynamics emerging from a non-vanishing Weyl tensor

Shore 2005, Nucl Phys B, 717, 86118

Quantum gravity models that modify the dispersion relation of photons

Gleiser & Kozameh 2001, PRD, 64, 8, 083007

$\beta(\nu)$

disfavored by data

Eskilt 2022, A&A, 662, A10

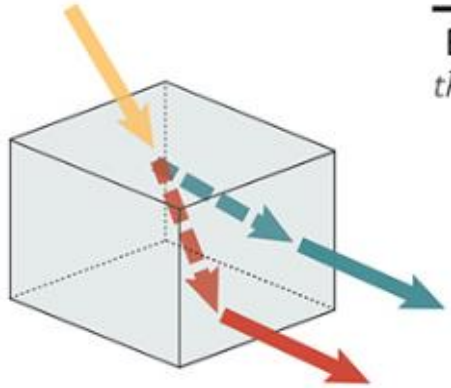

BIREFRINGENCE *Birefringence describes the optical property where a ray of light is split by polarization into two rays taking slightly different paths.*

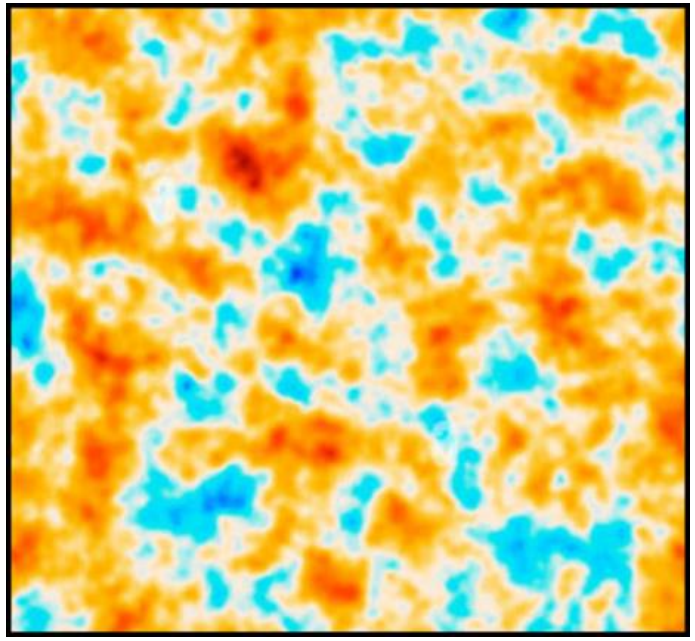

Improve instrument calibration

- Provides tighter constraints and does not directly depend on foregrounds (subject to the foreground residuals)
- Optimal strategy for ground-based experiments as new calibration sources allow a precise measurement of polarization angles

BICEP3: rotating polarized source
systematic error of <0.1° with a ≈0.03° statistical uncertainty on the calibration of polarization angles

Cornelison & Vergès Proc SPIE Int Soc Opt Eng 12190 (2022) 829

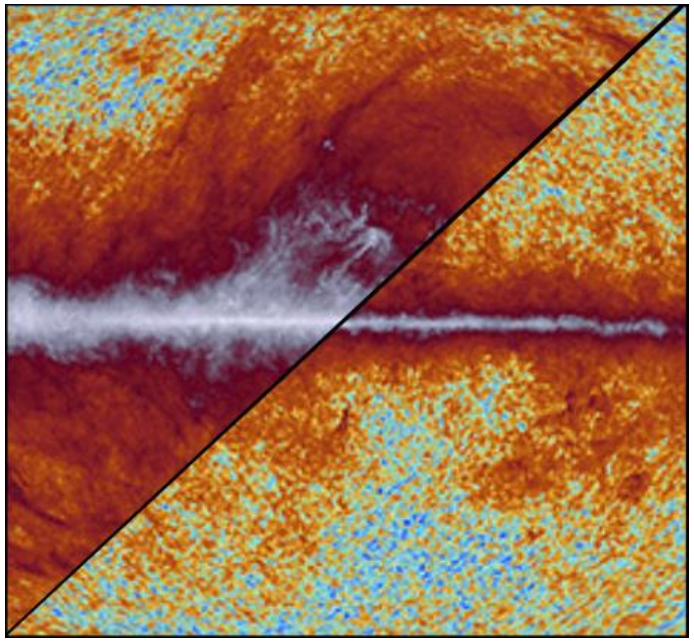

Use Galactic foregrounds as calibrator

- (Currently) optimal strategy for satellite missions where calibration is limited by prior knowledge of astrophysical sources
- Proven to be robust against instrumental systematics but sensitive to dust EB

PDP et al 2022 [arXiv:2210.07655]
PDP et al 2022, PRL, 128, 091302

Tightest constraint to date coming from
Planck PR4 + WMAP-9y $\beta = 0.342° \pm 0.093°$

Eskilt & Komatsu 2022, PRD, 106, 063503

Minami et al 2019, PTEP, 083E02
Minami 2020, PTEP, 063E01
Minami & Komatsu 2020, PTEP, 103E02

Observed signal is a rotation of the CMB and Galactic foreground emissions

$$\begin{pmatrix} E^{\rm o}_{\ell m} \\ B^{\rm o}_{\ell m} \end{pmatrix} = \begin{pmatrix} \cos(2\alpha) & -\sin(2\alpha) \\ \sin(2\alpha) & \cos(2\alpha) \end{pmatrix} \begin{pmatrix} E^{\rm fg}_{\ell m} \\ B^{\rm fg}_{\ell m} \end{pmatrix} + \begin{pmatrix} \cos(2\alpha+2\beta) & -\sin(2\alpha+2\beta) \\ \sin(2\alpha+2\beta) & \cos(2\alpha+2\beta) \end{pmatrix} \begin{pmatrix} E^{\rm cmb}_{\ell m} \\ B^{\rm cmb}_{\ell m} \end{pmatrix}$$

so the observed EB is

$$C_\ell^{EB,{\rm o}} = \frac{\tan(4\alpha)}{2}\left(C_\ell^{EE,{\rm o}} - C_\ell^{BB,{\rm o}}\right) + \frac{1}{\cos(4\alpha)} C_\ell^{EB,{\rm fg}} + \frac{\sin(4\beta)}{2\cos(4\alpha)}\left(C_\ell^{EE,{\rm cmb}} - C_\ell^{BB,{\rm cmb}}\right)$$

Planck Collaboration XI. 2020, A&A, 641, A11
Martire et al 2022, JCAP, 04, 003

Build a Gaussian likelihood to simultaneously determine both angles

$$-2\ln\mathcal{L} = \sum_{b=1}^{N_{\rm bins}} \left(\mathbf{A}\bar{C}_b^{\rm o} - \mathbf{B}\bar{C}_b^{\rm cmb}\right)^T \mathbf{M}_b^{-1} \left(\mathbf{A}\bar{C}_b^{\rm o} - \mathbf{B}\bar{C}_b^{\rm cmb}\right) + \sum_{b=1}^{N_{\rm bins}} \ln|\mathbf{M}_b|$$

Only two ingredients needed:

Cross-correlation of frequency bands of any CMB experiment

$$\bar{C}_b^{\rm o} = \left(C_b^{E_iE_j,{\rm o}}\ C_b^{B_iB_j,{\rm o}}\ C_b^{E_iB_j,{\rm o}}\right)^T$$

Theoretical prediction for CMB angular power spectra

Planck PR4 (NPIPE reprocessing)

Planck Collaboration 2020, A&A, 643, A42

The NPIPE pipeline processes raw, uncalibrated detector data from both LFI and HFI into polarized frequency and detector-set maps. NPIPE fits and corrects for gain fluctuations, ADCNL, bolometric transfer-function residuals and bandpass mismatch by fitting time-domain templates while solving for the polarized map.

NPIPE achieves a smaller noise by:

(1) including data acquired during repointing maneuvers between scans

(2) better modeling the data via a short baseline offset model for noise, suppressing degree-scale noise residuals

(3) multi-frequency polarization model used in calibration greatly reduces large-scale polarization uncertainty but introduces a pipeline transfer-function that suppresses CMB polarization power at $\ell < 20$

(4) second-order analog-to-digital conversion nonlinearity (ADCNL) model

The net effect on polarization is a scale-dependent reduction in the total uncertainty:

(1) $\sim$ 50 % lower N_ℓ at $\ell \sim 10$

(2) 20–30 % lower N_ℓ at $\ell \sim 100$

(3) 10–20 % lower N_ℓ at $\ell \sim 1000$ (also in temperature)

Planck PR4 (NPIPE reprocessing)

Reprocessing of raw LFI and HFI *Planck* data

Scale-dependent reduction of total uncertainty due to

- Addition of data acquired during repointing maneuvers
- Improved modeling of instrumental noise and systematics

Planck Collaboration 2020, A&A, 643, A42

- NPIPE 100, 143, 217, 353 GHz data
- Focus on small-scale information (ℓ>50) to target the birefringence angle from recombination
- Cross-correlating A/B detector splits → β, α_i (i=1,…,8)
- Start by considering a null foreground EB

PDP et al 2022, PRL, 128, 091302

Consistent results across 4 independent pipelines

Pipeline	Implementation	Pseudo-C_ℓ
JRE	Posterior distribution via MCMC	PolSpice
MT		Xpol
YM		NaMaster
PDP	Analytical minimization	

PDP et al 2022 [arXiv:2210.07655]

Minami & Komatsu 2020, PRL, 125, 221301

Planck 2018 (PR3)

100, 143, 217, 353 GHz data

Half-mission splits → β, α_i (i=1,…,4)

High-ℓ data → bin C_ℓ/M_ℓ from ℓ_{min}=51 to ℓ_{max}=1490 with $\Delta\ell$ = 20 spacing

Specific mask for each band

Neglecting foreground EB

$\beta = 0.35^\circ \pm 0.14^\circ$ (2.4σ)
for nearly full-sky

PDP et al 2022, PRL, 128, 091302

Planck 2020 (PR4 or NPIPE)

100, 143, 217, 353 GHz data

A/B detector splits→ β, α_i (i=1,…,8)

High-ℓ data → bin C_ℓ/M_ℓ from ℓ_{min}=51 to ℓ_{max}=1490 with $\Delta\ell$ = 20 spacing

Common mask for all bands

Correcting for foreground EB

$\beta = 0.30^\circ \pm 0.11^\circ$ (2.7σ)
for nearly full-sky

For nearly full-sky: β = 0.30° ± 0.11° (2.7σ) → Consistent with and more precise than previous measurements!

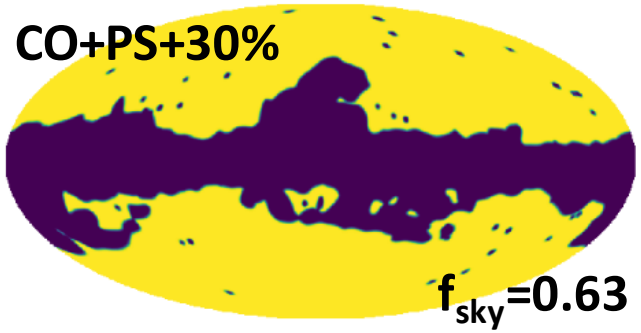

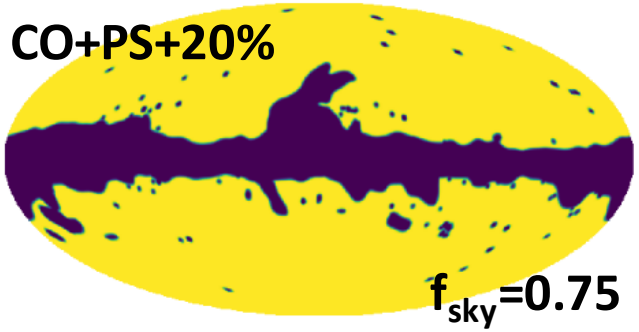

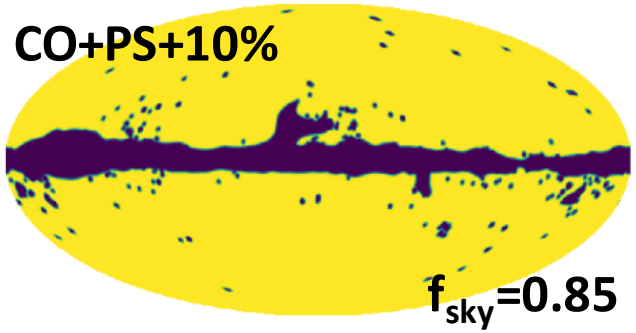

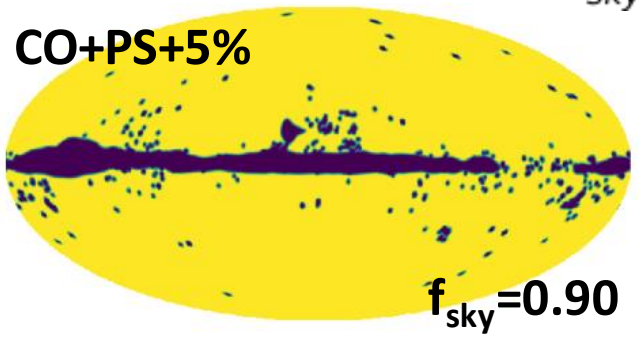

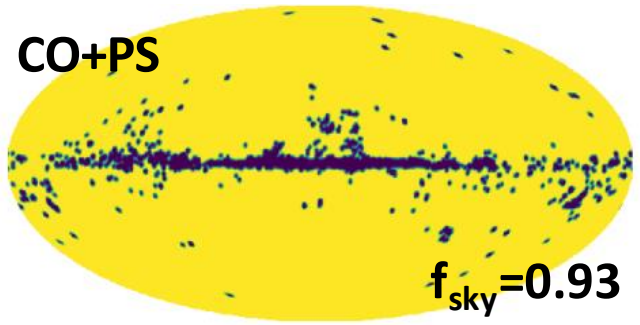

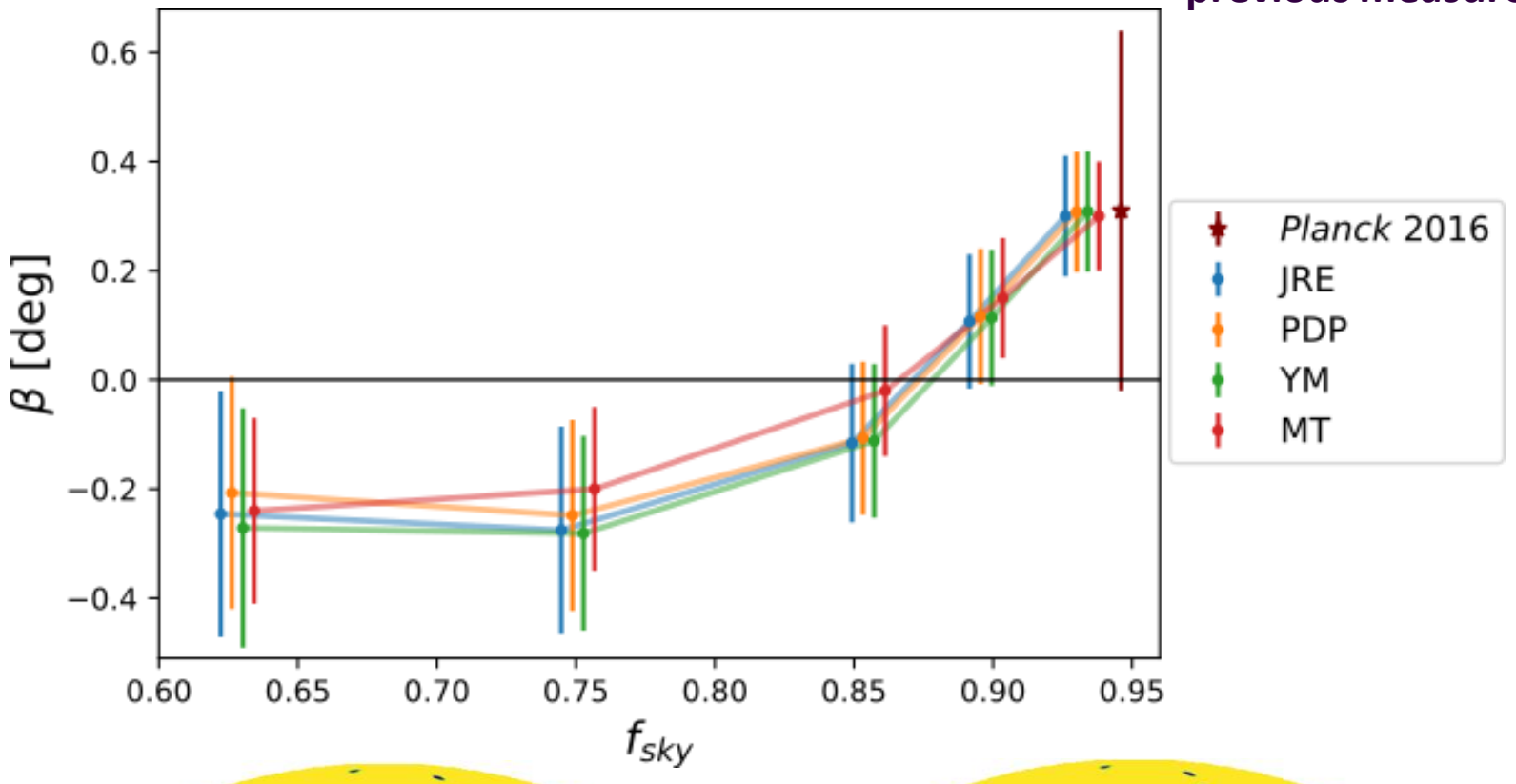

… but our inferred value of α depends on Galactic dust

Dust EB biases our estimation of miscalibration angles, dragging with them the measurement of β

Misalignment of dust filaments and Galactic magnetic fields produces TB and EB

Clark et al 2021, ApJ, 919, 53

- Dust TB > 0 detected by *Planck*

  Planck Collaboration XI. 2020, A&A, 641, A11

- Expected dust EB > 0

Indirect detection of dust EB

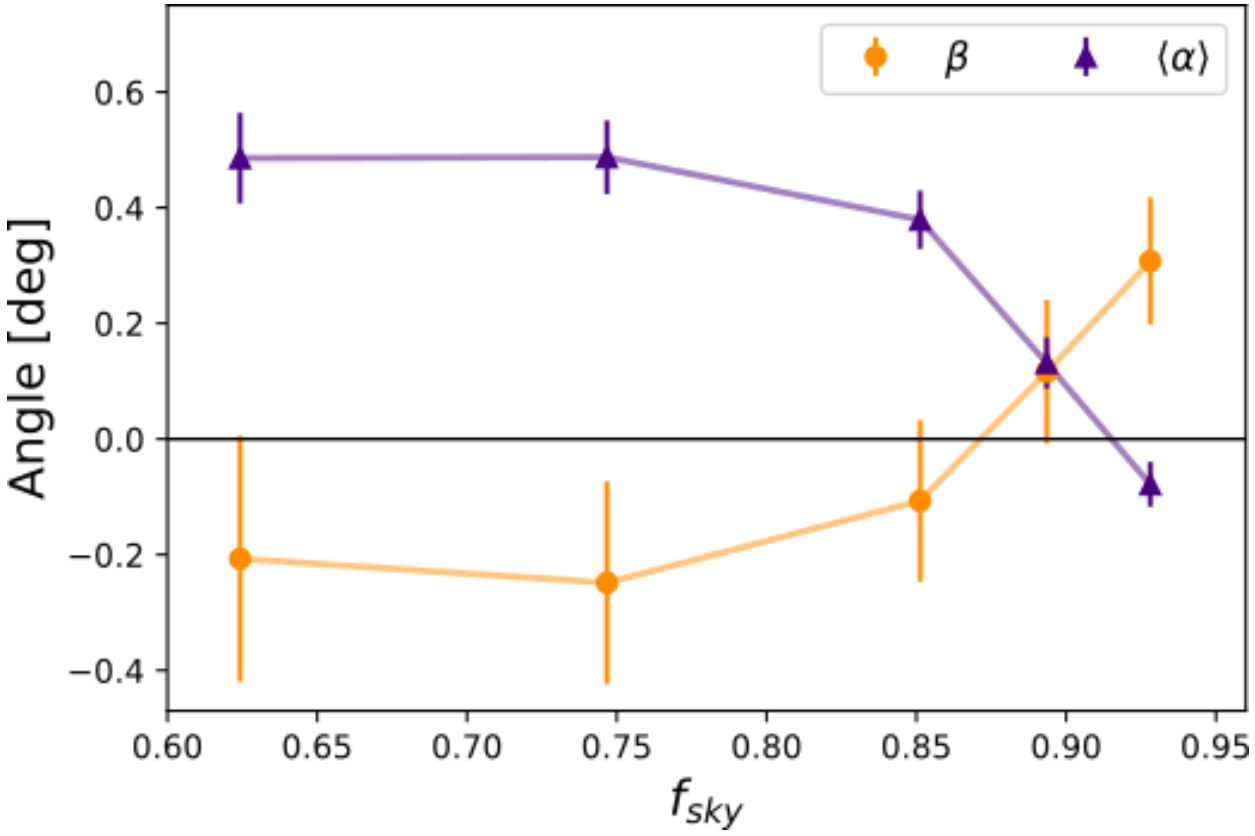

The EB signal created by birefringence exists regardless of the Galactic mask ...

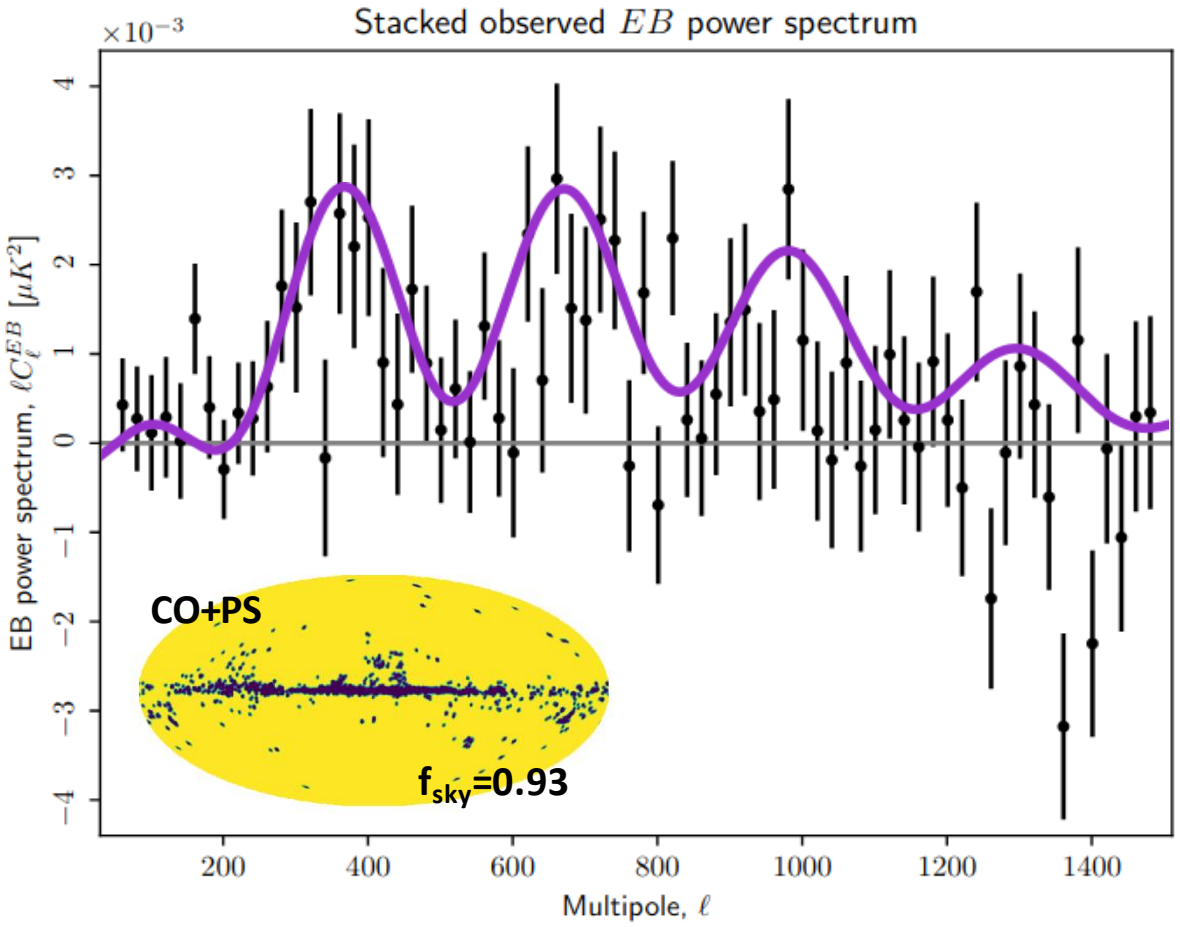

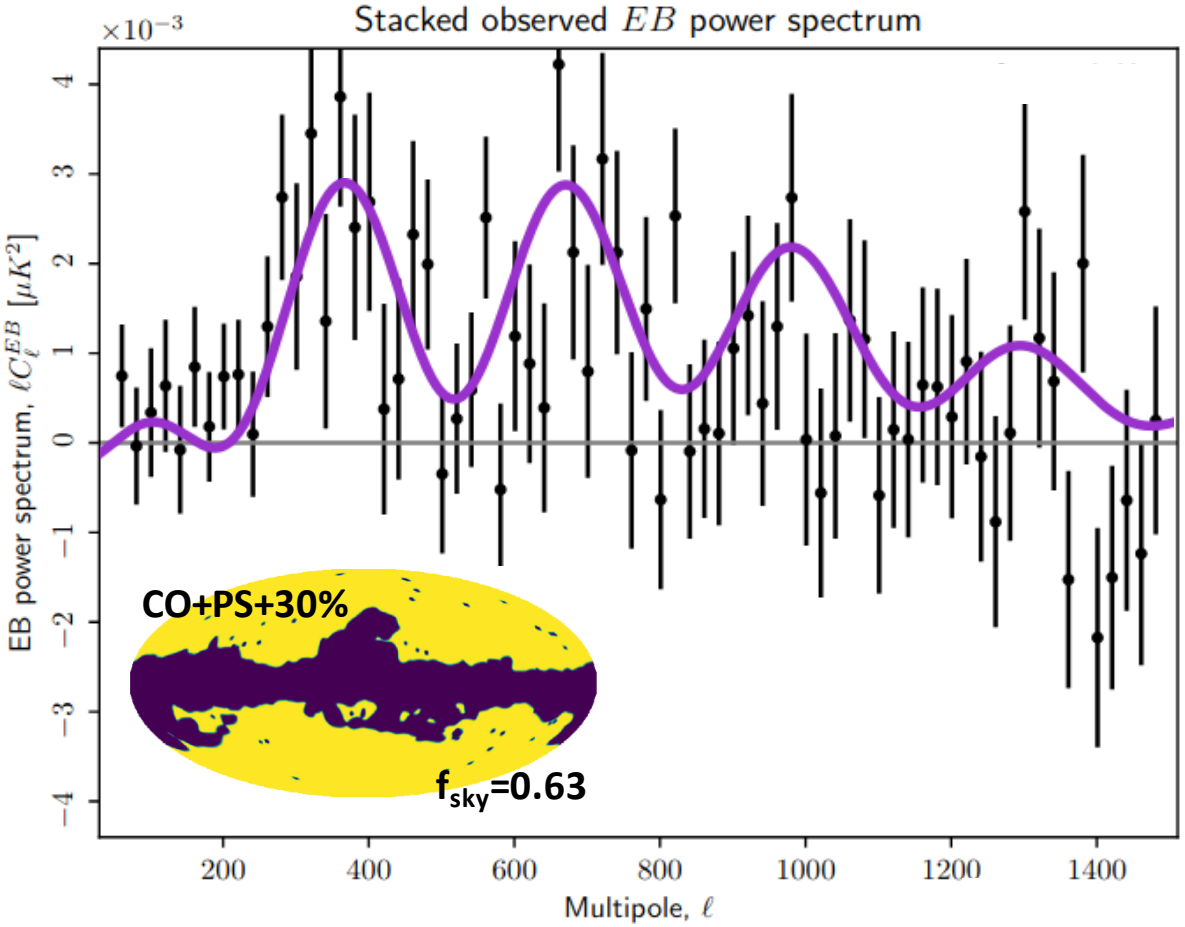

Eskilt & Komatsu 2022, PRD, 106, 063503

… but our inferred value of α depends on Galactic dust

Observed foreground signal can be rewritten as

$$C_\ell^{EB,\mathrm{fg,o}} = \tfrac{1}{2}\sin(4\alpha)\left(C_\ell^{EE,\mathrm{fg}} - C_\ell^{BB,\mathrm{fg}}\right) + \cos(4\alpha) C_\ell^{EB,\mathrm{fg}}$$
$$= \tfrac{1}{2}\sqrt{4\left(C_\ell^{EB,\mathrm{fg}}\right)^2 + \left(C_\ell^{EE,\mathrm{fg}} - C_\ell^{BB,\mathrm{fg}}\right)^2}\,\sin(4\alpha + 4\gamma_\ell)$$

Within the small angle approximation

$$\gamma_\ell \approx \frac{C_\ell^{EB,\mathrm{fg}}}{C_\ell^{EE,\mathrm{fg}} - C_\ell^{BB,\mathrm{fg}}}$$

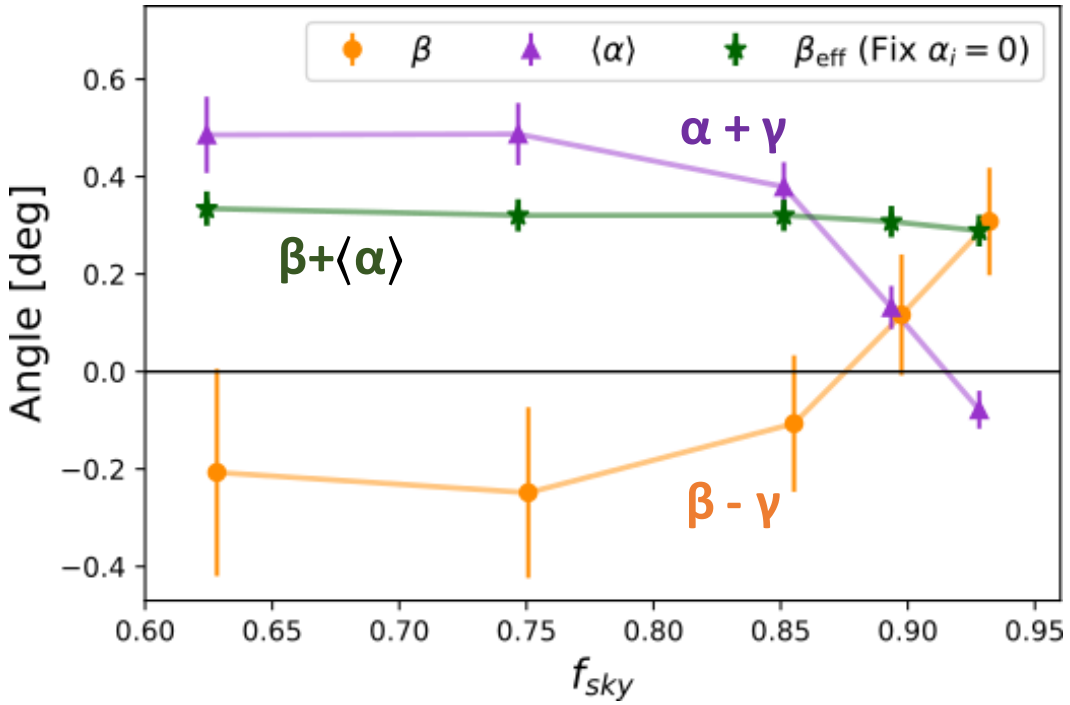

If $C_\ell^{EB,\mathrm{fg}} \propto C_\ell^{EE,\mathrm{fg}} - C_\ell^{BB,\mathrm{fg}}$

then $\gamma_\ell = \gamma$ → degenerate with α

- measure α + γ and β - γ
- does not affect α + β → By fixing α_i=0 we effectively measure β+⟨α⟩

Planck Collaboration XI. 2020, A&A, 641, A11

Planck reported dust TB > 0 → Plausible dust EB > 0 → Expect ↑α and ↓β

Observed foreground signal can be rewritten as

$$C_\ell^{EB,\mathrm{fg,o}} = \tfrac{1}{2}\sqrt{4\left(C_\ell^{EB,\mathrm{fg}}\right)^2 + \left(C_\ell^{EE,\mathrm{fg}} - C_\ell^{BB,\mathrm{fg}}\right)^2}\,\sin(4\alpha + 4\gamma_\ell)$$

Within the small angle approximation $\gamma_\ell \approx \dfrac{C_\ell^{EB,\mathrm{fg}}}{C_\ell^{EE,\mathrm{fg}} - C_\ell^{BB,\mathrm{fg}}}$

If $C_\ell^{EB,\mathrm{fg}} \propto C_\ell^{EE,\mathrm{fg}} - C_\ell^{BB,\mathrm{fg}}$ **then** $\gamma_\ell = \gamma$ → **degenerate with α**

- measure α + γ and β - γ
- does not affect α + β

Synchrotron

Synch EB **statistically compatible with null**

Martire et al 2022, JCAP, 04, 003

No physical process known to produce synch EB

Dust

Misalignment between dust filaments and Galactic magnetic fields creates TB and EB correlations

Clark et al 2021, ApJ, 919, 53

Planck reported :

- Dust TB > 0
- A hint of dust EB > 0 (still statistically compatible with null)

Planck Collaboration XI. 2020, A&A, 641, A11

→ Expect γ > 0 leading to ↑α and ↓β

Planck Collaboration LVII. 2020, A&A, 643, A42

PDP et al 2022 [arXiv:2210.07655]

NPIPE end-to-end simulations

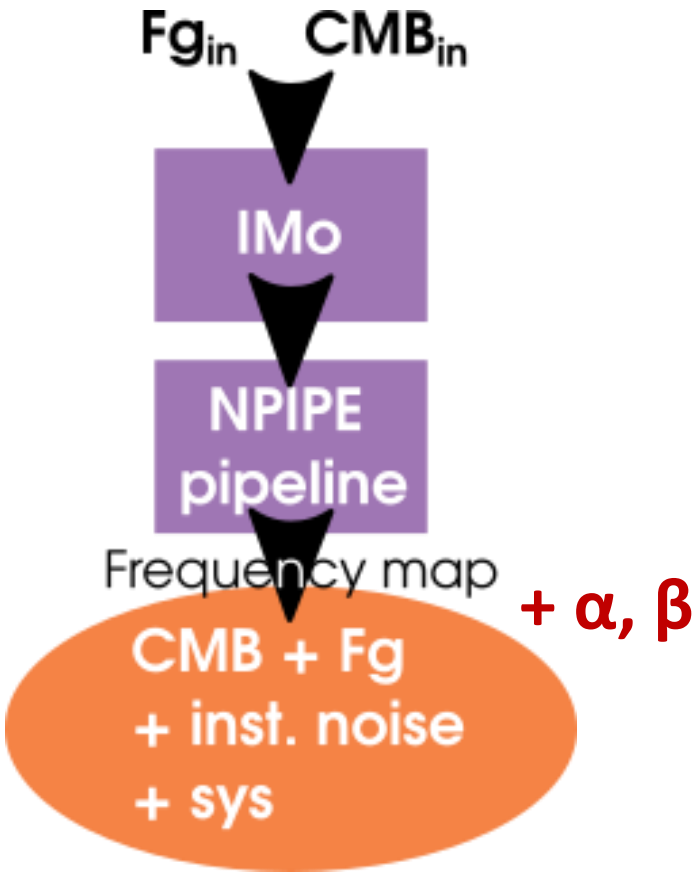

Ignoring dust EB

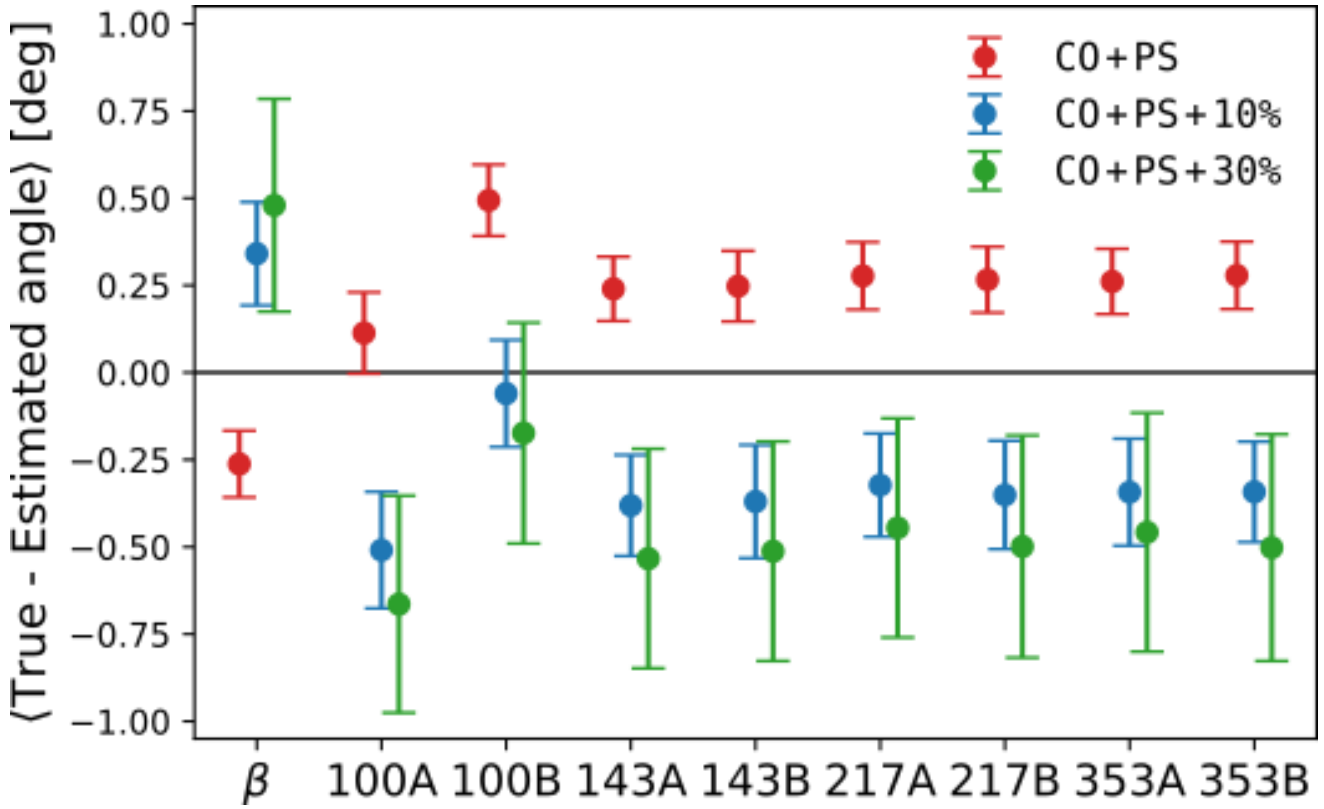

Average over 100 simulations
Error bar = simulations dispersion

Planck Collaboration LVII. 2020, A&A, 643, A42

PDP et al 2022 [arXiv:2210.07655]

NPIPE end-to-end simulations

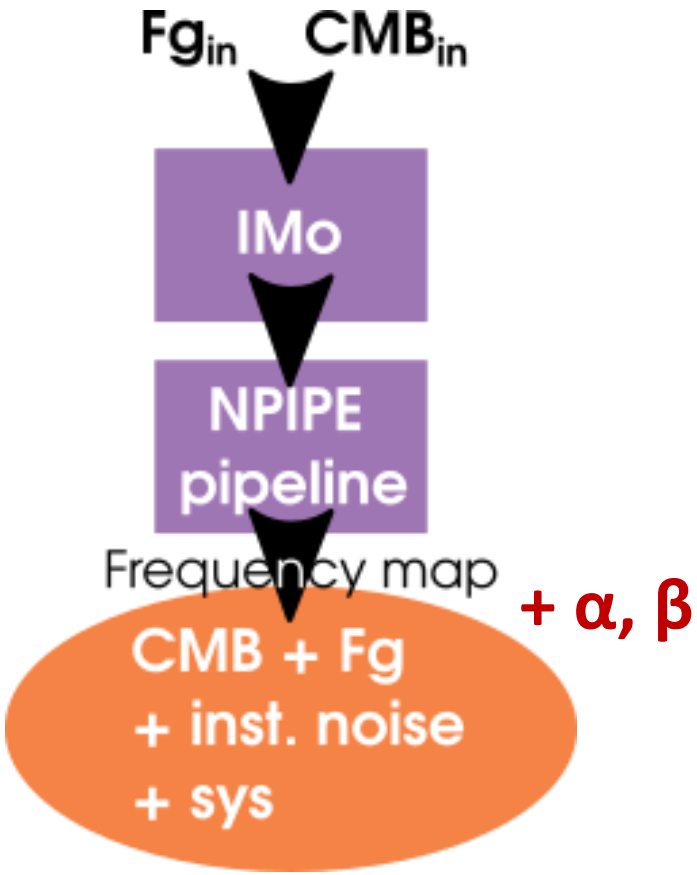

Correcting for dust EB

Exact description of the fiducial foreground model

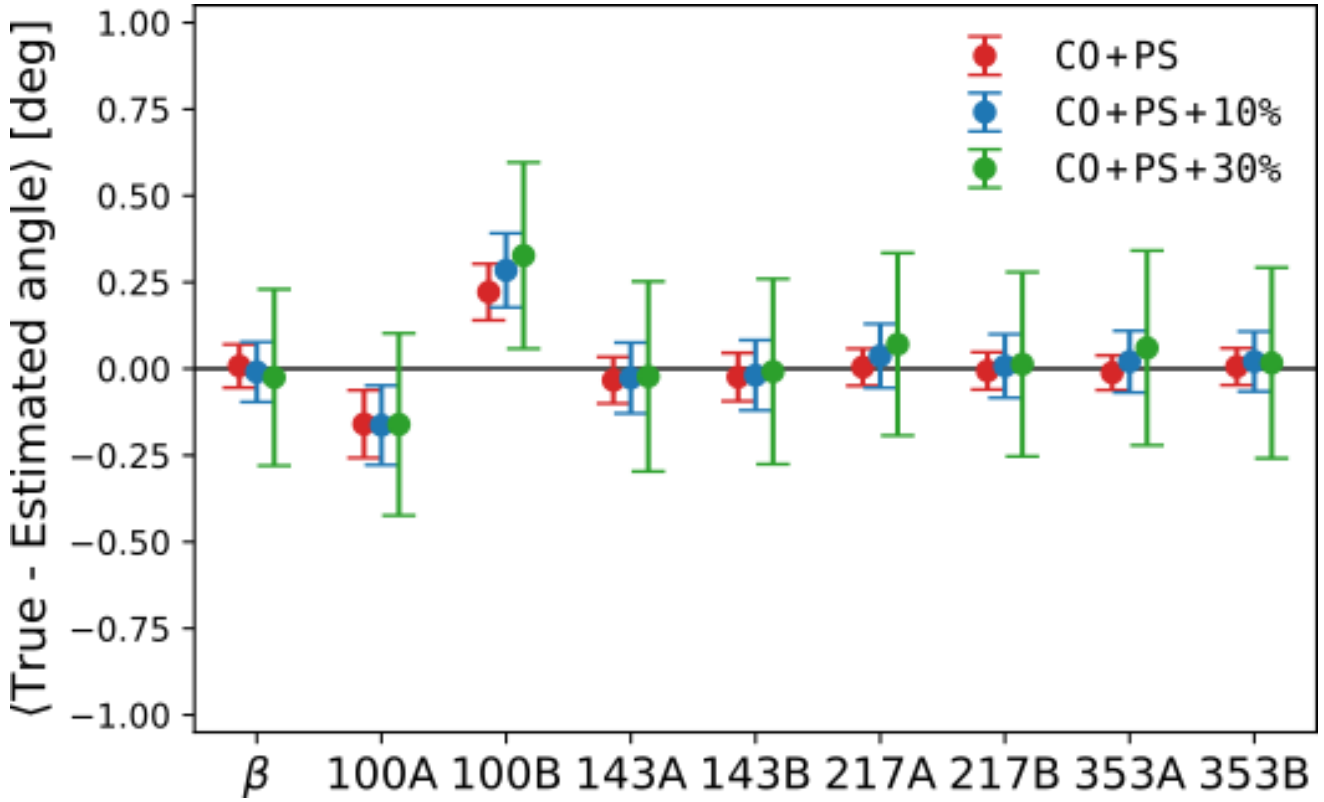

Average over 100 simulations

Error bar = simulations dispersion

Planck Collaboration LVII. 2020, A&A, 643, A42

PDP et al 2022 [arXiv:2210.07655]

NPIPE end-to-end simulations

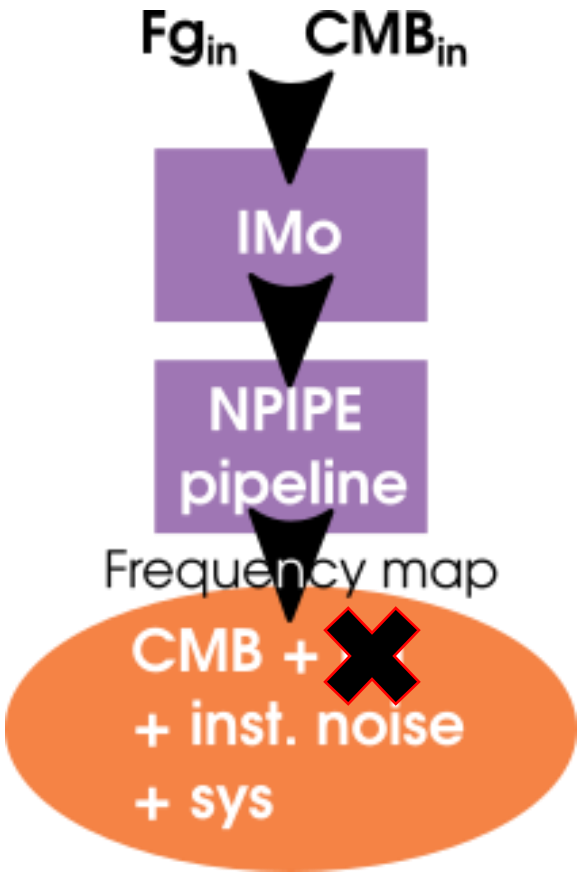

Removing foregrounds

Sims of CMB + Noise + Systematics

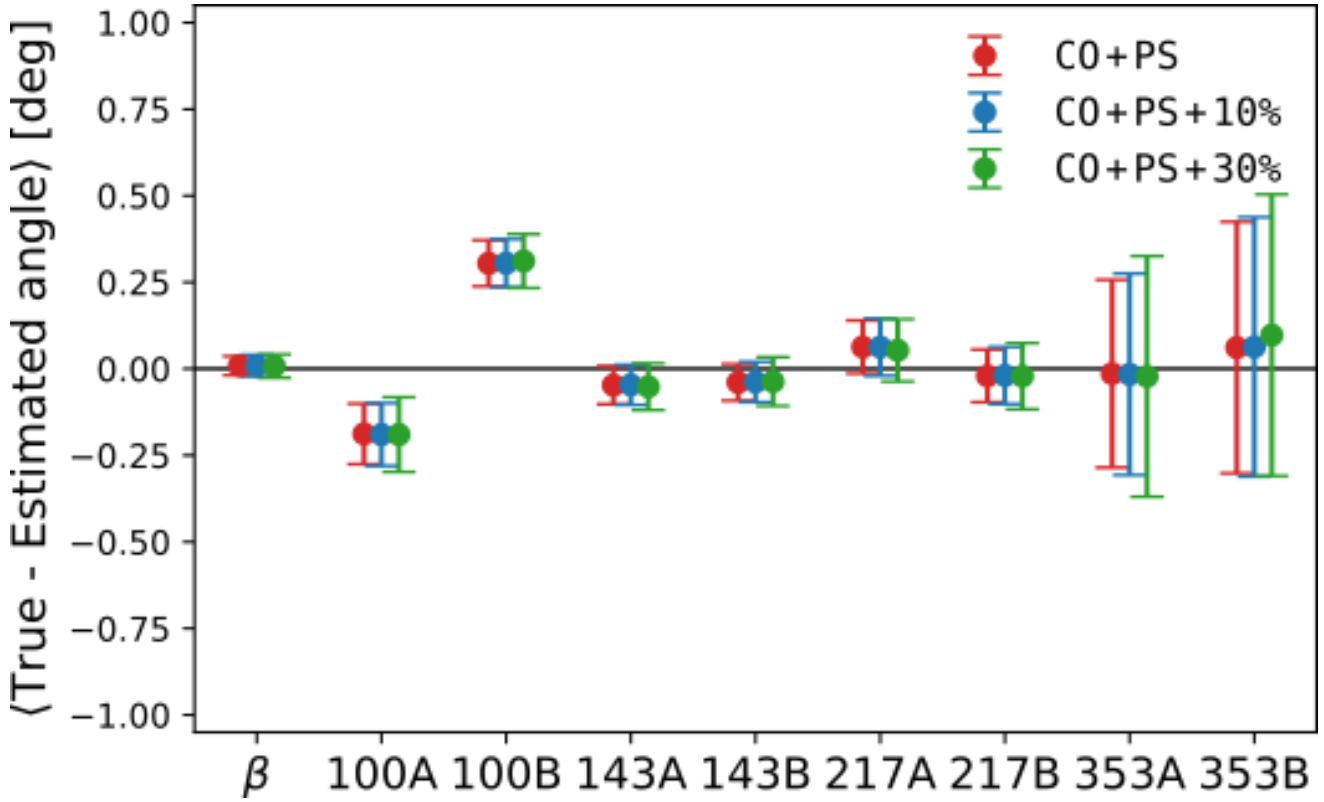

Average over 100 simulations

Error bar = simulations dispersion

Huffenberger et al 2020, ApJ, 899, 31
Clark et al 2021, ApJ, 919, 53

Misalignment between the filamentary dust structures of the ISM and the plane-of-sky orientation of the Galactic magnetic field

Filament
Magnetic Field

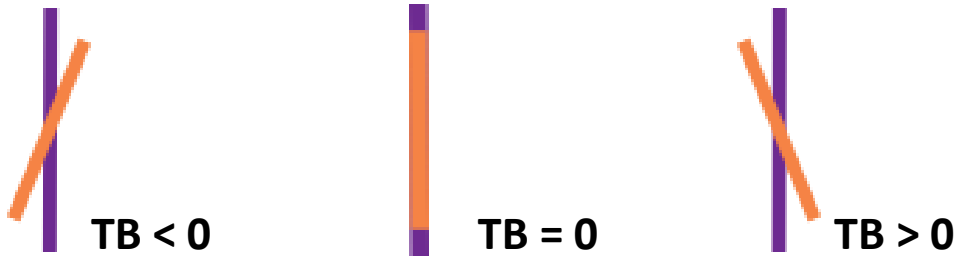

TB < 0
TE > 0
EB < 0

TB = 0
TE > 0
EB = 0

TB > 0
TE > 0
EB > 0

$$C_\ell^{TB,\mathrm{dust}} \propto \sin(2\psi)$$
$$C_\ell^{TE,\mathrm{dust}} \propto \cos(2\psi)$$
$$C_\ell^{EB,\mathrm{dust}} \propto \sin(4\psi)$$

Sign and magnitude of EB can be predicted by measuring TE and TB

$$C_\ell^{EB,\mathrm{dust}} = r_\ell^{TB,\mathrm{dust}} \sqrt{C_\ell^{EE,\mathrm{dust}} C_\ell^{BB,\mathrm{dust}}} \sin\left(2 \arctan\left(\frac{C_\ell^{TB,\mathrm{dust}}}{C_\ell^{TE,\mathrm{dust}}}\right)\right)$$

Our take

Small angle approximation

$C_\ell^{BB,\mathrm{dust}} \propto C_\ell^{EE,\mathrm{dust}}$ **thus** $\sqrt{C_\ell^{EE,\mathrm{dust}} C_\ell^{BB,\mathrm{dust}}} \to C_\ell^{EE,\mathrm{dust}}$

$|r_\ell^{TB,\mathrm{dust}}| \to A_\ell$ **free amplitude parameter** $0 \leq A_\ell \ll 1$

$$C_\ell^{EB,\mathrm{dust}} \approx A_\ell C_\ell^{EE,\mathrm{dust}} \frac{C_\ell^{TB,\mathrm{dust}}}{C_\ell^{TE,\mathrm{dust}}}$$

Huffenberger et al 2020, ApJ, 899, 31
Clark et al 2021, ApJ, 919, 53
Cukierman et al 2022 [arXiv:2208.07382]

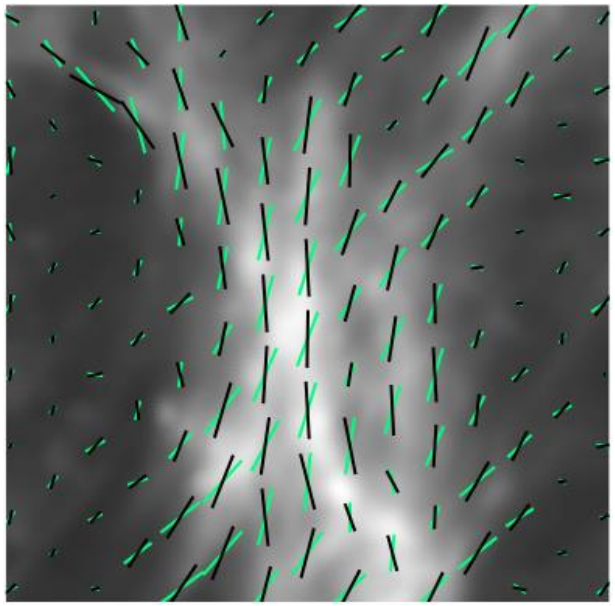

Misalignment between the dust filaments of the ISM and the plane-of-sky orientation of the Galactic magnetic field sources TE, TB, EB correlations

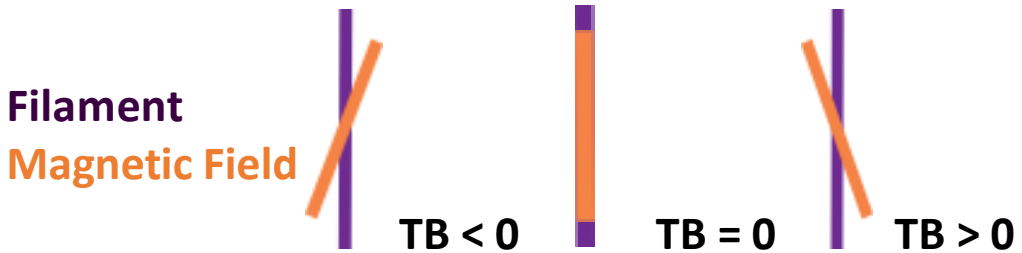

TB < 0
TE > 0
EB < 0

TB = 0
TE > 0
EB = 0

TB > 0
TE > 0
EB > 0

$$C_\ell^{TB,\mathrm{dust}} \propto \sin(2\psi)$$
$$C_\ell^{TE,\mathrm{dust}} \propto \cos(2\psi)$$
$$C_\ell^{EB,\mathrm{dust}} \propto \sin(4\psi)$$

Sign and magnitude of EB predicted from EE, TE, and TB

$$C_\ell^{EB,\mathrm{dust}} \approx A_\ell C_\ell^{EE,\mathrm{dust}} \frac{C_\ell^{TB,\mathrm{dust}}}{C_\ell^{TE,\mathrm{dust}}}$$

Take dust C_ℓ to be that of NPIPE @ 353GHz

A_ℓ **free amplitude parameter** $0 \leq A_\ell \ll 1$

Caveats and limitations

- **Assumes that all dust is sourcing the misalignment while only filaments are expected to produce EB**
- **Noisy proxy as it is built from Planck polarization measurements**

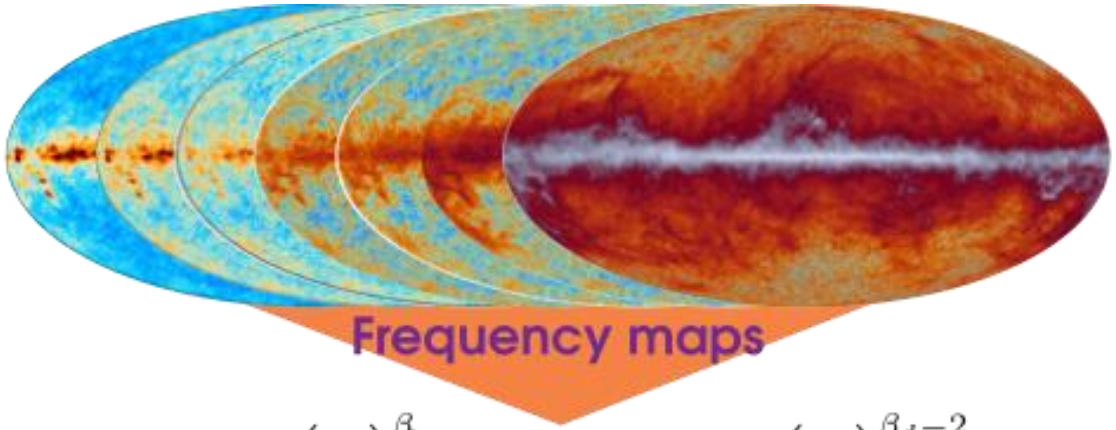

Frequency maps

$$\begin{pmatrix} Q \\ U \end{pmatrix}_p = \begin{pmatrix} q^{\rm cmb} \\ u^{\rm cmb} \end{pmatrix}_p + \frac{1}{f(\nu)} \left(\frac{\nu}{\nu_s}\right)^{\beta_s} \begin{pmatrix} q^{\rm synch} \\ u^{\rm synch} \end{pmatrix}_p + \frac{1}{f(\nu)} \left(\frac{\nu}{\nu_d}\right)^{\beta_d - 2} \frac{B(\nu, T_d)}{B(\nu_d, T_d)} \begin{pmatrix} q^{\rm dust} \\ u^{\rm dust} \end{pmatrix}_p$$

CMB Synch Dust

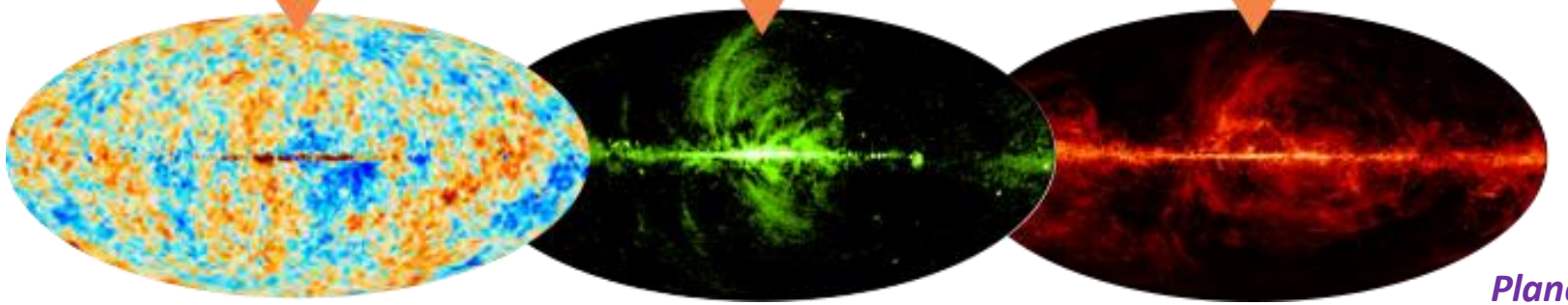

$f(\nu)$ **conversion from thermodynamic to antenna units**

$B(\nu, T)$ **Planck's law**

Power law synchrotron and one-component modified blackbody dust models

Commander

Planck Collaboration IV. 2020, A&A, 641, A4

Take the Commander sky model as our foreground model

$$C_\ell^{EB,\rm o} = \frac{\tan(4\alpha)}{2}\left(C_\ell^{EE,\rm o} - C_\ell^{BB,\rm o}\right) + \frac{\mathcal{D}}{\cos(4\alpha)} C_\ell^{EB,\rm fg} + \frac{\sin(4\beta)}{2\cos(4\alpha)}\left(C_\ell^{EE,\rm cmb} - C_\ell^{BB,\rm cmb}\right)$$

Commander

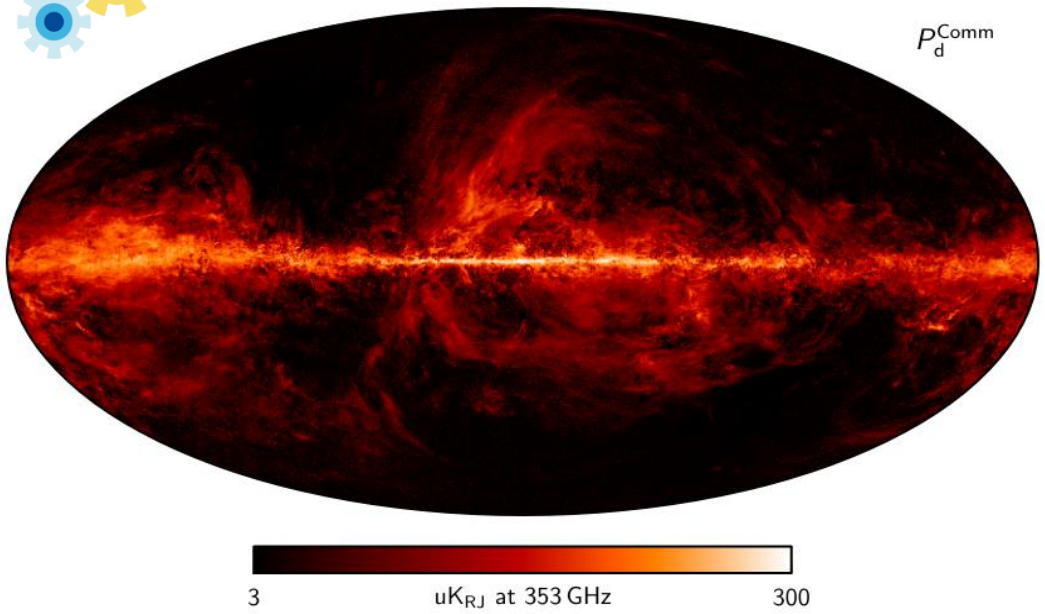

$$\frac{1}{f(\nu)}\left(\frac{\nu}{\nu_d}\right)^{\beta_d-2}\frac{B(\nu,T_d)}{B(\nu_d,T_d)}\begin{pmatrix}q^{\mathrm{dust}}\\ u^{\mathrm{dust}}\end{pmatrix}_p$$

Caveats and limitations

- **Limited signal-to-noise of EB template leads to a 20% underestimation of uncertainties**

  PDP et al 2022 [arXiv:2210.07655]

  → High-precision measurements from next-generation experiments

- **Spurious EB correlations through ignoring instrumental polarization angles in the SED model**

  → Inclusion of polarization angles in SED

  de la Hoz et al 2022, JCAP, 03, 032

- **Spurious EB correlations from the integration of different dust clouds along the line-of-sight**

  Vacher et al 2022 [arXiv:2210.14768]

  → Dust model beyond the single modified blackbody

NPIPE end-to-end simulations

Simulations of CMB + Foregrounds + Noise + Systematics

Baseline analysis (ignoring foreground EB)

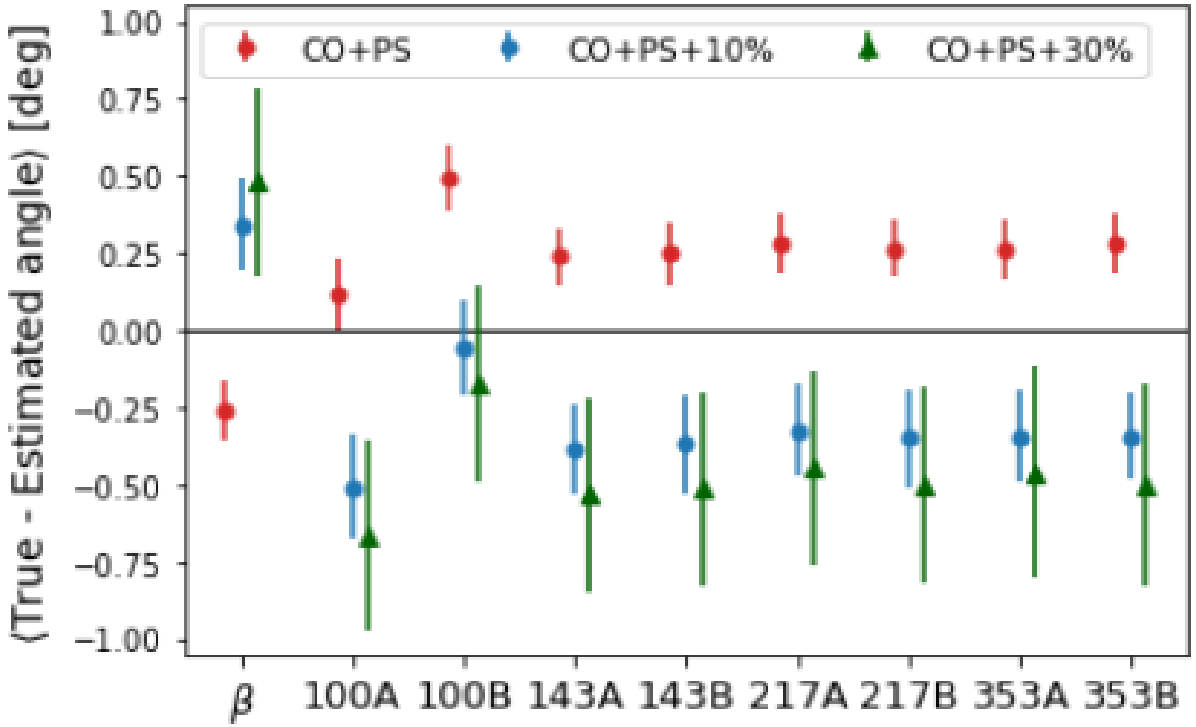

Modeling foreground EB (Commander)

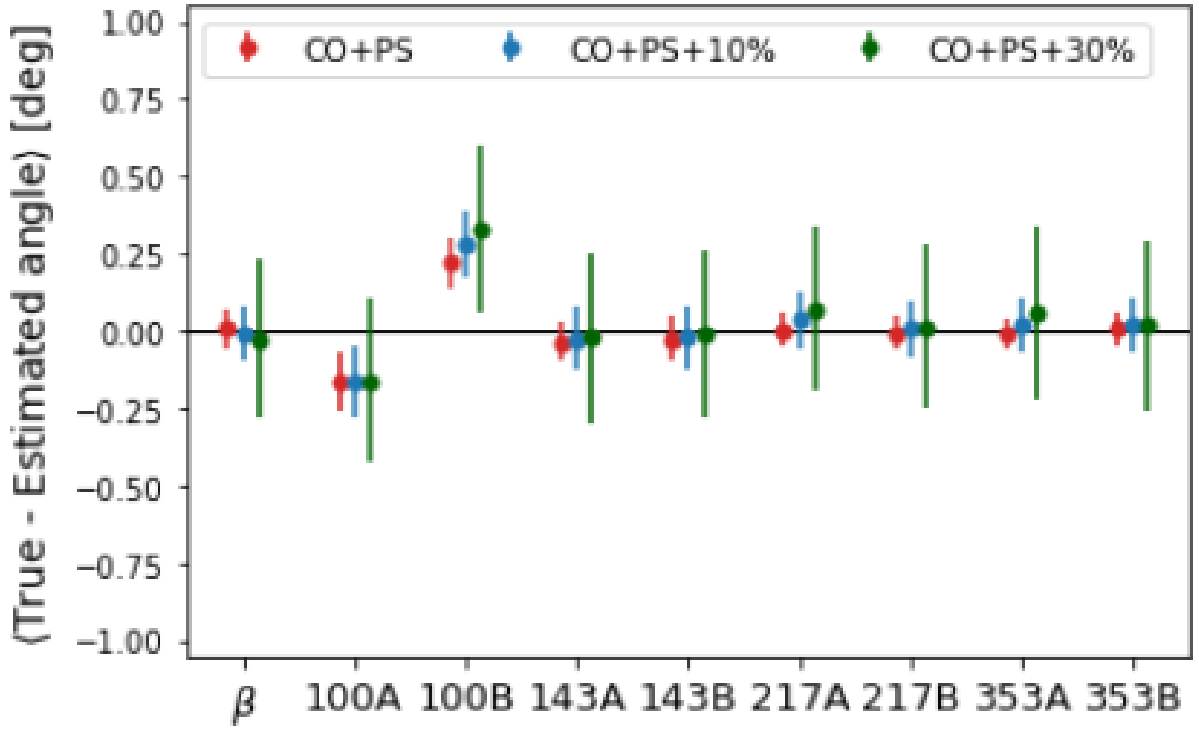

Average over 100 simulations
Error bar = simulations dispersion

PDP et al 2022 [arXiv:2210.07655]

Quantifying systematics with NPIPE end-to-end simulations

PDP et al 2022 [arXiv:2210.07655]

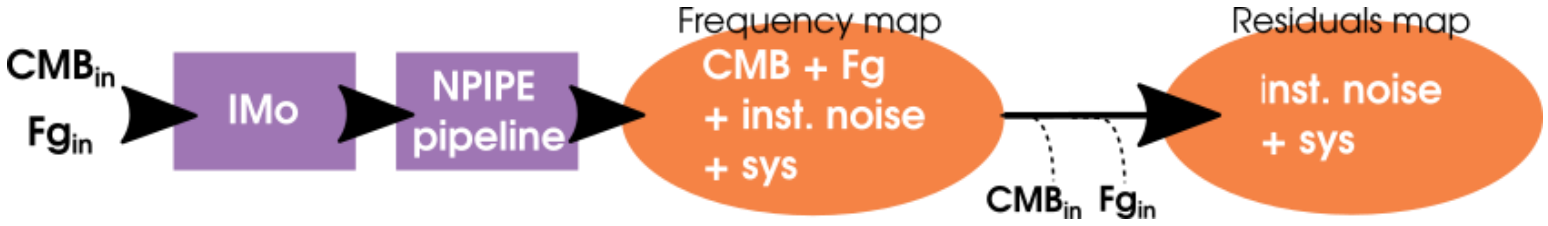

Simulations of CMB + Noise + Systematics

No foreground to break the α+β degeneracy

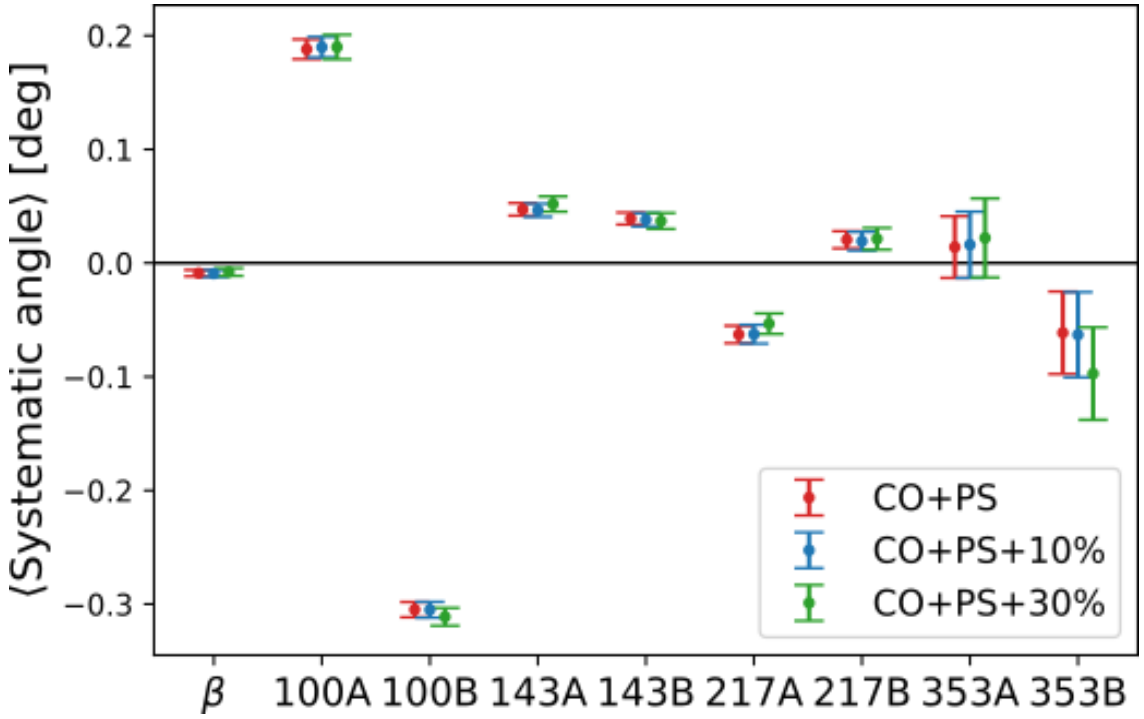

Average over 100 sims

Error bar = sim' dispersion / sqrt(100)

different angle for each detector split → α_i

same angle for all frequency bands → β

	From sims	σ_{stat} fit to data
$\langle\alpha_{100A}\rangle$ =	0.188° ± 0.009°	0.13°
$\langle\alpha_{100B}\rangle$ =	- 0.305° ± 0.007°	0.13°

→ cross-polarization effect

$\langle\alpha_{143A}\rangle$ =	0.047° ± 0.006°	0.11°
$\langle\alpha_{143B}\rangle$ =	0.039° ± 0.005°	0.11°
$\langle\alpha_{217A}\rangle$ =	- 0.063° ± 0.008°	0.11°

→ beam leakage

α_{sys} don't need to agree with data

→ simulations can't include the real α_i in the data

Negligible impact on β

$\langle\beta_{sys}\rangle$ = - 0.009° ± 0.003° 0.11°

Intensity-to-polarization leakage → $C_\ell^{EB} \propto C_\ell^{TT}$

Cross-polarization effect → $C_\ell^{EB} \propto C_\ell^{EE}$

A combination of both → $C_\ell^{EB} \propto C_\ell^{TE}$

Beam leakage

$$C_\ell^{EB} = \omega^2_{\ell,\mathrm{pix}} \sum_{XY} W_\ell^{EB,XY} C_\ell^{XY,\mathrm{cmb}}$$

$$XY \in \{TT, EE, BB, TE\}$$

QuickPol's polarization matrices

Hivon et al 2017, A&A, 598, A25

PDP et al 2022 [arXiv:2210.07655]

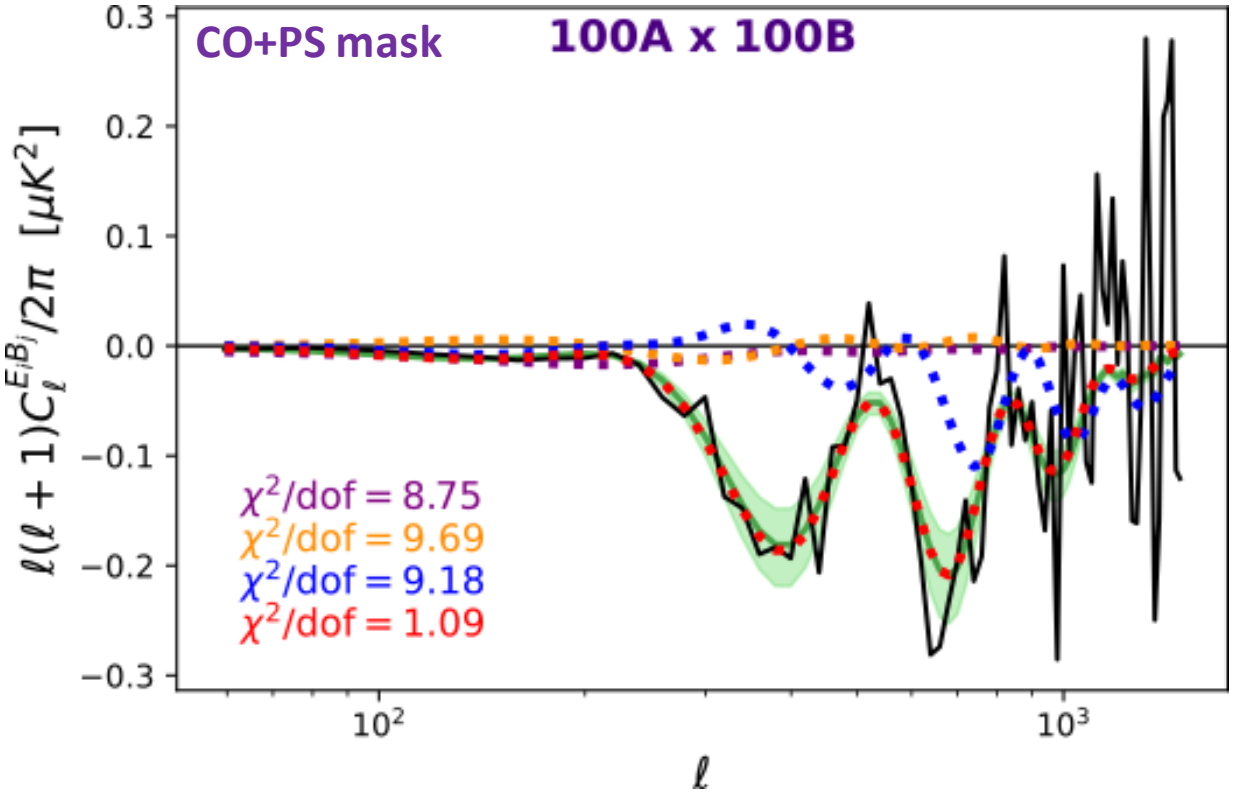

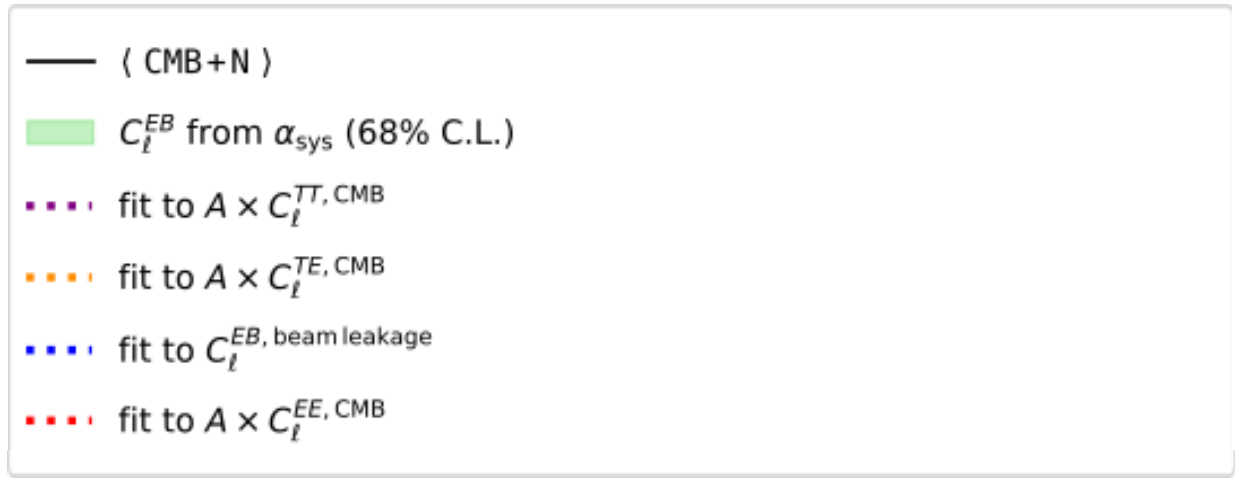

Particularly dangerous since our estimator relies on finding a signal resembling EE^{cmb} in EB

Intensity-to-polarization leakage → $C_\ell^{EB} \propto C_\ell^{TT}$

Cross-polarization effect → $C_\ell^{EB} \propto C_\ell^{EE}$

A combination of both → $C_\ell^{EB} \propto C_\ell^{TE}$

Beam leakage

$$C_\ell^{EB} = \omega^2_{\ell,\mathrm{pix}} \sum_{XY} W_\ell^{EB,XY} C_\ell^{XY,\mathrm{cmb}}$$

$$XY \in \{TT, EE, BB, TE\}$$

QuickPol's polarization matrices

Hivon et al 2017, A&A, 598, A25

PDP et al 2022 [arXiv:2210.07655]

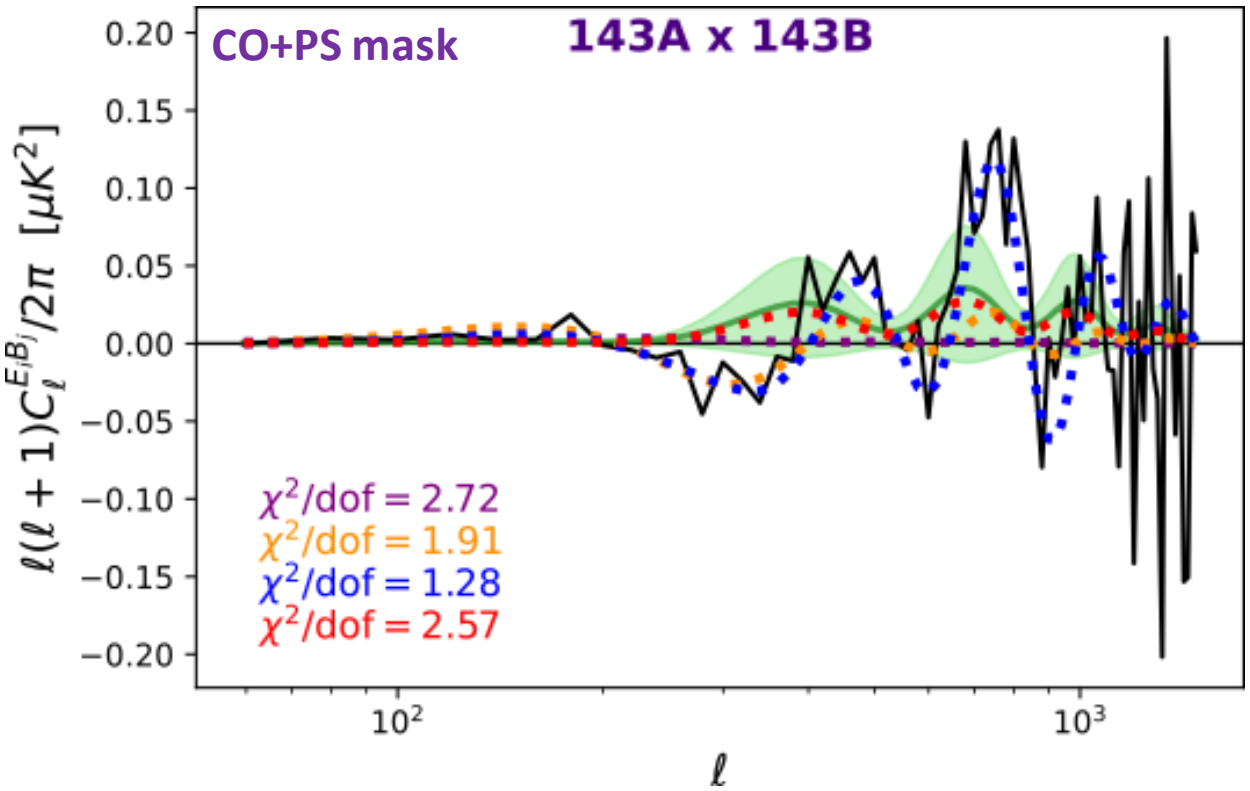

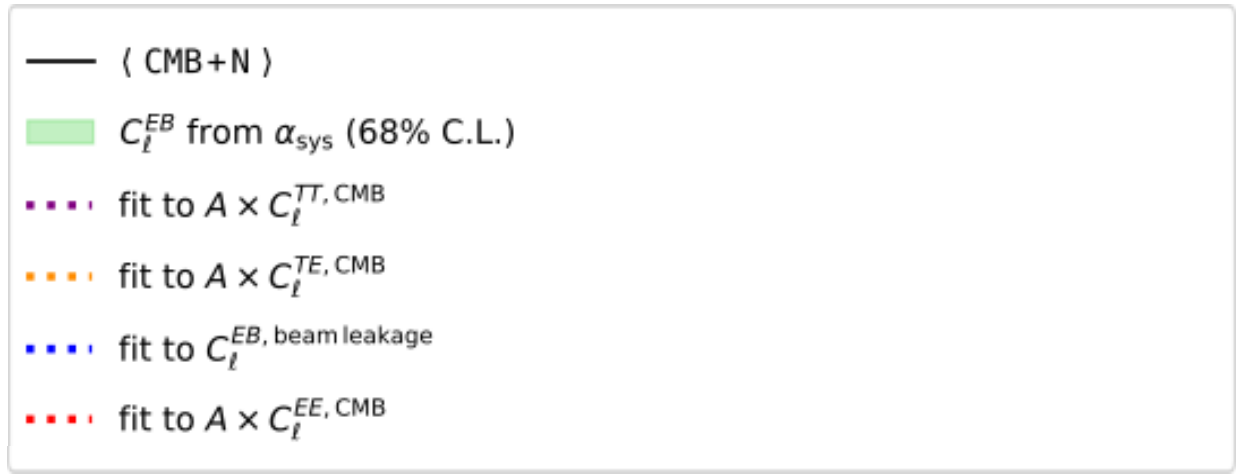

The estimator is trying to accommodate beam leakage as a rotation of EE

Frequency-dependent constraints on cosmic birefringence from the LFI and HFI Planck data release 4

Eskilt 2022, A&A, 662, A10

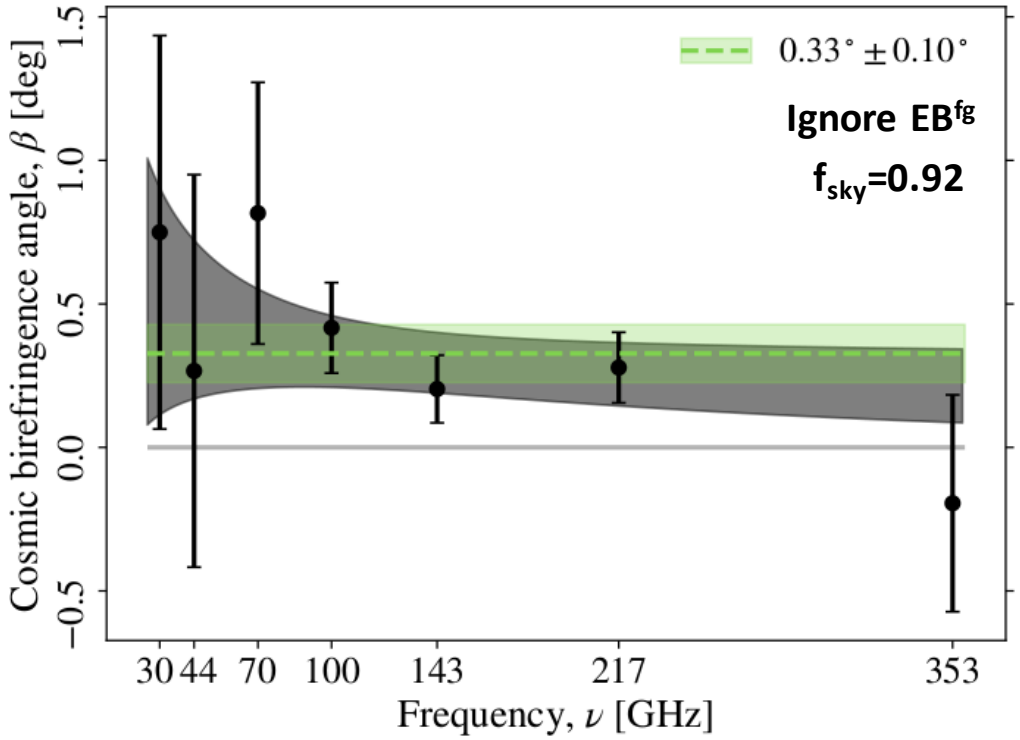

$$\beta_\nu = \beta_o(\nu/\nu_o)^n \begin{cases} \beta_o = 0.29^{+0.10}_{-0.11}\text{deg} \\ n = -0.35^{+0.48}_{-0.47} \end{cases}$$

First follow-up work adding *Planck* low-frequency bands

→ β = 0.33° ± 0.10° (3.3σ) for nearly full-sky data

Forcing an integer index

n	$\Delta\chi^2$ - Ignore EB^{fg}	$\Delta\chi^2$ - Model EB^{fg}
2	8.21	9.45
1	4.67	5.60
0	0.00	0.00
-2	2.25	3.01

Data seems to favor a frequency-independent birefringence

→Quantum gravity theories $\beta \propto \nu^2$

→Lorentz-violating electrodynamics $\beta \propto \nu$

→Chern-Simons coupling to a light pseudoscalar field $\beta \propto \nu^0$

→Faraday rotation from primordial magnetic fields $\beta \propto \nu^{-2}$

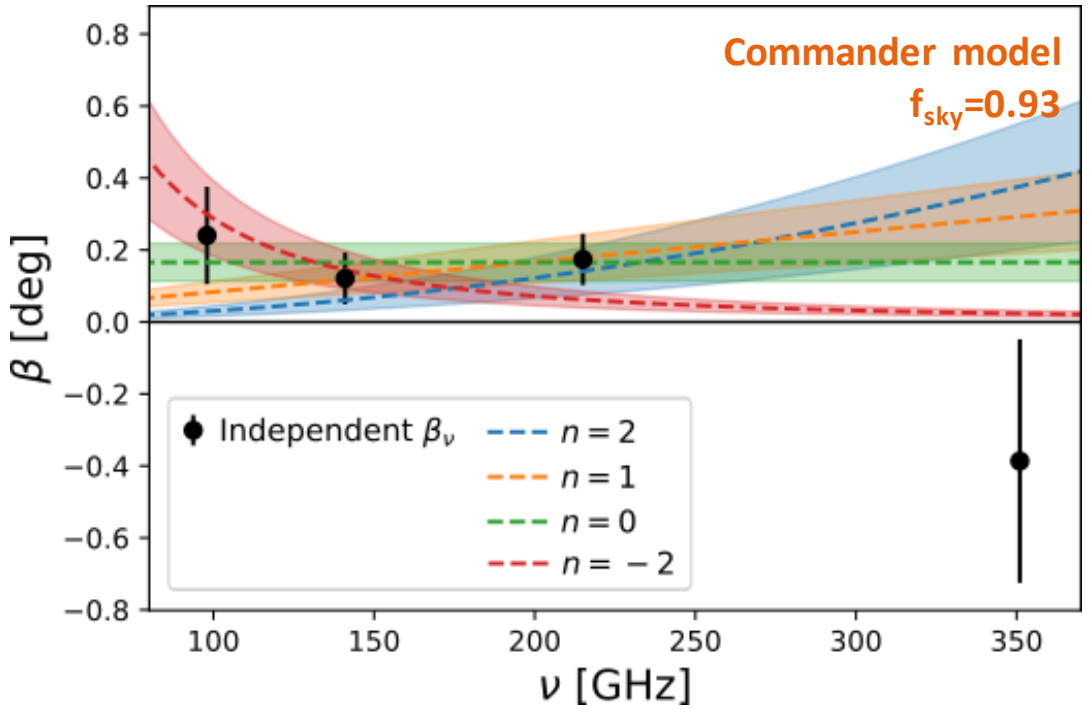

n	β_0 [deg]	$\Delta\chi^2$
2	0.07±0.03	5.08
1	0.13±0.04	1.77
0	0.17±0.05	0.00
-2	0.13±0.05	2.15

Independent β_ν for each frequency

$\beta_\nu=\beta_0\nu^2$ **Quantum gravity** models that modify the dispersion relation of photons

Gleiser & Kozameh 2001, PRD, 64, 8, 083007

$\beta_\nu=\beta_0\nu$ Superluminal **Lorenzt-violating electrodynamics** emerging from a non-vanishing Weyl tensor

Shore 2005, Nucl Phys B, 717, 86118

$\beta_\nu=\beta_0$ Chern-Simons coupling to a **light pseudoscalar field** like that of axion-like particles

$\beta_\nu=\beta_0\nu^{-2}$ **Faraday rotation** from Galactic or Primordial magnetic fields

Subramanian 2016, Rep Prog Phys, 79, 076901

Data seems to favor a **frequency-independent birefringence**

See **Eskilt 2022, A&A, 662, A10** for a more detailed analysis

Constraining power of CMB observations on ALP parameter space

Fujita et al 2021, PRD, 103, 063508

Assuming:

- A simple potential $V(\phi) = \frac{1}{2} m_\phi^2 \phi^2$
- A scale-invariant power spectrum for the ALP field

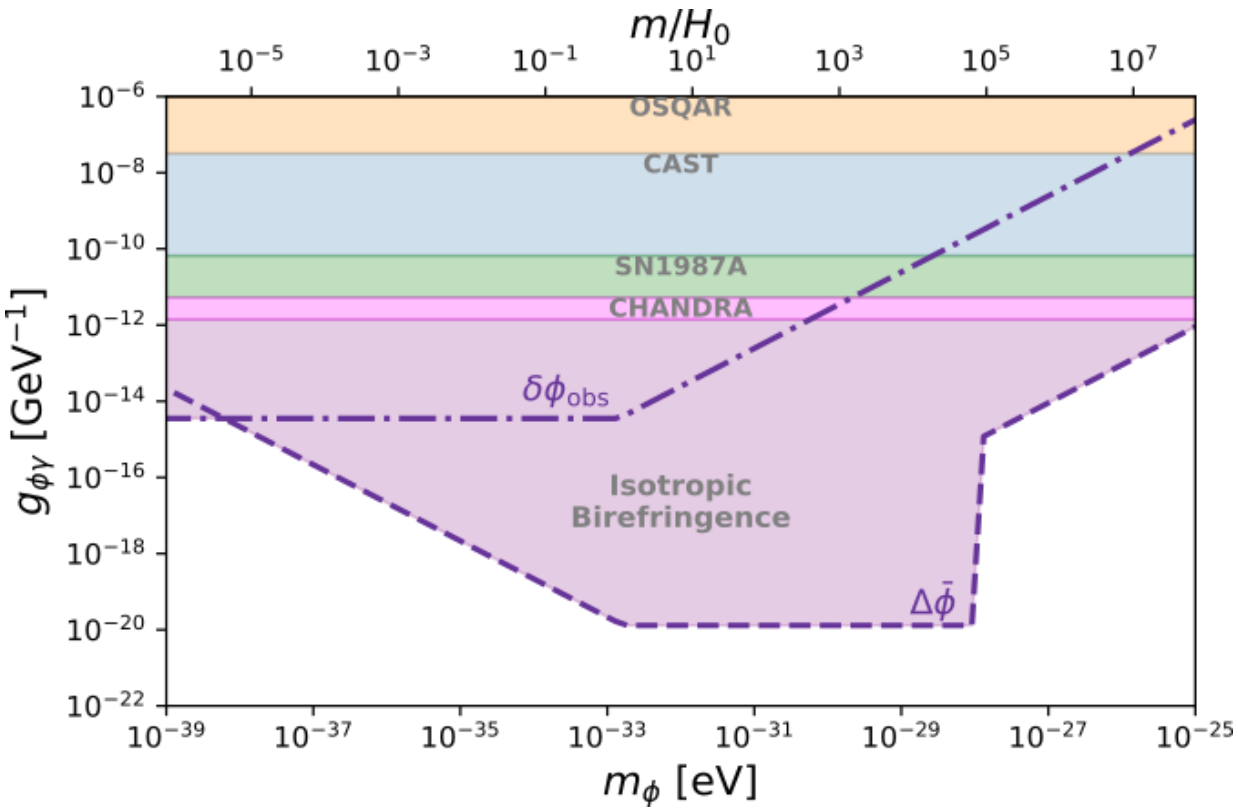

- A spatially flat FLRW universe, leading to EoM

$$\bar{\phi}'' + 2\mathcal{H}\bar{\phi}' + a^2 m_\phi^2 \bar{\phi} = 0$$
$$\delta\phi'' + 2\mathcal{H}\delta\phi' - \nabla^2\delta\phi + a^2 m_\phi^2 \delta\phi = 0$$

- The largest allowed ALP abundance

$$\Omega_\phi \begin{cases} \Omega_\Lambda = 0.69 & m_\phi \leq 9.26 \times 10^{-34}\text{eV} \\ 0.006h^{-2} & 10^{-32}\text{eV} \leq m_\phi \leq 10^{-25.5}\text{eV} \end{cases}$$

Planck Collaboration VI. 2020, A&A, 641, A6

- r<0.032 Tristram et al 2022, PRD, 105, 083524
- β≈0.30°

Chern-Simons coupling to a light ($m < 10^{-27}$eV) pseudoscalar field

$$\mathcal{L} = -\frac{1}{2}\partial^\mu\phi\partial_\mu\phi - V(\phi) - \frac{1}{4}F_{\mu\nu}F^{\mu\nu} + \frac{1}{4}g_{\phi\gamma}\phi F_{\mu\nu}\tilde{F}^{\mu\nu}$$

Marsh 2016, Phys Rep, 643, 1

Axion-like particles (ALP)

Initially proposed to solve the strong-CP problem

Evolved beyond the QCD axion to the more general axion-like particles from supersymmetry or string theories (10^{-33}eV < m < 10^{-18}eV)

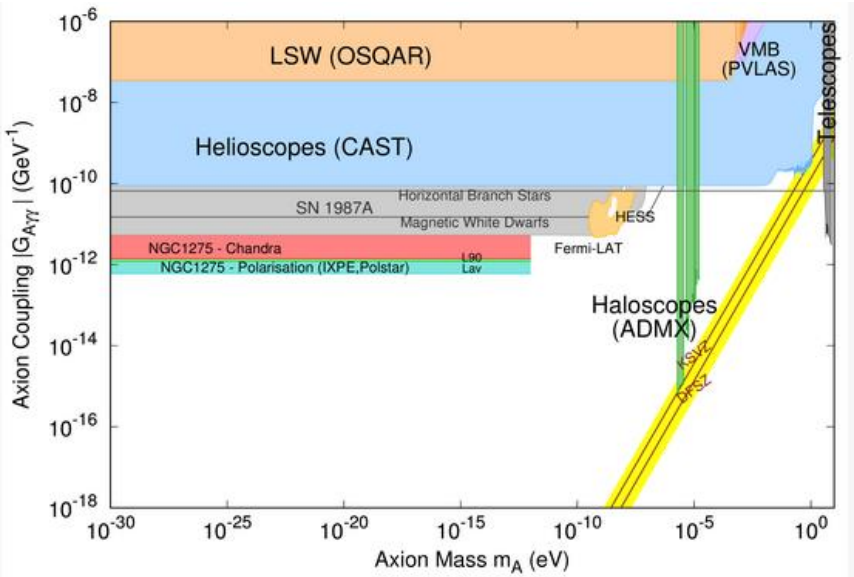

Day & Krippendorf 2018, Galaxies 2018, 6(2), 45

Kamionkowski & Riess 2022 [arXiv:2211.04492]

Early Dark Energy (EDE)

Early-time solution to the Hubble tension that modifies the sound horizon, increasing the H_0 inferred from CMB data

Fluid that behaves like a cosmological constant before matter-radiation equality (≈10% contribution to the total energy density briefly before recombination) and decays faster than radiation afterward so that late-time evolution is unchanged

Suppresses the growth of perturbations at early times, potentially increasing σ_8

→ worsening the tension between CMB and LSS measurements

Hill et al 2020, PRD, 102, 043507

Poulin et al 2019, PRL, 122, 221301
Hill et al 2020, PRD, 102, 043507

Global U(1) shift symmetry, broken by non-perturbative effects (instantons)

$$V(\phi) = m_\phi^2 f^2 \left[1 - \cos\left(\frac{\phi}{f}\right)\right]^n$$

Integer values of n

Around the minimum behaves as

$$w_\phi = \frac{n-1}{n+1}$$

$$\Omega_\phi \propto a^{-3(w_\phi+1)}$$

Axion-like particles (ALP)

$$n = 1$$

$$V(\phi) \to \frac{1}{2} m_\phi^2 \phi^2$$

$$\Omega_\phi \propto a^{-3}$$

ALP dilute like matter

Early Dark Energy (EDE)

$$n \geq 3$$

$$\Omega_\phi \propto a^{-4.5}$$

(or steeper)

EDE dilutes faster than radiation

Nakatsuka et al 2022, PRD, 105, 123509

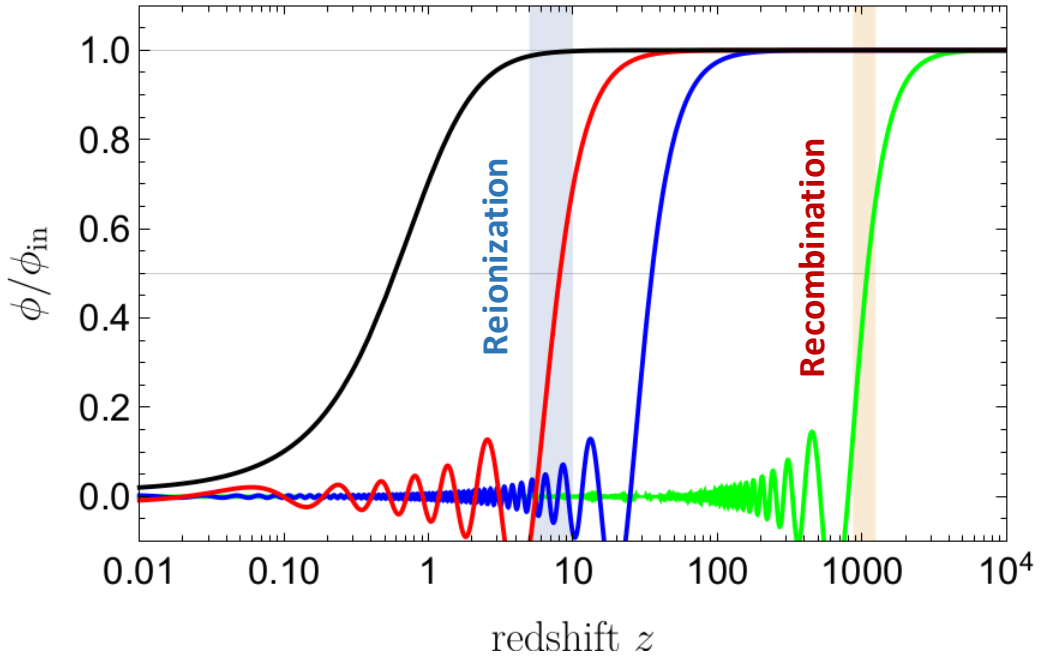

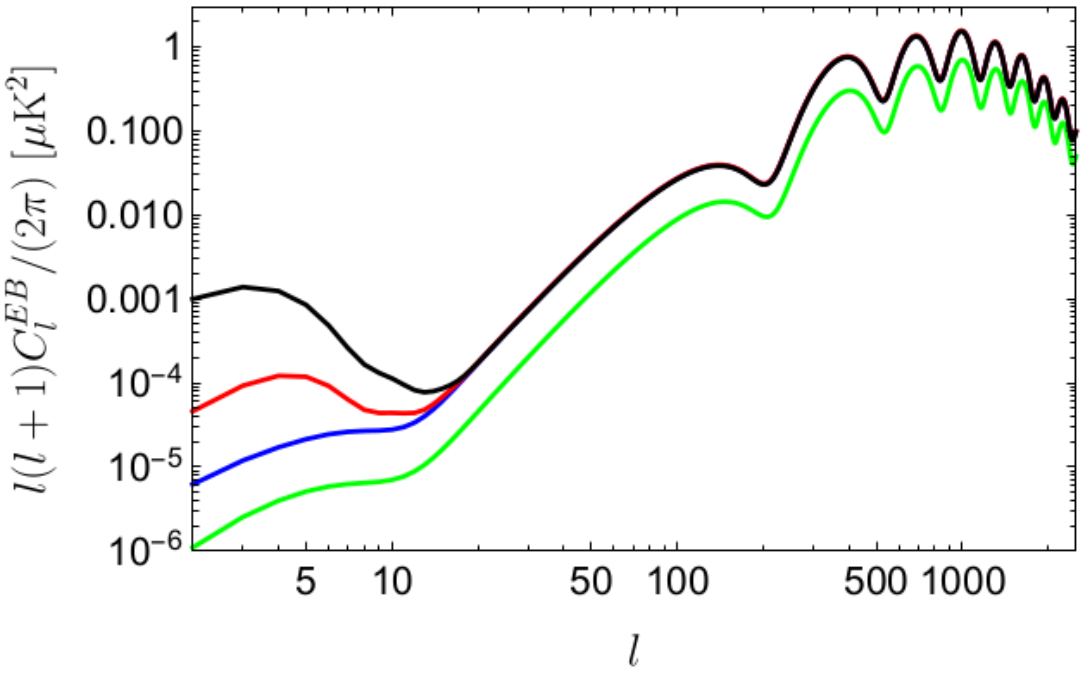

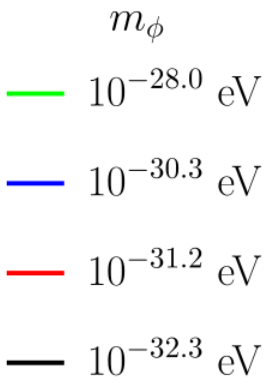

$$\beta = -\frac{1}{2} g_{\phi\gamma} \int \frac{\partial \phi}{\partial t} dt$$

Birefringence depends on the value of the field at photon emission and absorption

$$\beta(z) = \begin{cases} 0 & \text{for} \quad z = 0 \\ \beta_{\rm rei} & \text{for} \quad 0 < z \leq 10 \\ \beta_{\rm rec} & \text{for} \quad 10 < z \end{cases},$$

CMB photons emitted at recombination and reionization will suffer different rotations

$$C_\ell^{EB,{\rm o}} \approx \frac{1}{2} \sin(4\beta_{\rm rec}) C_\ell^{E_{\rm rec}E_{\rm rec}} + \frac{1}{2} \sin(4\beta_{\rm rei}) C_\ell^{E_{\rm rei}E_{\rm rei}} + \sin(2\beta_{\rm rec} + 2\beta_{\rm rei}) C_\ell^{E_{\rm rec}E_{\rm rei}}$$

For fields undergoing a significant evolution during the epoch of recombination…

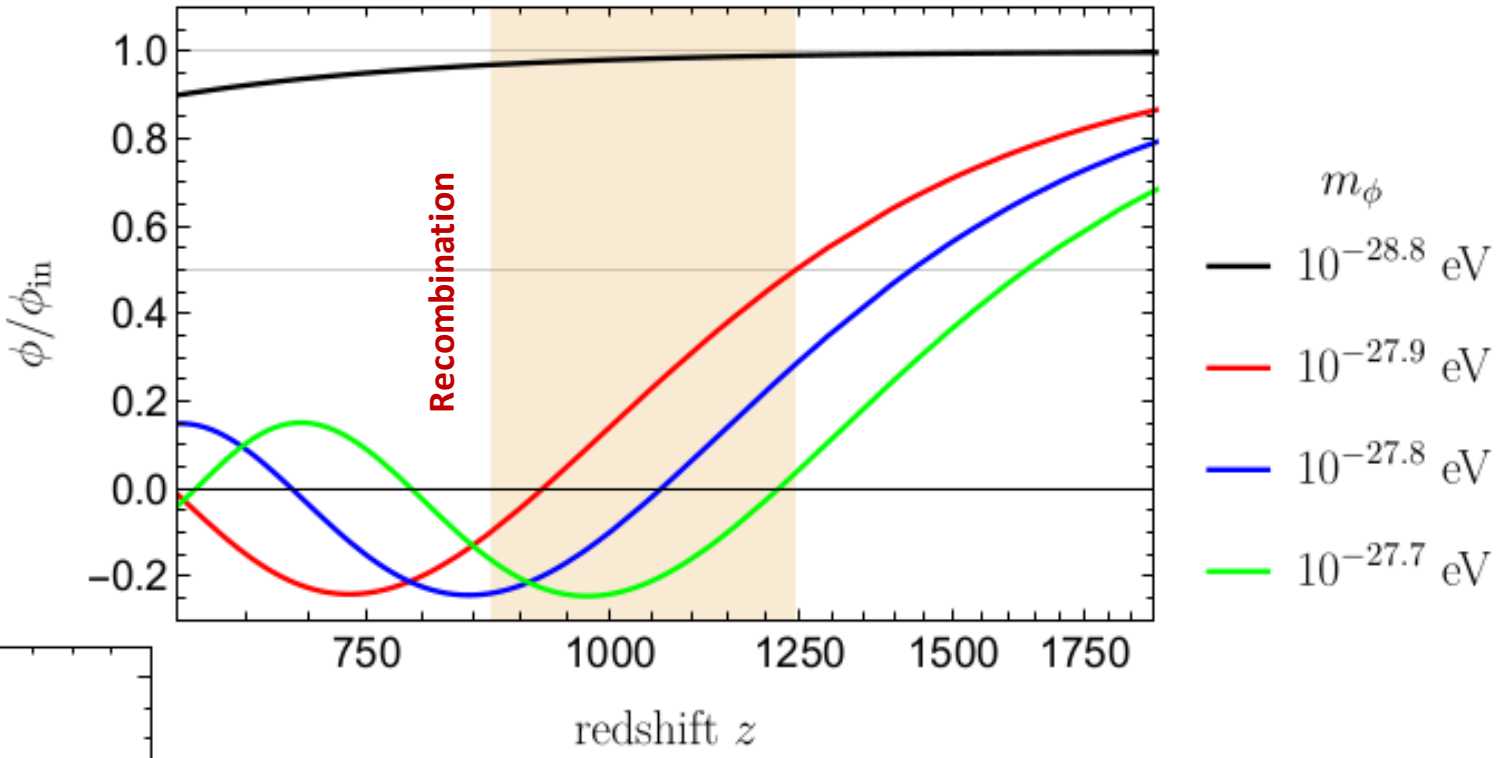

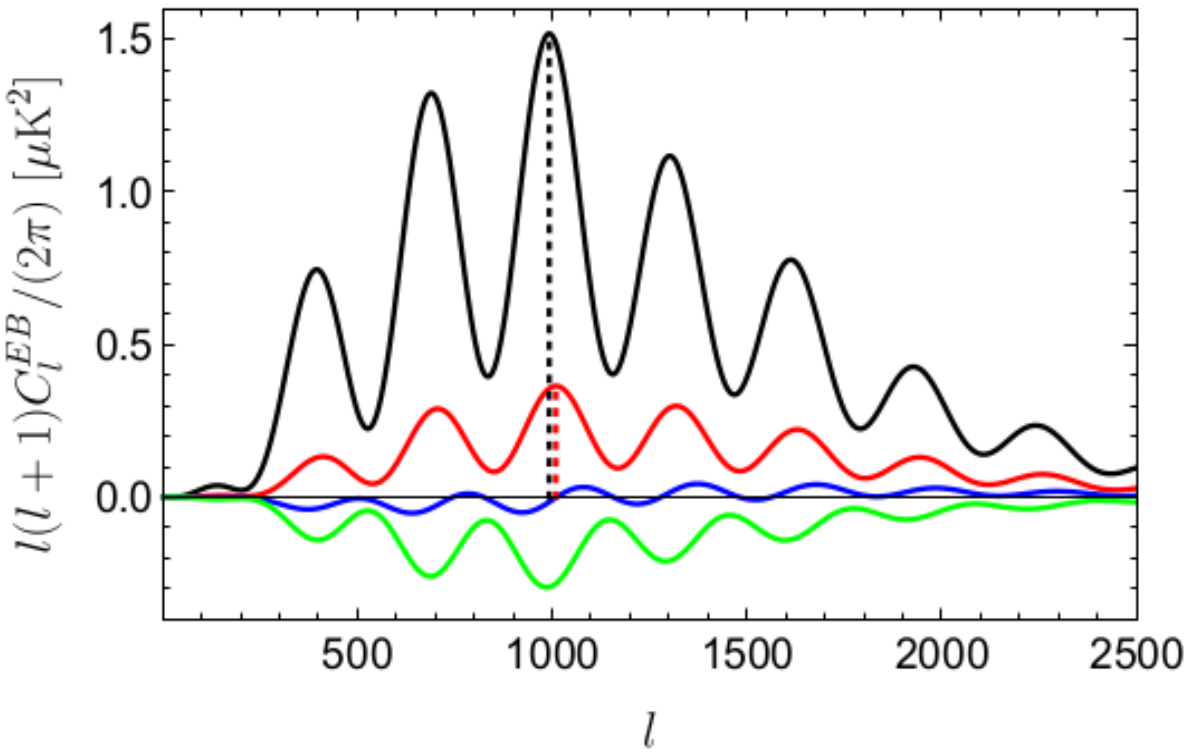

… the EB spectrum produced by birefringence no longer resembles a constant rotation of EE

Murai et al 2022 [arXiv:2209.07804]

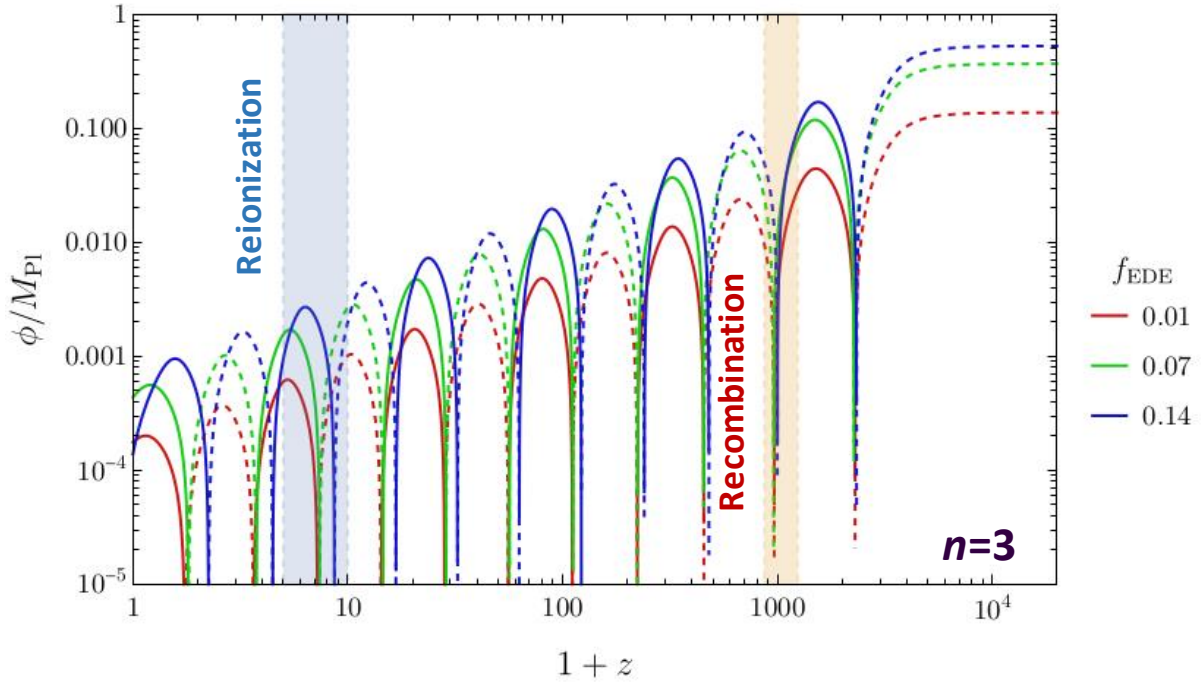

By definition, the EDE field must evolve before recombination

EB no longer resembles a constant EE rotation

EB is strongly dependent on the EDE model (*n* and f_{EDE})

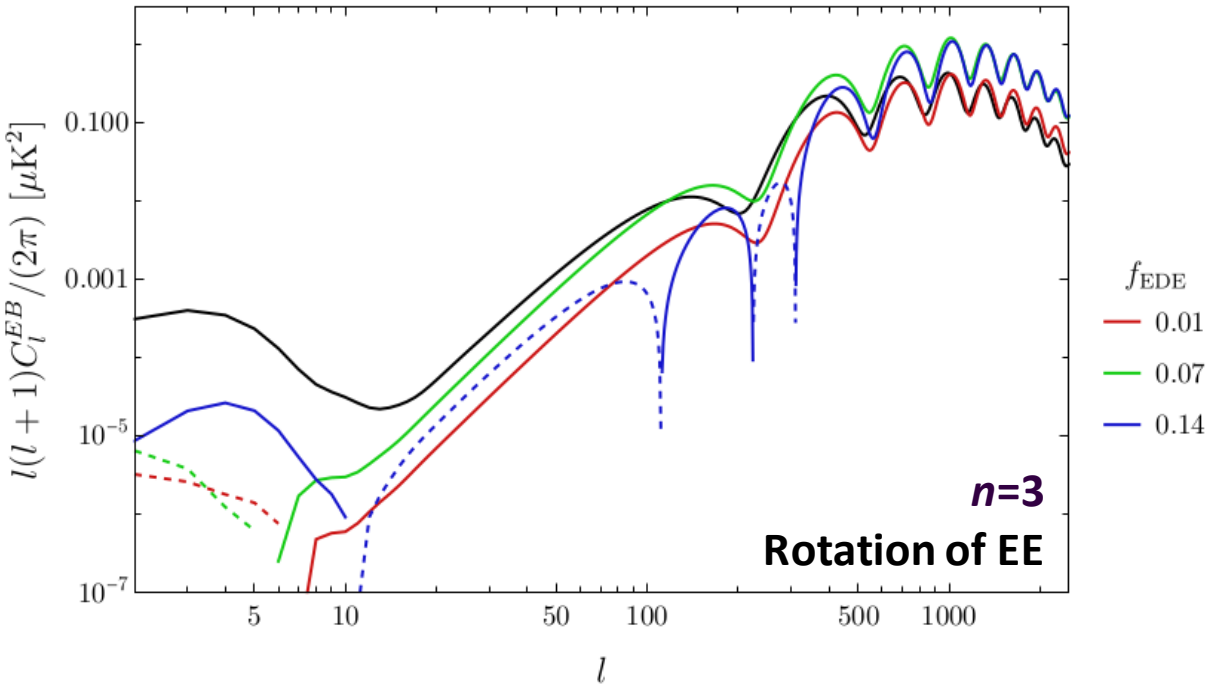

CMB data alone can discern between ALPs and EDE as the source of birefringence

→ in the next decade, experiments like CMB-S4 will have enough sensitivity

WIP:

Obtain the first measurement of β from the epoch of reionization using only low-ℓ information